CHAPTER I

BACKGROUND AND SIGNIFICANCE

A stem cell is an undifferentiated cell with the ability to undergo long-term self renewal and produce differentiated progeny. Adult stem cells have vital roles in maintaining tissue integrity and function throughout the life of an organism. Stem cells respond to local signals within their specialized microenvironment, or niche, to both maintain their identity and regulate their activity. They also respond to external stimuli such as injury, hormones, and diet, and modulate their activity accordingly. The use of adult stem cells for therapeutic purposes, such as tissue regeneration and organ development, holds great promise for the treatment of disease and injury. However, many adult stem cell-based therapies have had limited success, likely due to the complexity of their regulation, which requires the precise coordination of signals arising from multiples tissues/organs. A better understanding of the mechanisms that modulate stem cell activity is vital for the development of successful stem-cell based therapies.

Adult stem cells

The human body is composed of trillions of cells and dying cells must be replaced to maintain cell numbers. While the majority of our cells are terminally differentiated and no longer undergo cell division (e.g. neurons and red blood cells), our bodies contain a small number of undifferentiated stem cells capable of long-term self-renewal and the production of daughter cells (Weissman, 2000). Stem cells can be classified based on the number of different cell types they can produce, or their potency. Totipotent embryonic

stem cells are generated by the fusing of sperm to egg and give rise to all cells of the embryonic and extra embryonic lineages and pluripotent stem cells give rise to all the cells of the embryonic lineage only. Adult stem cells, or somatic stem cells, produce differentiated cells within a restricted lineage and are classified as multipotent (multiple related cell types), oligopotent (several cell types), or unipotent (one cell type) (Lukaszewicz et al., 2010).

Most, if not all adult organs contain stem cells, including the brain, bone marrow, blood, blood vessels, skeletal muscle, skin, teeth, heart, gut, liver, testis, and ovarian epithelium (Terskikh et al., 2006). Additional tissues, including the kidney and pancreas, may also contain stem cells, but the exact location and identity of those cells remain elusive (Gupta and Rosenberg, 2008; May et al., 2010). A stem cell's unique ability to self-renew and produce daughter cells has been exploited to identify potential stem cell populations by lineage tracing. While lineage tracing may be the gold-standard method for stem cell identification, its use is largely limited to model organisms that can be genetically manipulated. Furthermore, only some stem cell populations, such as *Drosophila* germline stem cells, or GSCs, remain consistently active and can be easily marked by labeling methods. Some types of mammalian adult stem cells are believed to be primarily quiescent, making their identification more difficult and dependent, rather, on the availability of specific cellular markers (Li and Clevers, 2010).

Intrinsic factors and local regulation via the niche

Stem cells respond to stimuli such as injury, hormones, and diet, and divide to restore tissue homeostasis or promote tissue expansion (Drummond-Barbosa, 2008). The

signals and mechanisms that activate stem cells are not well understood in mammalian systems due to the difficulties associated with identifying, labeling, and imaging stem cells in highly complex tissues. Studies in lower model organisms, such as *Drosophila melanogaster* and *Caenorhabditis elegans* have greatly contributed to our knowledge regarding conserved stem cell mechanisms such as stem cell control via the niche.

A niche is a highly specialized microenvironment that provides signals necessary for stem cell maintenance and activity (Spradling et al., 2001). Since the detailed characterization of the GSC stem cell niche in *Drosophila* (which will be reviewed in detail later) stem cell niches have been identified in other systems, including those supporting other types of GSCs and mammalian hematopoetic stem cells (HSCs). For instance, the *C. elegans* germ line contains a niche made up of a single cell type, a distal tip cell (DTC), which produces a Notch ligand necessary to suppress GSC differentiation by activating transcription of the RNA-binding proteins FBF-1 and -2. These proteins are specifically expressed in the GSCs and promote their maintenance by repressing the translation of regulators of meiotic cell cycle entry, *gld-1* and *gld-3* (Kimble and Crittenden, 2007). In the mammalian testis, spermatogonial stem cell identity is maintained by glial cell-line-derived neurotropic factor (GDNF) produced by sertoli cells of the niche (Wong et al., 2005). In the HSC niche, both endosteal and perivascular cells have roles in HSC maintenance via Notch and Kit signaling, and additional factors (He et al., 2009; Mitsiadis et al., 2007).

Local signals act by impinging upon various intrinsic mechanisms that repress stem cell differentiation. Epigenetic mechanisms maintain stem cell identity as demonstrated in studies of HSCs mutant for DNA methyltransferases (Tadokoro et al.,

2007) and in studies implicating the regulation of chromatin structure in the suppression of differentiation and the repression of cell cycle inhibitors in mammalian HSCs and neural stem cells, or NSCs (He et al., 2009). Also, asymmetric stem cell division ensures that stem cells remain in contact with the niche to receive maintenance promoting signals while the displaced daughter cell differentiates (Fuller and Spradling, 2007).

Systemic regulation via environmental signals

Systemic signals from environmental stimuli can be received either directly by a stem cell or be relayed via local signals from the niche (Figure 1.1). The effect of diet on *Drosophila* female GSCs is currently the best-understood stem cell response to an environmental signal. GSCs respond to diet by up regulating insulin signaling activity within the GSC to increase proliferation rates and within the niche to regulate maintenance via E-cadherin-mediated adhesion to niche cap cells, numbers of cap cells, and Notch signaling (Hsu and Drummond-Barbosa, 2009; Hsu et al., 2008; LaFever and Drummond-Barbosa, 2005).

Other examples of stem cell populations responding to systemic signals have been demonstrated, but are mechanistically unclear. NSCs in rats can respond to stroke-induced signals that lead to a proliferative response not only at the site of the stroke, but also at distant regions (reviewed in Drummond-Barbosa, 2008). This response depends on the presence of insulin-like growth factor-1, or IGF-1 (Yan et al., 2006). Other hormones also play key roles in regulating stem cells. Androgens and estrogens have stimulatory and pro-survival effects on adult neurogenesis (Spritzer and Galea, 2007; Tanapat et al., 1999).

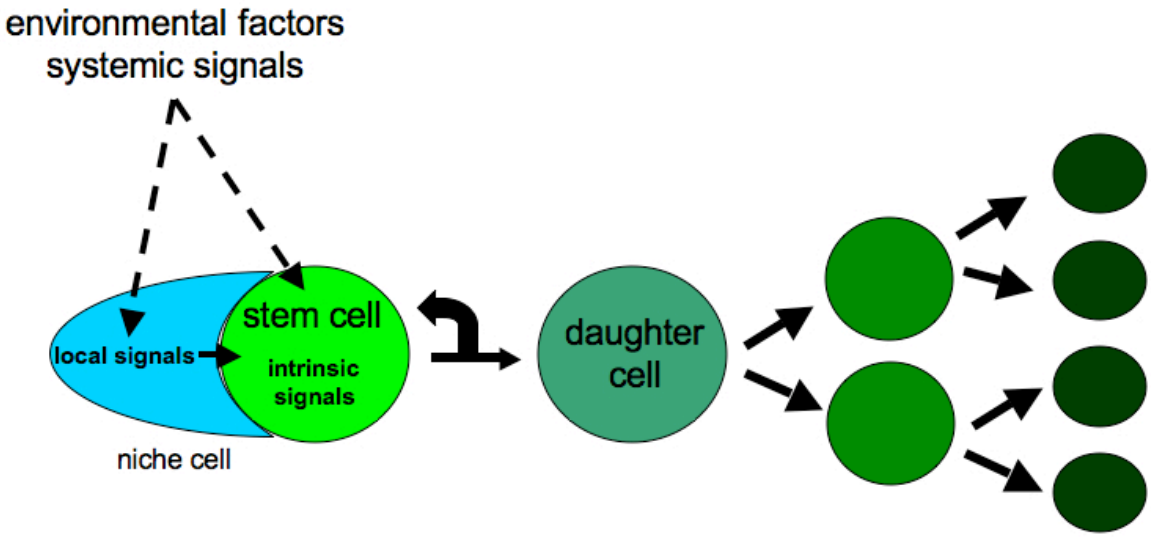

Figure 1.1. Adult stem cells respond to environmental factors, systemic signals and local signals via the niche. A stem cell divides to produce a daughter cell while also replacing itself. A daughter cell can undergo further transit amplifying divisions and produce differentiated progeny within a restricted lineage. Signals arising from stimuli such as injury, hormones, or dietary factors can be received either directly by a stem cell or indirectly via its niche. These extrinsic signals impinge upon stem cell intrinsic signals to regulate maintenance, growth, and proliferation.

Follicle-stimulating hormone (FSH) promotes glial cell-line-derived neurotropic factor (GDNF) expression, which, as previously mentioned, is secreted by niche cells to regulate mammalian testis GSC maintenance (Drummond-Barbosa, 2008). Dietary factors also regulate various stem cell populations. Dietary phosphate restriction decreases the proliferation rates of mesenchymal stem cells (MSCs) in neonatal pigs (Alexander et al., 2010). Diet may also play a role in adult hippocampal neurogenesis, which is supported by NSCs (Stangl and Thuret, 2009).

Many stem cell regulatory mechanisms appear to be evolutionarily conserved throughout metazoa, including the stimulatory effects of insulin signaling on stem cell proliferation and the role of the niche in repressing stem cell differentiation (Drummond-Barbosa, 2008). As such, further studies in organisms such as *Drosophila*, with its relatively simple ovarian stem cell biology, easily identified stem cell progeny, and particularly powerful genetic tools, holds much promise to further our understanding of the key mechanisms of mammalian stem cell regulation.

The *Drosophila* ovary, a model to study adult stem cell regulation

Ovarian cell biology

Due to its simple anatomy, molecular markers, and a linear arrangement between stem cells and their differentiated progeny, the *Drosophila* ovary is one of the premiere model systems for the study of stem cell regulation *in vivo*. In the *Drosophila* female, two ovaries are made up of fifteen to twenty individual ovarioles, or strings of progressively more mature follicles, held together by a muscle sheath (Figure 1.2A,B). The germarium is located at the anterior-most region of the ovariole (Spradling, 1993). Residing within

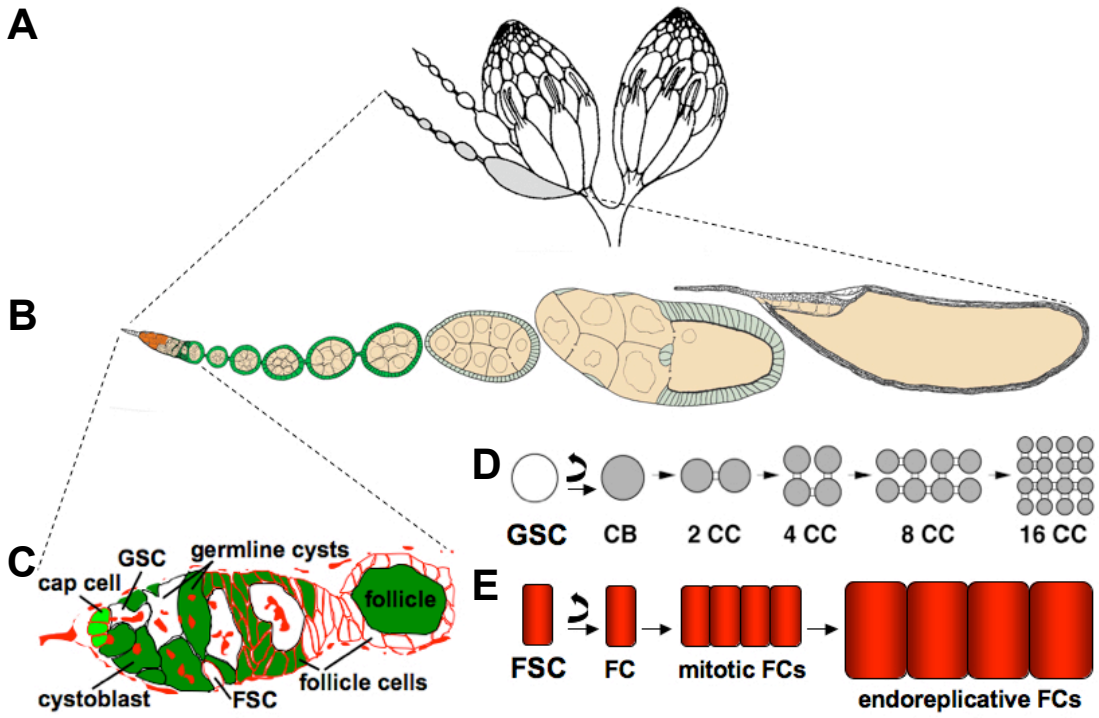

Figure 1.2. The *Drosophila* ovary. (A) A pair of ovaries is made up of individual subunits called ovarioles **(B)**. **(C)** The germarium, at the anterior of each ovariole, contains two populations of stem cells. GSC, germline stem cell. FSC, follicle stem cell. Cell membranes and fusomes are outlined in red. The progeny arising from a green GSC or FSC are marked in green. **(D)** A GSC divides to replace itself and produce a daughter cell that divides four times with incomplete cytokinesis to produce a sixteen cell-cyst (16 CC). CB, cystoblast. 2-16 cell-cyst, 2-16 CC. **(E)** A FSC divides to replace itself and produce a daughter cell that divides an additional 8-9 time to produce a mitotic follicle cell clone of about 650 follicle cells. Those cells switch to an endoreplicative program at stage seven of follicle development. FC, follicle cell.

the germarium are two populations of stem cells, the germline (GSCs) and follicle stem cells (FSCs), which give rise to all the cells within a follicle (Morrison and Spradling, 2008) (Figure 1.2C).

GSCs reside in a specialized microenvironment, or niche, made up of several different cell types, including escort cells, terminal filament cells, and cap cells (Figure 1.2C). Each germarium contains about two to three GSCs that can be identified both by their juxtaposition to niche cap cells and their stereotypical fusome morphology, a germline specific organelle that undergoes morphological changes with the GSC cell-cycle (de Cuevas and Spradling, 1998). A GSC divides four times with incomplete cytokinesis to form a 16-cell cyst connected by ring canals (Figure 1.2D). One of the two cells with four ring canals becomes the oocyte, while the remaining fifteen cells become nurse cells. Each cyst acquires a monolayer of follicle cells arising from the FSCs to form a complete follicle that then exits the germarium. The follicle grows and matures through seven pre-vitellogenic stages, then undergoes vitellogenesis, or yolk uptake, starting at stage eight. Rapid growth of the oocyte occurs throughout additional stages resulting in a mature stage fourteen egg (Spradling, 1993).

FSCs are located mid-way through the germarium. Lineage labeling experiments demonstrate that each germarium contains exactly two FSCs corresponding to the anterior-most Fasciclin III negative follicle cells in germarial region 2A/B that are also slightly larger than their daughters (Margolis and Spradling, 1995). A FSC mitotically divides to produce a daughter cell that forms a clone by further dividing eight to nine times up to stage six of follicle development (Nystul and Spradling, 2010) (Figure 1.2E). At stage seven, follicle cells switch to an endoreplicative cell cycle program consisting of

alternating G1 and S phases, resulting in the amplification of DNA necessary to support high levels of yolk and chorion protein secretion (Deng et al., 2001; Spradling, 1993).

Ovarian stem cells are regulated by local signals from the niche

As previously mentioned, the stem cell niche plays a major role in controlling stem cell behavior by producing factors necessary for stem cell maintenance. Communication between niche cells and stem cells has been studied in detail in the *Drosophila* ovary and systemic signals can impinge on the niche to modulate GSC behavior (Figure 1.3). Two of the major signals produced by the niche cap cells are Decapentaplegic (Dpp) and Glass bottom boat (Gbb), both vertebrate bone morphogenic protein (BMP) 2/4 homologs. BMPs are members of the transforming growth factor β (TGFβ) family, a family of proteins that elicit a broad range of cellular responses including repression of mammalian stem cell proliferation (Morrison et al., 1997). *Drosophila* BMPs are short-range signals that activate signaling through their receptors, thickveins (Tkv), saxophone (Sax), and punt (Put), to repress transcription of the differentiation factor, bag of marbles (Bam). Active BMP signaling is essential for GSC maintenance as loss of *dpp* or *gbb* results in GSC differentiation and overexpression of *dpp* blocks GSC differentiation (Xie and Spradling, 1998). In addition to BMPs, Hedgehog signaling and Piwi, both of which are regulated by Yb in the niche cells, are also required for GSC self-renewal and proliferation (Xie et al., 2008) (Figure 1.3).

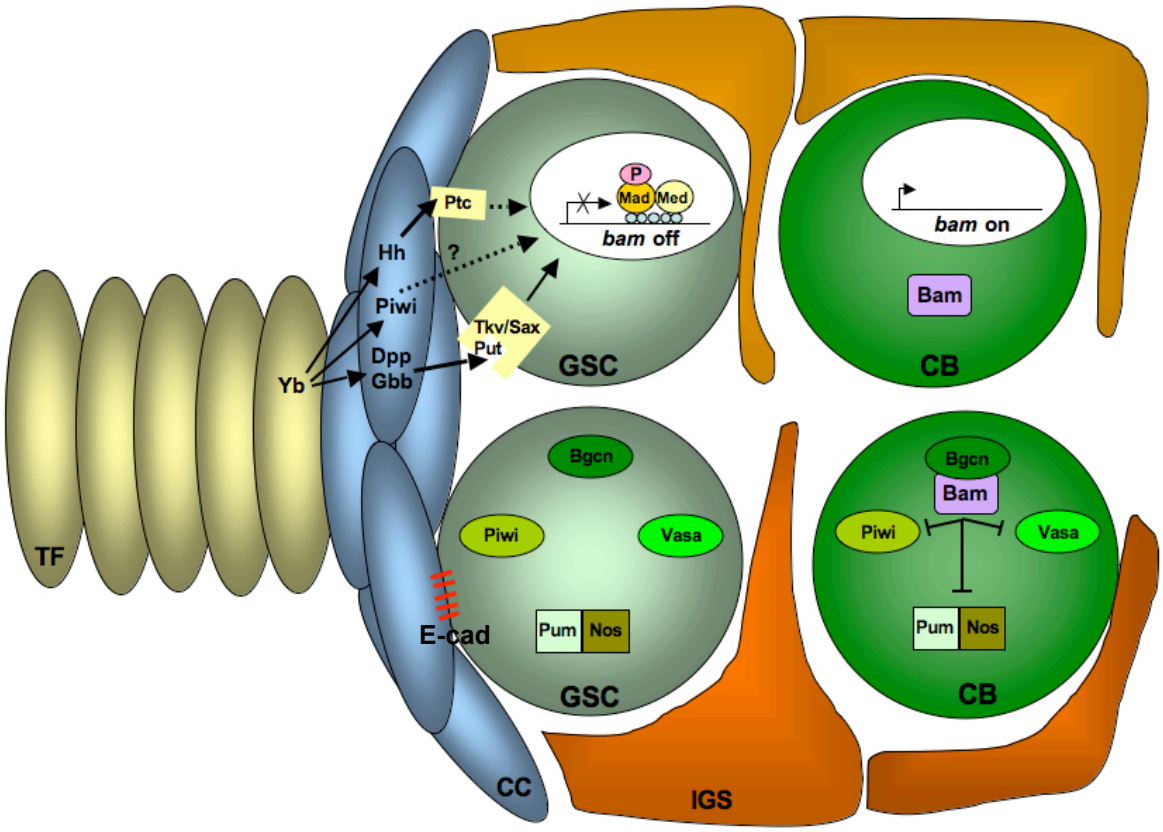

Figure 1.3. Regulation of GSCs via the niche. GSCs are maintained within the niche by E-cadherin (E-cad)-mediated adhesion (red lines between cap cells and GSC) and by niche cap cell secreted Dpp/Gbb-mediated repression of the differentiation factor *bam*. Cystoblasts, displaced from the niche, no longer receive the short-range Dpp/Gbb ligands so Bam is derepressed, forms a complex with Bgcn, and represses several intrinsic factors required for GSC identity. TF, terminal filament (gold). CC, cap cell (blue). GSC, germline stem cell (light green). CB, cystoblast (dark green). IGS, inner germarial sheath cells (orange). Figure modified from Wong et al., 2005.

GSC intrinsic factors

Intrinsic factors also regulate GSC activity and one class of GSC intrinsic factors are the chromatin remodeling factors, ISWI and Stonewall, which regulate different differentiation pathways that together allow for long-term GSC self-renewal (Xi and Xie, 2005). ISWI is an ATP-dependent chromatin remodeling factor proposed to regulate GSC maintenance by promoting the silencing of *bam* expression, while Stonewall exerts its effects on GSC maintenance by regulating the expression of the self-renewing factor nanos (nos). *nos* and other translational regulators including *pumilio (pum)*, *pelota (pelo)*, and *vasa (vas)* all inhibit GSC differentiation in a *bam*-independent manner (Zhang, 2009). Nos and Pum together form a complex that represses RNA translation of differentiation-promoting genes (Barker et al., 1992). Pelo is thought to degrade mRNAs for differentiation-promoting genes, while Vas serves as a germline-specific translation initiation factor. Piwi, a protein involved in the production of piRNAs, intrinsically regulates GSC proliferation (Cox et al., 1998). *bam* expression inhibits Piwi, Pum, Vas, and Nos activity in the displaced daughter cell, thus permitting differentiation (Figure 1.3) (Wong et al., 2005). Finally, Cyclin B also appears to have a role in GSC maintenance, suggesting that cell cycle control may be linked to self-renewal in GSCs (Zhang, 2009); however, studies from our lab indicate that insulin signaling mutant GSCs have altered cell-cycle profiles without an effect of their maintenance (described in a later section) so proliferation and maintenance can clearly be uncoupled under certain circumstances (Hsu and Drummond-Barbosa, 2009).

Nutrient-sensing pathways

Organisms must take in nutrients to provide energy and the building blocks for cell growth and proliferation. Whole body nutritional status is sensed and communicated at both the cellular and systemic levels. Nutrient-sensing evolved from the basic Target of rapamycin, or TOR, and AMPK signaling pathways found in single cell organisms such as yeast, to include the insulin/IGF signaling pathway, which relays systemic information on whole body nutritional status in multicellular organisms. Together these pathways make up a highly sophisticated network, providing multiple layers of regulatory mechanisms that couple cell growth and proliferation to the demands of an organism (Hietakangas and Cohen, 2009). While the importance of nutrition in stem cell regulation appears obvious, stem cell nutrient-sensing mechanisms are just beginning to be elucidated.

Insulin signaling

The insulin signaling pathway plays key roles in growth, metabolism, stress resistance, lifespan, and reproduction. When vertebrates feed, secretion of insulin from the pancreas results in systemic insulin pathway activation in peripheral tissues, resulting in glucose uptake, energy storage, and increased cellular growth and proliferation (Jensen and De Meyts, 2009). The importance of proper systemic insulin signaling regulation is underlined by the damage caused to multiple organ systems from Type I and II Diabetes, diseases characterized by the autoimmune destruction of pancreatic β-cells and long-term resistance to circulating insulin, respectively.

In *Drosophila*, the orthologs for mammalian insulin are called *Drosophila* insulin-like peptides, or DILPs (Brogiolo et al., 2001). There are seven *dilps* with specific spatio-

temporal expression patterns, which suggests the ligands may have functional differences (Ikeya et al., 2002). Recent analysis of single and combinatorial *dilp* null mutations show, however, that DILPs can act redundantly, synergistically, and can even compensate for reduced expression of other DILPs (Gronke et al.). DILPs are secreted upon feeding by a mechanism involving signaling from the fat body (Geminard et al., 2009) and they bind and activate a single insulin receptor in *Drosophila*, dInR, that combines the roles of both the mammalian insulin and IGF receptors (Yenush et al., 1996). The *Drosophila* IRS1-4 ortholog, *chico*, binds activated dInR and serves as a link to the PI3K and Ras/MAPK branches of the insulin signaling pathway (Bohni et al., 1999; Oldham et al., 2002). The PI3K branch leads to activation of Akt kinase and subsequent inhibition of the transcription factor FOXO, a negative regulator of the insulin signaling pathway. Inhibition of FOXO increases rates of cellular proliferation (Junger et al., 2003; Kramer et al., 2003; Puig et al., 2003). Akt also feeds into the Target of rapamycin (TOR) signaling pathway (see next section) leading to an increase in protein translation and cell growth.

Target of rapamycin (TOR) signaling

TOR kinase

TOR is a serine/threonine kinase and the founding member of the phosphoinositol kinase-related kinase (PIKK) family. It is a large protein of 2549 amino acids and is divided into several domains. These include a series of tandem HEAT repeats, that contribute to interactions with other regulatory proteins; a conserved, but functionally undefined FAT domain; an FRB domain necessary for the sensitivity of TORC1 to

rapamycin; a kinase domain; and a FATC domain that is thought to couple TOR stability to the redox state of the cell (Figure 1.4) (Hay and Sonenberg, 2004).

TOR was identified in yeast as the Target of Rapamycin, an antifungal agent purified from *Streptomyces hygroscopicus*. Rapamycin treatment of the budding yeast *Saccharomyces cerevisiae* leads to *TOR1* and *TOR2* dependent growth inhibition. Yeast TOR homologs have since been identified in fungi, plants, and animals, demonstrating a high level of conservation (Inoki et al., 2005). Indeed, the entire TOR signaling network is highly conserved in eukaryotes and consists of phosphotidylinositol 3 kinase (PI3K), Phosphatase and tensin homolog (PTEN), the serine/threonine-protein kinase Akt, 5'-AMP-activated protein kinase (AMPK), Tuberous sclerosis protein 1 and 2 complex (TSC1/2), Regulatory-associated protein of TOR (Raptor), Rapamycin-insensitive companion of TOR (Rictor), eukaryotic translation initiation factor eIF4e binding protein (4E-BP), and ribosomal protein S6-p70-protein kinase (S6K). Intriguingly, TSC1/2, which inhibits TOR activity and serves as a major point of convergence between nutrient-sensing pathways, appears to have evolved last and is present only in unikonts (eukaryotic cells with one or no flagellum (Serfontein et al., 2010). Each member of the TOR signaling network will be discussed in further detail later.

TOR forms two functional complexes: TORC1 and TORC2. The nutritionally-insensitive complex TORC2 includes the protein Rictor, has roles in cytoskeletal dynamics and can phosphorylate Akt at an insulin-independent site to further activate TORC1 (Figure 1.5). The nutritionally and rapamycin-sensitive TORC1 includes Raptor and has major roles in promoting cell growth by regulating protein translation rates

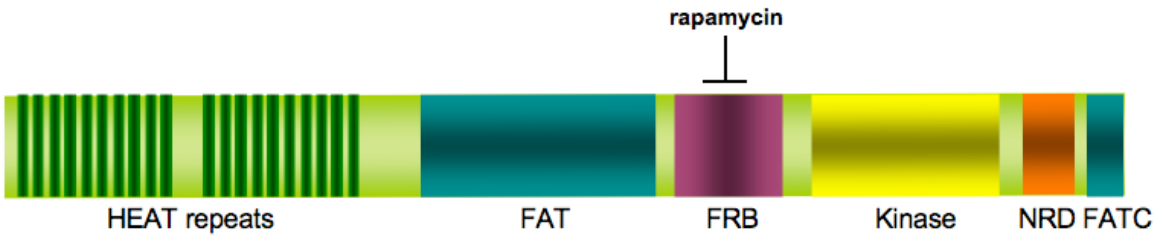

Figure 1.4. TOR protein domains. HEAT repeats contribute to interactions with other TOR regulatory proteins. The FAT domain is conserved, but functionally undefined. The FRB domain confers rapamycin sensitivity. The serine/threonine kinase domain is required for TOR kinase activity. Phosphorylation of the negative regulatory domain, or NRD domain can lead to increased TOR activity. The FATC domain that is thought to couple TOR stability to the redox state of the cell. Figure modified from Hay and Sonenberg, 2004.

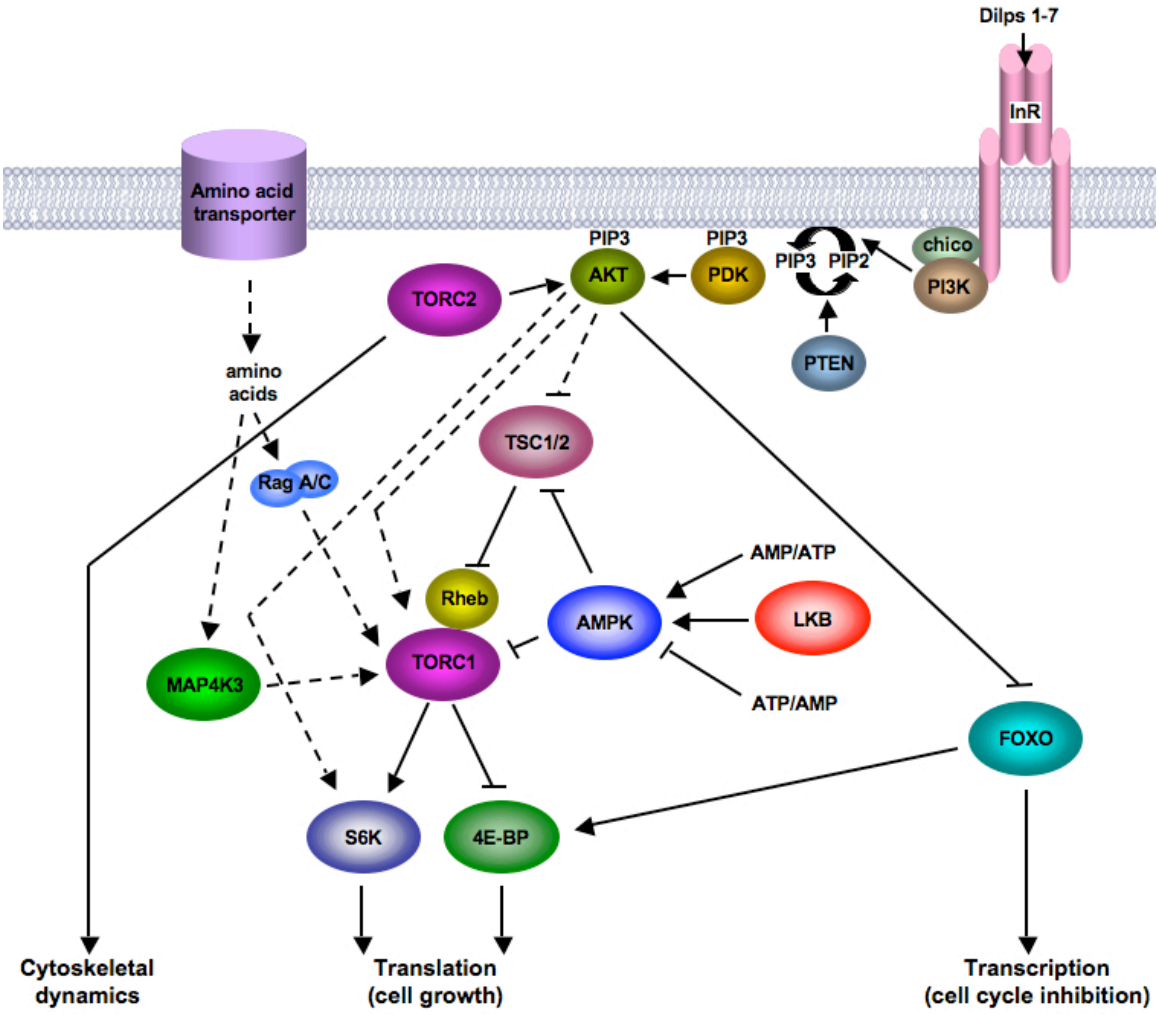

Figure 1.5. TOR receives nutritional inputs from multiple sources. Energy, nutrient, and hormone/mitogen signals are integrated at the level of TOR kinase. AMPK is activated under low ATP conditions and acts to inhibit TOR. Amino acids are sensed via an unclear mechanism involving Rag proteins and MAP4K3 and stimulate TOR activity. Insulin signaling is sensed at the level of TSC1/2, S6K, or TOR itself. Together these pathways coordinate rates of cell growth, survival, and proliferation to the nutritional status of the organism.

(Liao et al., 2008). The remainder of this introduction will focus on TORC1, which is more relevant to the topics of this thesis.

TOR complex 1 regulation

Multiple inputs, including insulin signaling, energy levels, amino acids, cellular stresses, and even hormones, act both cooperatively and independently to modulate TORC1 activity (Figure 1.5). For instance, full activation of the TOR kinase by insulin requires amino acids, but the presence of amino acids in a cell culture can activate TOR even in the absence of growth factor signaling (Liao et al., 2008).

Amino acid regulation of TOR requires both Rheb, a Ras-related GTP-binding protein that interacts with and activates TORC1, and the Rag GTPases, which are also members of the Ras family of GTP-binding proteins. The mechanism by which amino acids stimulate TOR activity is unclear. One study demonstrated that amino acids trigger the release of intracellular Ca^{2+} and activates human vacuolar protein sorting 34 (hVps34), a lipid kinase that targets phox homology (PX) domain-containing proteins to early endosomes where TOR is present (Gulati et al., 2008). More recently, it was demonstrated in mammalian cell culture that a trimeric complex of proteins, coined the "Ragulator", forms in response to amino acids and localizes Rag proteins to the surface of lysosomes to form a docking site for TOR. Rheb then is proposed to activate TOR, but whether endogenous Rheb is actually localized on endosomes is unclear (Sancak et al., 2010). It remains unclear whether these mechanisms occur *in vivo*. For instance, loss of the single *Drosophila Vps34* ortholog does not alter TOR signaling, suggesting Vps34 does not act upstream of TOR in *Drosophila* (Juhasz et al., 2008).

Amino acid independent stimuli, including AMPK activity, insulin, and hormones are thought to regulate TOR activation at the level of TSC1/2. TSC2, also known as tuberin in mammals, is a GTPase-activating protein that inactivates Rheb, and, thereby inhibits TOR activity. TSC1, or hamartin, is required for the localization and stability of TSC2; therefore, loss of either TSC1 or 2 leads to TOR hyperactivation and tissue overgrowth (Catania et al., 2001). In humans, benign tumor growth is a characteristic of Tuberous Sclerosis, a genetic disorder caused by a mutation in either *Tsc1* or *Tsc2*.

Proper ATP/AMP ratios are maintained to support the energy requirements of a cell. AMPK is activated by AMP, the end product of ATP hydrolysis, and AMPK then phosphorylates and activates TSC2. Enhanced TSC2 activity reduces TOR activity under energetically unfavorable conditions (Inoki et al., 2003). TOR activity is also modulated by direct AMPK-mediated phosphorylation of the TORC1 component, Raptor (Gwinn et al., 2008).

Insulin is thought to regulate TOR activity by Akt-mediated phosphorylation of TSC2 on numerous sites, resulting in the inactivation of the complex and release of TOR suppression (Pan et al., 2004). However, there are inconsistencies regarding this simplistic model. For instance, in *Drosophila*, TSC2 Akt-specific phosphorylation mutants are viable, fertile, and exhibit normal body size and growth rates, suggesting that Akt-mediated TSC2 phosphorylation may not be functionally important for Akt-mediated growth (Dong and Pan, 2004; Schleich and Teleman, 2009). Other genetic data support a model wherein insulin activates TOR in parallel to TSC1/2 (Pan et al., 2004). Several potential models have been proposed to explain these results. One group identified *Drosophila* Melted, a conserved PH-domain protein that sequesters the TSC1/2 complex

and the FOXO transcription factor at the cell membrane upon insulin signaling activation and leads to increased TOR activity by inhibition of negative regulators of TOR (Teleman et al., 2005b). Insulin signaling may also directly regulate S6K activity, a downstream effector of TOR, in a TOR-independent manner. Support for this idea comes from a study showing that expression of a mutant form of S6K that cannot associate with TOR leads to cellular resistance to rapamycin treatment but maintained responsiveness to insulin pathway inhibitors (Inoki et al., 2005).

In mammals, hormones can also regulate TOR activity. Both Prostaglandin F2α and Follicle Stimulating Hormone (FSH) stimulate Akt phosphorylation and inhibit TSC2 in luteal and granulosa cells of the ovary, respectively, thus activating TOR and is downstream effectors (Arvisais et al., 2006; Kayampilly and Menon, 2007).

TOR effectors

The Raptor component of TORC1 contains a TOR signaling motif, or TOS, which serves as a docking site for proteins to associate with TOR (Schalm and Blenis, 2002). TOS motifs are found in all known TOR substrates, including both 4E-BP and S6K. One of the main roles for TOR is the regulation of protein translation. Both 4E-BP and S6K regulate translation of a specific group of mRNAs that contain 5'-terminal oligopyrimidine tracts and encode ribosomal proteins and translation elongation factors. 4E-BP competes with the eukaryotic initiation factor 4G, or eIF4G, for binding to eIF4E and prevents the assembly of the eIF4F complex. TOR-mediated phosphorylation of 4E-BP inhibits binding to eIF4E and relieves repression of translation. Phosphorylation by TOR activates S6K and increases translation rates by controlling the phosphorylation

status of a number of downstream translational components (Hay and Sonenberg, 2004). In mammalian cell culture, the three 4E-BPs control cell proliferation while S6K1 and S6K2 control growth, but this uncoupling of growth and proliferation does not appear to be conserved in *Drosophila* (Dowling et al., 2010).

d4E-BP and dS6K mutations in *Drosophila* have been characterized. Loss of dS6K results in a severe body size reduction, resulting from a decrease in cell size but not number. Increased dS6K activity in *dTor* hypomorphic mutants rescues growth, strongly suggesting dS6K is the major growth mediator downstream of dTOR. In agreement with S6K as the major TOR-dependent growth effector, loss of d4E-BP has no effect on cell size or number in *Drosophila* and adult mutants have only mild metabolic defects. Ectopic overexpression of a hyperactivated form of d4E-BP, however, leads to reduced cell size (Miron and Sonenberg, 2001).

TOR control of cell death and autophagy

In addition to regulating rates of translation and, thus, cell growth, TOR activity has been linked to other cellular and metabolic processes, including autophagy, apoptosis, fat storage, feeding behavior, cell-cycle regulation, and aging (Arsham and Neufeld, 2006; Diaz-Troya et al., 2008; Wang and Proud, 2009). Here I will present an overview of the role of TOR in cell death, while metabolic and cell-cycle regulatory roles for TOR are discussed in later sections.

When nutrients are severely low, eukaryotic cells activate a process called macroautophagy, a “self-eating” mechanism whereby proteins, organelles, and cytoplasm are broken down in intracellular structures called autophagosomes for use as a nutrient

source. Autophagy is controlled by a group of conserved autophagy-related (Atg) proteins, one of which TOR has been demonstrated to suppress. In yeast, TOR phosphorylates Atg13 and inhibits the formation of a protein kinase complex consisting of Atg1, Atg13, and Atg17, which are among the earliest acting Atg components in the signaling cascade (Chang et al., 2009).

An additional way TOR may regulate autophagy is via Vps34. As mentioned earlier, mammalian Vps34 activates TOR signaling in an amino acid dependent manner. A null mutation of *Drosophila* Vps34 blocks larval starvation-induced autophagy. This study and others demonstrate that Vps34 is involved in early autophagosome formation. The seemingly conflicting roles of Vps34 to both activate TOR and to promote autophagy might be explained by different functional pools of Vps34 within the cell, but this has not yet been demonstrated (Chang et al., 2009).

Some autophagy is necessary to promote cell survival, but excessive autophagy can promote cell death. One way TOR modulates autophagy activity is via S6K. Again, this seems to be a conflicting role for S6K, which is also promotes cellular growth. One explanation may be that the coupling of a positive and negative autophagy regulator within a single pathway could serve in a negative feedback loop allowing for the magnitude of autophagy stimulation caused by reduced TOR activity to be limited by reduced S6K activity downstream of TOR (Chang et al., 2009).

TOR also signals to inhibit apoptosis, a second and distinct type of cell death from autophagy. Apoptosis can be triggered by induction of p53, which is suppressed by insulin signaling (Trotman and Pandolfi, 2003). In mouse embryonic hepatocytes, the effect of

PI3K on the inhibition of p53 is mediated by TOR, which promotes the translation of the p53 negative regulator, Mdm2 (Moumen et al., 2007).

AMP-activated protein kinase signaling

AMP kinase

This section briefly reviews the role of AMP-activated protein kinase, or AMPK, as an energy sensor. Although no experiments involving AMPK were performed in this thesis project, AMPK is an important upstream regulator of the TOR signaling pathway and a demonstrated downstream mediator of adipokine signaling in mammals, which will be introduced later (Marshall, 2006).

AMPK is a serine-theronine kinase that acts as a cellular energy sensor. Its activity increases with cell stress, especially those stresses that lower ATP and increase AMP levels within a cell. AMPK is a heterotrimeric protein with three highly conserved subunits: two regulatory subunits, β and γ, and a catalytic subunit, α. In mammals, two or three different isoforms exist for each AMPK subunit, resulting in twelve different combinations of AMPK trimers that appear to provide tissue specificity (Canto and Auwerx, 2010). In *Drosophila* each subunit has a single isoform; therefore, mutation of a single gene eliminates AMPK activity (Williams and Brenman, 2008).

AMPK regulation

The basic mechanism for the activation of AMPK involves the binding of either ATP or AMP to the γ subunit of the AMPK complex. ATP binding maintains AMPK enzyme activity low while the replacement of ATP with AMP promotes a mild activation

of the kinase through an allosteric mechanism. This exchange also renders AMPK a poorer substrate for phosphatases, resulting in a greater than 1000 fold increase in enzyme activity. Maximum activity occurs, however, when AMPK is phosphorylated (Canto and Auwerx, 2010).

The best characterized upstream activating kinase for AMPK is the LKB1 serine-threonine kinase. LKB1 acts as a master kinase for all thirteen members of the AMPK-related kinase family so AMPK activation specificity must be obtained through additional mechanisms (Canto and Auwerx, 2010). Additional upstream AMPK kinases (AMPKKs) are thought to modulate AMPK activity, including calmodulin-dependent protein kinase kinase (CaMKK) and possibly the ATM serine-theronine kinase. In addition to AMPK regulation by kinases, studies in yeast have shown that phosphatase activity toward AMPKα is important for determining net AMPK activity (Williams and Brenman, 2008).

AMPK effectors and regulated cellular processes

As previously mentioned, AMPK phosphorylates TSC2 and raptor, leading to TORC1 inhibition, reduced protein metabolism and increased cellular autophagy (Figure 1.5) (Gwinn et al., 2008; Inoki et al., 2003; Lippai et al., 2008). In addition, AMPK activation stimulates glucose uptake in skeletal muscle via GLUT4 translocation to the plasma membrane, increases transcription of genes involved in ATP production and the use of lipids as energy, decreases glycogen synthesis rates, and promotes fatty acid oxidation to increase ATP levels. These roles for AMPK allow a cell to sense and respond to low ATP levels by mobilizing energy stores and priming the cell to quickly respond to nutrients when they again become available (Canto and Auwerx, 2010).

In *Drosophila*, loss of AMPK results in small larvae with reduced fat storage levels and early larval lethality. Interestingly, AMPK has been demonstrated to be a non-cell autonomous regulator of cell growth—i.e. growth defects in the mutant larvae are due to dysfunctional peristaltic activity resulting in decreased food intake. Indeed, transgenic restoration of dAMPKα to *dAMPKα* mutant visceral musculature restores gut function and organismal/systemic growth (Bland et al., 2010). Other studies have uncovered roles for AMPK in the regulation of cell polarity during energy stress in the embryonic cuticle, ovarian follicular cells, and in neurons (Lee et al., 2007; Mirouse et al., 2007). AMPK activates non-muscle regulatory light chain (MRLC) and expression of an active form of MRLC rescues the epithelial cell polarity defects caused by AMPK loss in *Drosophila* embryonic cuticle. This mechanism appears to be conserved in mammalian cells as AMPK activation induced by energy deprivation can polarize and induce a brush border formation in an unpolarized epithelial cell line, LS174T. (Lee et al., 2007).

Cell-cycle regulation by nutrient-sensing pathways

Cell growth and division are normally coordinated to ensure that a cell does not divide until it reaches a critical size. Nutrients affect both of these cellular processes and can regulate cell division indirectly via growth and directly via modulation of cell-cycle regulators (Wang and Proud, 2009). In this section I will review the dietary control of cell-cycle progression.

Mitotically dividing cells follow a four phase program: G1 (Growth phase 1), S (DNA replication), G2 (Growth phase 2), and M (mitosis, or cell division) (Figure 1.6). The G1/S and G2/M transitions are driven by Cyclin/Cdk complexes, which are

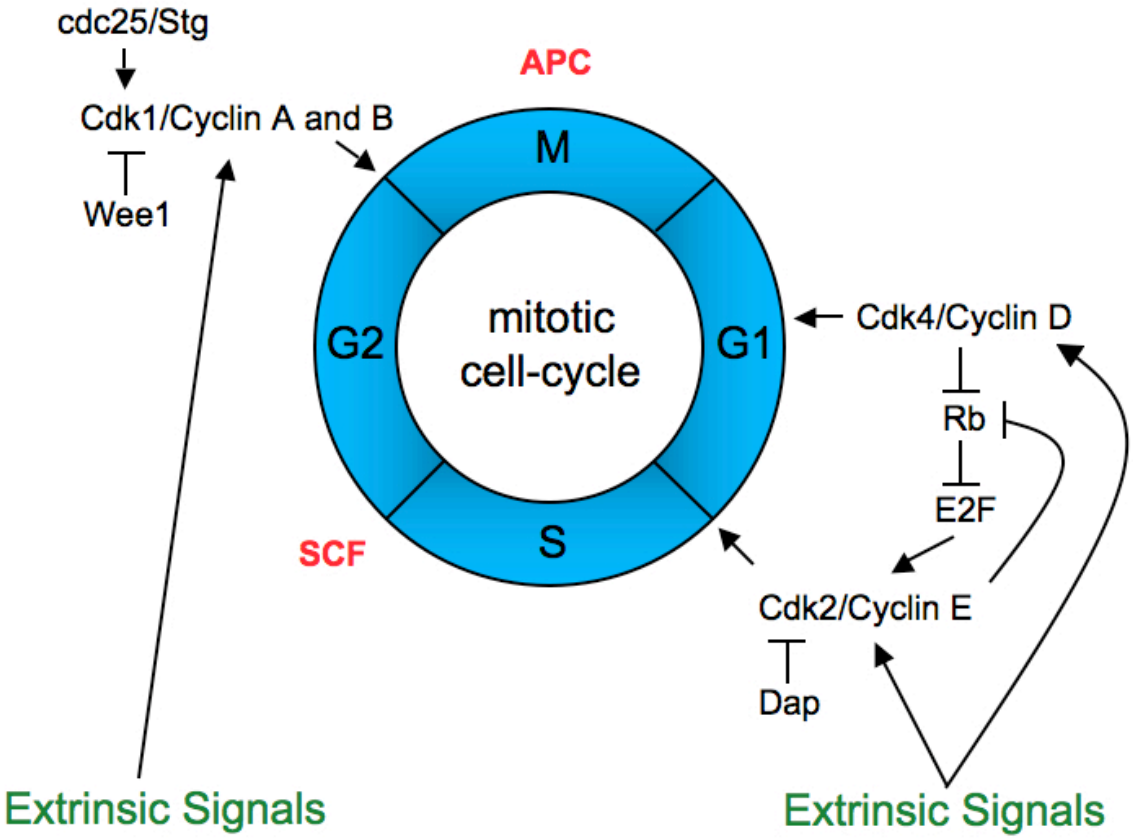

Figure 1.6. The *Drosophila* mitotic cell-cycle. The mitotic cell cycle is driven by Cyclin A and B at the G2/M transition and by Cyclin D and E at the G1/S transition. Extrinsic signals impinge upon the cell cycle at both G1/S, the historical "nutrient-checkpoint", and also at G2/M by an unclear mechanism. Cdk, cyclin-dependent kinase. Rb, retinoblastomia. Dap, Dacapo, the *Drosophila* p21/p27 homolog. Stg, String, the *Drosophila* cdc25 homolog. The APC degrades mitotic cyclins. The SCF degrades G1/S cyclins.

downregulated by SCF (Skp, Cullin, F-box containing complex) in G1/S and the APC (anaphase promoting complex)-mediated proteolytic degradation in G2/M (Lee and Orr-Weaver, 2003). In many cell types a major nutrient checkpoint occurs during G1 to prohibit entry into S-phase until the cell reaches critical mass (Lee and Orr-Weaver, 2003). Extrinsic signals, including growth factors, activate the Cdk2/Cyclin E and Cdk4/Cyclin D complexes. Both complexes drive the G1/S transition by phosphorylating Retinoblastoma (Rb) a protein that binds and inhibits the transcription factor E2F. Free E2F transcribes genes encoding DNA replication proteins necessary for S-phase and even Cyclin E itself, which is involved in a feed-forward mechanism to maintain E2F activity (Lee and Orr-Weaver, 2003). Recent evidence suggests the G2/M transition also responds to dietary inputs. Fission yeast, for example, have two known nutrient checkpoints at both the G1/S and G2/M transitions (Shiozaki, 2009) and budding yeast are delayed at G2 when placed in a nitrogen-free medium, a phenotype that had been previously masked by the G1 nutrient-dependent arrest (Nakashima et al., 2008).

TOR and the cell-cycle

It is well known that treatment of cells with rapamycin, an inhibitor of TORC1, leads to a G1 delay or cell cycle exit in many cell types. Studies have also shown that TOR regulates the G1/S transition by modulating the expression of G1/S phase regulators, including p27, p21, and Cyclins (Wang and Proud, 2009). More recently, roles for TOR at other stages of the cell-cycle have been uncovered, including those at the G2/M transition. In budding yeast, a G2 delay due either to a temperature sensitive TORC1 component or by treatment with rapamycin can be rescued by overexpression of the yeast polo-like

kinase (Cdc5). It was proposed that TORC1 may be required for the nuclear translocation of Cdc5 that is necessary for mitotic entry (Nakashima et al., 2008). In mammalian cells, TOR seems to regulate G2/M progression via its effect on Cdk1/Cyclin B activity, albeit by an unknown mechanism (Smith and Proud, 2008). Clues may lie in the effects of TSC1/2, the upstream TOR negative regulator complex, on G2/M progression. *Drosophila Tsc2* mutant cells fail to progress from G2 to M and instead undergo cycles of endoreplication (amplification of DNA without mitosis). It was observed that Cyclin A and B fail to move into the nucleus in these cells so mitotic progression cannot occur (Ito and Rubin, 1999). An interaction between mTSC1, or hamartin, and mTSC2, or tuberin, with CDK1 (which is responsible for nuclear transport of Cyclins B and A) further suggest a direct role for TSC1/2 in cell-cycle progression (Catania et al., 2001). Whether or not this role for TSC1/2 is TOR-dependent or -independent is still unknown.

Insulin and the cell-cycle

Roles for insulin signaling on cell-cycle progression have also been demonstrated. Treatment of *Drosophila* cell culture with insulin delays G2/M progression and speeds G1/S progression, a phenotype potentially explained by elevated TOR activity (Wu et al., 2007). Insulin can also regulate the cell-cycle by inhibiting the transcription factor FOXO, a downstream negative regulator of cell proliferation. In mammalian cells, increased FOXO activity due to poor nutritional conditions leads to a G1 arrest via increase of p27 levels and a G2/M delay via decreased Cyclin B and Polo-like kinase levels (Burgering and Kops, 2002).

Drosophila ovarian stem cells and their progeny respond to diet

The ovarian response to diet

The *Drosophila* ovary is highly responsive to diet. On a rich diet (molasses, agar, and wet yeast paste) egg production is 60-fold higher than on a poor diet (molasses and agar only) (Figure 1.7A) (Drummond-Barbosa and Spradling, 2001). While most of the egg production difference is due to a vitellogenenic block at stage eight of follicle development and early cyst death in region 2A/B of the germarium, there is a four-fold reduction in rates of GSC division and follicle growth (Drummond-Barbosa and Spradling, 2001) (Figure 1.7B). Loss of the IRS homolog in *Drosophila*, *chico*, results in an inability to upregulate rates of ovarian proliferation on a rich diet, implicating insulin signaling in the ovarian response to diet (Figure 1.7C).

The role of insulin signaling in the regulation of germline stem cells and their progeny

As a technician in the Drummond-Barbosa laboratory from 2003-2005, I further investigated the role of insulin signaling in *Drosophila* oogenesis. I found that brain-DILP producing cells are required for the ovarian response to diet. I also found that germline loss of *dInR* reduces GSC proliferation rates, delays follicle growth, and fails to progress through vitellogenesis, indicating DILPs are directly received by GSCs and their progeny in response to diet (Figure 1.8) (LaFever and Drummond-Barbosa, 2005). Dr. Hwei-Jan Hsu, a former postdoctoral trainee in our laboratory, analyzed the role of insulin signaling on the GSC cell-cycle. She demonstrated that GSCs in *dInR* and *chico* mutant flies fed a rich diet had a longer G2 phase that could be suppressed by removing *dFOXO*, a negative downstream regulator (Hsu et al., 2008). Dr. Hsu also demonstrated that GSCs

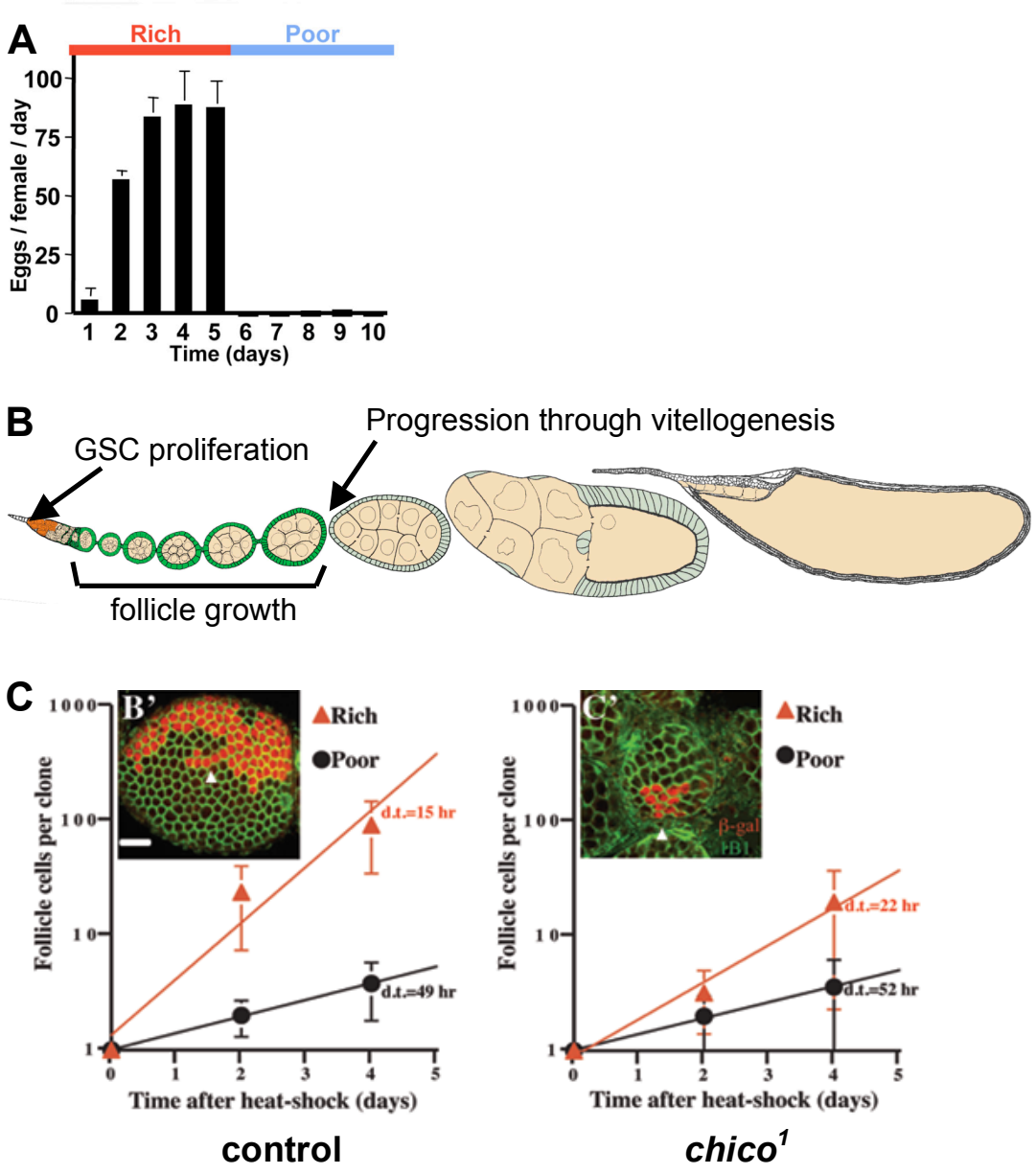

Figure 1.7. The ovarian response to diet. (A) Egg production is 60-fold higher on a rich versus a poor diet (Drummond-Barbosa and Spradling, 2001). **(B)** Diet regulates oogenesis by controlling GSC proliferation, follicle growth, and progression through vitellogenesis. **(C)** *chico* mutant flies are unable to upregulate rates of oogenesis in response to diet (Drummond-Barbosa and Spradling, 2001).

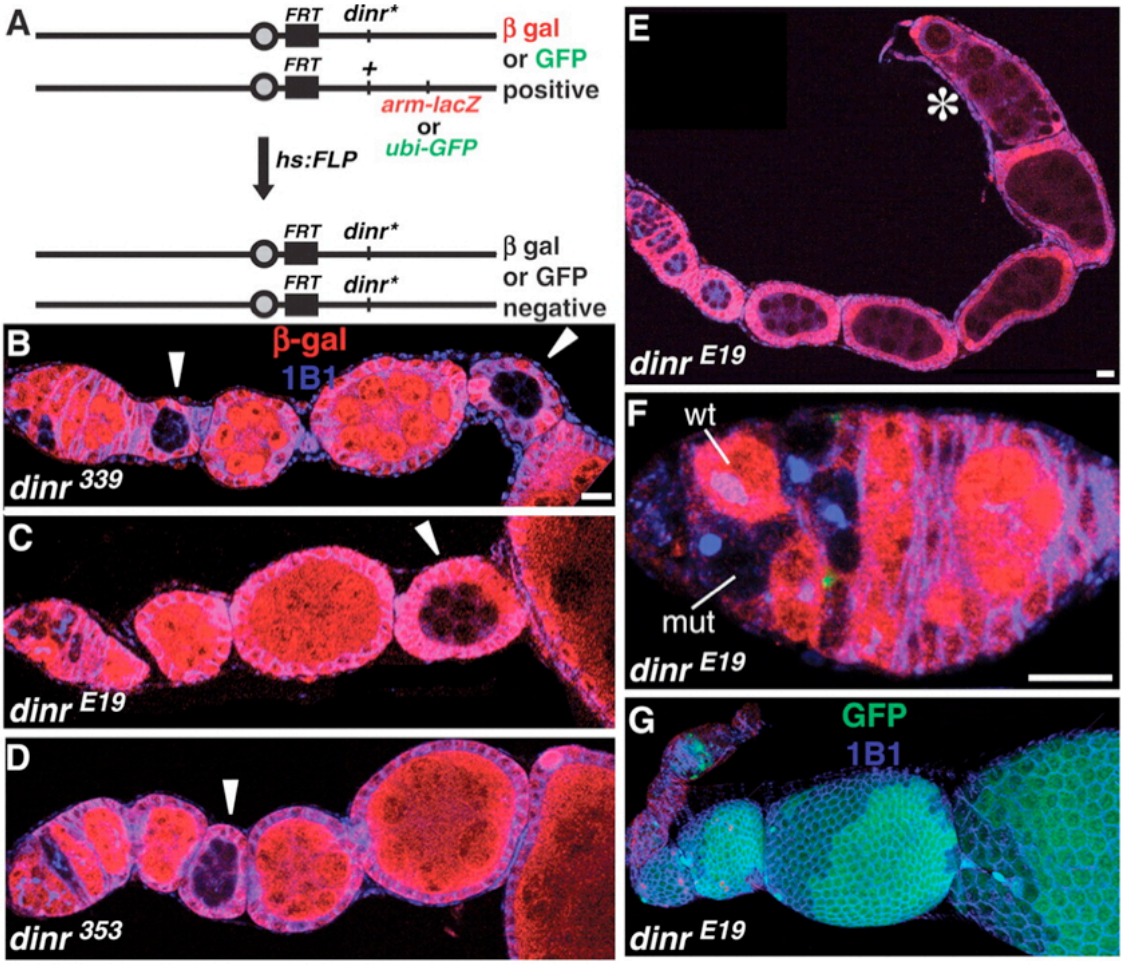

Figure 1.8. *dinr* is cell-autonomously required in the germ line for normal rates of GSC division, cyst development, and progression through vitellogenesis. (A) The *FLP/FRT* technique was used to generate mosaic ovarioles containing *dinr* homozygous mutant cells in the context of nearby heterozygous tissue. Flies carrying a wild-type *dinr* allele (+) in trans to a mutant or control *dinr* allele (*dinr**) were heat-shocked (hs) to induce FLP-mediated recombination between the FRT sites. Stem cell–derived *dinr* homozygous mutant clones were recognized by the absence of ß-gal or green fluorescent protein (GFP) markers. (B to D) Homozygous (B) $dinr^{339}$, (C) $dinr^{E19}$, and (D) $dinr^{353}$ germline cysts (arrowheads) are developmentally delayed relative to heterozygous control cysts. (B), (C), and (D) are shown at the same magnification. (E) Ovariole containing a germ line that is a fully $dinr^{E19}$ homozygous mutant (and surrounded by wild-type follicle cells), showing a degenerating egg chamber (asterisk) that has failed to undergo vitellogenesis. (F) Example of mosaic germaria used to determine the relative division rate of $dinr^{E19}$ homozygous mutant (mut) and control (wt) GSCs. (G) Mosaic ovariole showing similar numbers of homozygous $dinr^{E19}$ mutant (GFP-negative) and control (GFP-positive) follicle cells. 1B1 antibodies (blue) highlight cell membranes, whereas antibodies to ß-gal (red) or GFP (green) mark control cysts. (E) and (G) are shown at the same magnification. Scale bars, 10 µm. (LaFever and Drummond-Barbosa, 2005)

have an atypical Cyclin E cell-cycle expression pattern. In most cells, Cyclin E acts as a G1/S marker. Its levels increase throughout G1 and drop off during early S-phase (Ekholm et al., 2001). In GSCs, Cyclin E is present throughout G2 and M phases as well (Hsu et al., 2008). Mammalian embryonic stem cells also have Cyclin E expression throughout their cell-cycle and a very short G1 phase (Fluckiger et al., 2006). Interestingly, *C. elegans* GSCs are also delayed in G2 under low insulin signaling conditions (Michaelson et al., 2010) as are male *Drosophila* GSCs (Ueishi et al., 2009). It is possible that GSCs respond to dietary inputs (e.g., insulin signaling) at the level of G2 due to inherent differences in their cell-cycle, resulting in a very short or perhaps absent G1 phase. Our results disagree with another study reported that insulin signaling regulates G1 in ovarian GSCs via microRNAs (Hatfield et al., 2005). The conclusions were based, however, on using Cyclin E as a G1 marker, largely invalidating their findings.

Insulin signaling in the niche regulates GSC maintenance non-cell autonomously. DILPs are received directly by the cap cells and signal through the InR/PI3K pathway to regulate both cap cell-GSC attachment (via E-cadherin) and cap cell number (via Notch signaling). Interestingly, as flies age, insulin signaling activity goes down--correlating with GSC loss over time. Providing aged flies with elevated levels of DILPs can suppress the normal GSC loss associated with aging (Hsu and Drummond-Barbosa, 2009). Together these results indicate that GSCs both directly and indirectly sense and respond to insulin signals for the proper regulation of their maintenance and proliferation.

Additional factors contribute to the dietary regulation of GSCs

Evidence from our laboratory suggests that factors in addition to DILPS regulate the *Drosophila* ovarian response to diet. First, overexpression of *DILP2*, while increasing both the total body size of the flies as previously reported (Brogiolo et al., 2001) and the total number of eggs produced on a rich diet, does not increase egg production on a poor diet (see Figure 1.9A). Expression of other adult DILPs, *DILP3* and *DILP5*, also fails to rescue the ovarian response to a poor diet (data not shown). This suggests that DILP levels are limiting when nutrients are abundant, but cannot bypass the response to a poor diet.

DILPs control GSC division rates primarily by modulation of the G2 phase of the cell-cycle, while diet regulates the GSC cell-cycle at both G1 and G2 phases (Hsu et al., 2008; LaFever and Drummond-Barbosa, 2005) (Figure 1.9B). We also know that insulin signaling is not the only moderator of G2 in GSCs. Dr. Hsu's work clearly demonstrates that the G2 delay associated with an *InR* or *chico* mutation can be rescued by loss of the downstream negative regulator, *dFOXO*, but only on a rich diet. This indicates that either additional unidentified factors repress G2 on a poor diet and/or that G2 stimulatory factors are absent on a poor diet. The mechanism leading to a lengthened GSC G1 phase in response to a poor diet is also unknown (Hsu and Drummond-Barbosa, 2009).

Finally, we have evidence that nutritional history affects cyst growth and follicle cell proliferation rates. Females raised on a rich diet then switched to a poor diet maintain higher ovarian proliferation rates than those raised and continuously maintained on a poor diet (Drummond-Barbosa and Spradling, 2001) (Figure 1.9C,D). This finding suggests

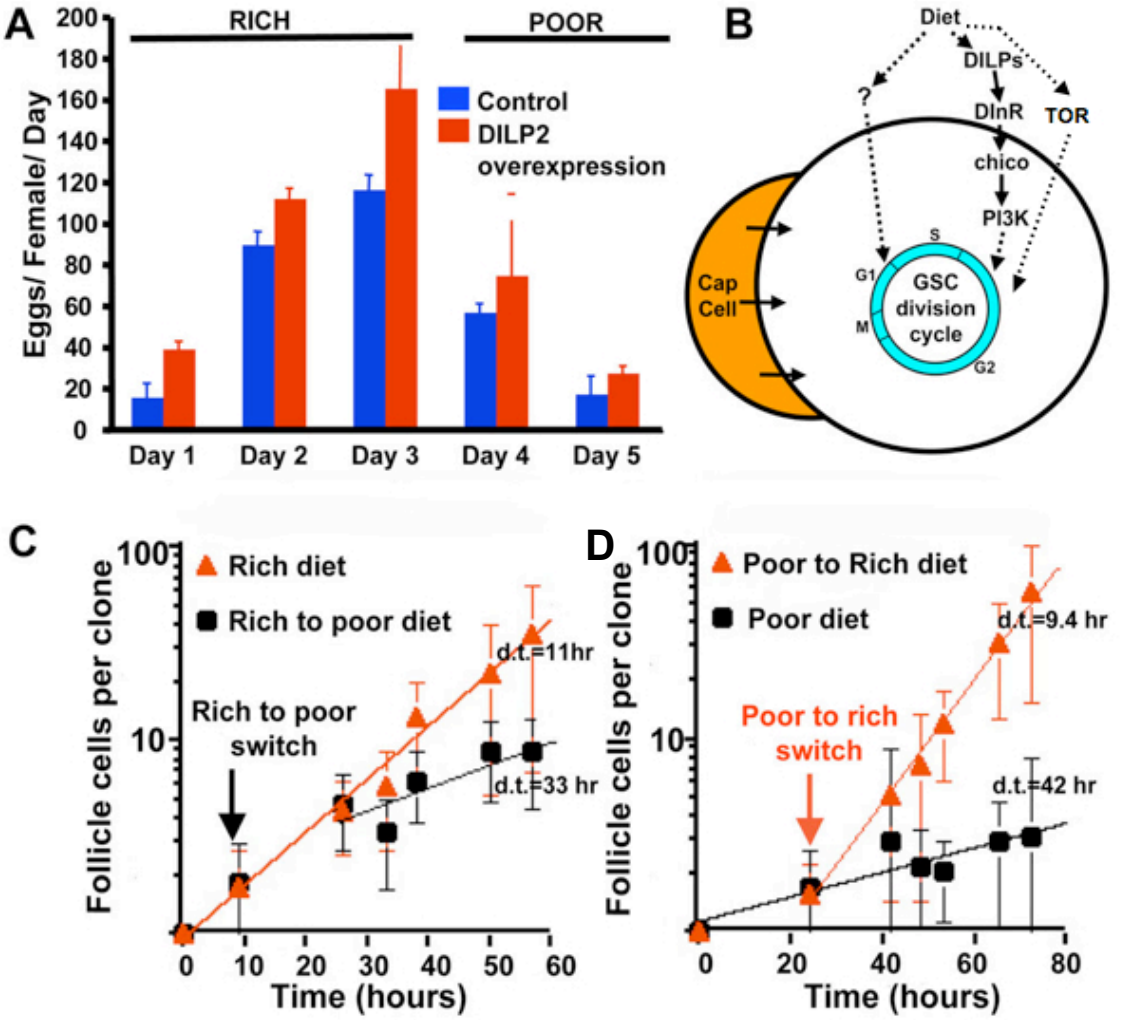

Figure 1.9. Additional factors contribute to the ovarian response to diet and DILPs. (A) Average daily egg production per control female or female overexpressing DILP2. On a rich diet (Days 1-3) egg production is higher in DILP2 overexpressing females, but egg production is unchanged on a poor diet (Days 4-5). **(B)** Model for the effects of insulin signaling on the GSC cell-cycle. Dotted lines and question marks indicate unknown factors and mechanisms that act at both G1 and G2. **(C)** Females with a rich diet history can maintain higher rates of ovarian cell proliferation over time than those with a poor diet history **(D)** (Drummond-Barbosa and Spradling, 2001).

that fat storage levels might be important for ovarian function and that additional signals regulating the ovarian response to diet may arise from the fat body.

Adipose tissue, a storage and endocrine organ in mammals

Adipose tissue is perhaps best known for its role as a energy storage organ, but it also plays key endocrine roles. Made up of adipocytes and a support system of blood vessels, nerve tissue and fibroblasts, adipose tissue provides many beneficial metabolic functions. Adipocytes can sense circulating nutrients, such as glucose and amino acids, and respond by secreting lipids, peptides, cytokines, complement factors, glycerol, and free fatty acids that act on peripheral tissues and maintain metabolic homeostasis (Avram et al., 2005).

Nutrient-sensing in adipose tissue

Four primary integrated nutrient-sensing pathways, the hexosamine, AMPK, TOR, and insulin signaling pathways, act within adipocytes to regulate a wide range of systemic processes via secreted factors. Examples of adipose tissue regulated processes include: energy homeostasis, blood glucose levels, nutrient storage balance, cell survival and repair, cell growth and proliferation, and central nervous system (CNS) metabolic regulatory mechanisms such as food intake. Each nutrient-sensing pathway triggers signaling cascades that are interconnected at multiple levels with other nutrient-sensing pathways (Marshall, 2006).

The hexosamine signaling pathway senses and responds to glucose availability. Upon insulin-stimulated glucose transport into the adipocyte, glucose is converted into

glucose-6-phosphate (G-6-P) for glycogen synthesis. Some G-6-P is further converted into fructose-6-phosphate (F-6-P) used for energy production via the TCA (tricarboxylic acid) cycle and for the production of lipids. F-6-P can be further modified to generate O-linked glycoproteins that control insulin resistance, cytokine secretion, and the secretion of adipokines, such as leptin and adiponectin (Marshall, 2006) (Figure 1.10).

Leptin and adiponectin, adipokines that modulate a variety of metabolic functions via systemic signaling to the CNS and other peripheral tissues, also participate in paracrine and autocrine signaling in adipocytes. They are both secreted from and bind their receptors on adipocytes to modulate nutrient-signaling pathways at the level of AMPK. AMPK signaling also feeds into the TOR signaling pathway, the main functions of which are to modulate rates of translation and inhibit autophagy in adipocytes. TOR signaling also feeds into the insulin signaling pathway at the level of Akt kinase. A major role for adipocyte insulin signaling is the regulation of Glut4 vesicle-mediated glucose transport. Insulin signaling also feeds into the TOR signaling pathway and the hexosamine signaling pathway; therefore, insulin can also modulate rates of protein translation, hormone secretion, and lipogenesis.

Metabolic imbalance caused by mutation or dysfunction of these nutrient-sensing pathways can lead to diseases such as cancer, inflammation, cardiovascular disease, dyslipidemia, obesity, and diabetes (Marshall, 2006). The large number of metabolic-related disease in humans has lead to a great research effort aimed at understanding these complex, interconnected pathways (Catania et al., 2010; Phillips and Kung, 2010; Viollet et al., 2010). Fat-secreted factors, or adipokines, in particular, have stimulated much

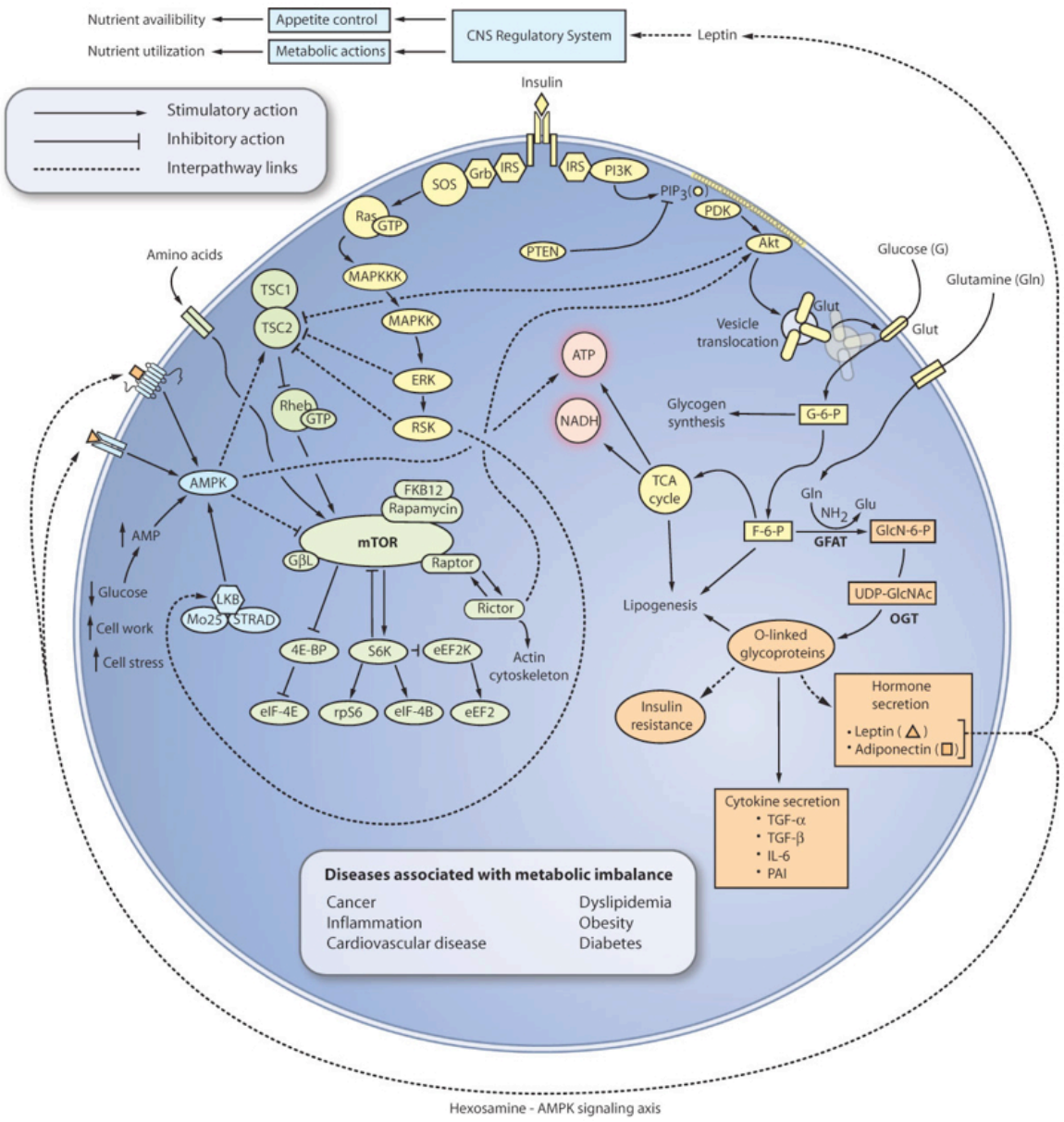

Figure 1.10. Nutrient-sensing in mammalian adipocytes. The hexosamine pathway (orange) senses glucose and modulates insulin resistance, cytokine secretion, lipogenesis, and hormone secretion. Insulin signaling (yellow) regulates glucose import via Glut4 vesicle transport and serves as a stimulatory input for the TOR signaling pathway (green). TOR also senses amino acids and AMPK activity and integrates nutrient signals to modulate rates of cellular protein synthesis and autophagy. AMPK signaling (blue) senses and balances ATP levels and is further regulated by autocrine adipokine signaling (leptin and adiopnectin). Leptin and adiponectin also act on peripheral tissues, including the CNS to modulate appetite and insulin sensitivity. Figure from Marshall, *Sci. STKE*, 2006.

interest due to their effects on the CNS regulatory system, including appetite control and their effects on peripheral tissue insulin-sensitivity, including muscle and liver. Adipokines also have reported roles in both stem cell regulation and ovarian function in mammals (Budak et al., 2006; DiMascio et al., 2007).

Adipokines

Adipokines are a structurally and functionally diverse family that regulate whole body insulin sensitivity and metabolic homeostasis (Staiger and Haring, 2005). These fat-derived molecules include proteins involved in the immune response, such as TNF-α; proteins involved in lipid metabolism, such as retinol binding protein; and many others, such as those involved in blood pressure regulation, angiogenesis, and fertility (Budak et al., 2006; Klein et al., 2006; Mitchell et al., 2005; Scherer, 2006; Staiger and Haring, 2005). The majority of adipokine research has focused on the roles of adiponectin and leptin in obesity, insulin resistance, and fertility. Leptin acts on the central nervous system to regulate appetite and body weight in addition to many other reported functions, including fertility (Staiger and Haring, 2005; Zhang et al., 1994). Leptin has multiple roles in fertility, ranging from initiation of puberty to facilitating implantation and pregnancy (Budak et al., 2006). Adiponectin has been associated with obesity, insulin resistance, and type II diabetes (Fu et al., 2005; Kadowaki et al., 2007; Oh et al., 2007; Whitehead et al., 2006). While loss of adiponectin has no reported effect on reproduction, transgenic mice overexpressing adiponectin are infertile (Combs et al., 2004).

Adiponectin signaling pathway

How adiponectin signaling interacts with insulin signaling is not completely understood, but the identification of the adiponectin receptors has led to some insights. These receptors, belonging to the progestin and adipoQ receptor (PAQR) family of proteins, contain seven transmembrane domains, but are both structurally and functionally distinct from G-protein coupled receptors (Yamauchi et al., 2003). The adiponectin receptors are highly conserved from yeast, which has one receptor (*PHO36*), to mammals, which have at least three adiponectin receptors (*mAdipoR1*, *mAdipoR2*, and *PAQR3*). Activation of these receptors increases the activity of 5'-AMP-activated protein kinase (AMPK), a sensor of cellular energy status (Kadowaki et al., 2006). Insulin signaling and AMPK levels converge on TOR kinase and thus control cellular growth and proliferation (Hardie, 2004). A recent report suggests that adiponectin can regulate insulin sensitivity at least in part through modulation of TOR (Wang et al., 2007).

Adiponectin and other adipokines as stem cell factors

Recent evidence indicates that adiponectin has a role as a stem cell factor. mAdipoR1 and 2 are expressed by components of the HSC niche and adiponectin has been demonstrated to increase HSC growth and maintain stem cell identity via a p38-MAPK-mediated pathway (DiMascio et al., 2007). Adiponectin treatment of damaged muscle tissues increases myogenic precursor proliferation and survival via both p38 MAPK and Akt activation (Chiarugi and Fiaschi, 2010). Other adipokines may also act as stem cell factors. For example, both visfatin and resistin levels are elevated by granulocyte colony-stimulating factor-inducted mobilization of HSCs (Tanaka et al., 2009). Leptin

regulates mouse spermatogenesis via activation of the STAT3 pathway, a known modulator of stem cell renewal and differentiation (El-Hefnawy et al., 2000). These studies suggest adipokines can regulation of mammalian stem cell and germ cell activity; including growth, proliferation, maintenance, and mobilization of stem cell populations.

The *Drosophila* fat body serves as a storage and endocrine organ

The *Drosophila* fat body, made up of adipocytes (fat cells) and oenocytes (liver-like cells), is found in sheets and masses attached to the integument layer and surrounding the gut throughout the adult (Figure 1.11) (Dean RLLMC, 1985; Gutierrez et al., 2007). Very little is known about the adult fat body, which arises from a different cell lineage to replace the larval fat body within three days of eclosion (Aguila et al., 2007). Studies on the larval fat body, however, clearly show that tissue has multiple endocrine roles. For instance, the larval fat body secretes an unknown mitogenic factor in response to nutrition that stimulates reactivation of the cell cycle in post-mitotic cells (Britton and Edgar, 1998) and promotes neural insulin secretion (Geminard et al., 2009). The larval fat body also acts as a central nutrient-sensing organ via an amino acid transporter, Slimfast (Slif). Downregulation of *slif* in the fat body inhibits growth through an unknown humoral mechanism that represses PI3K signaling in peripheral tissues (Colombani et al., 2003). While the factors that act downstream of nutrient sensing pathways in the larval fat body are unknown, potential candidates include the insulin growth factor binding protein homologs, ALS (acid-labile subunit) and Imp-L2 (also known as ecdysone-inducible gene L2). These proteins are secreted from the fat body and bind DILPs in the hemolymph to form a repressive trimeric complex resulting in reduced peripheral insulin signaling

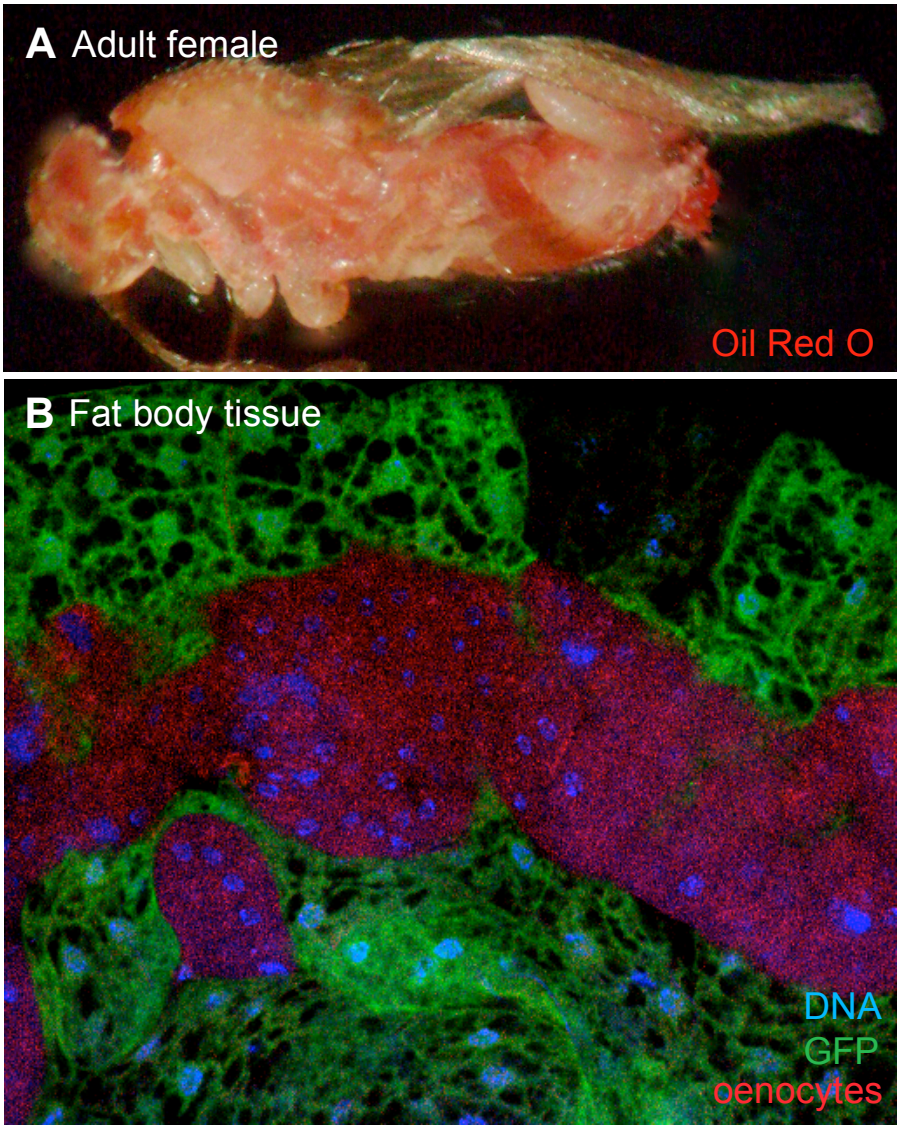

Figure 1.11. The *Drosophila* adult fat body. (A) A sagittal section through a whole female fly (anterior to left) stained with Oil Red O (neutral lipids) to mark the location of fat body tissue. **(B)** Adult fat body tissue expressing GFP (green) in fat cells. DNA, blue. Oenocytes, red, are autofluorescent at red wavelengths.

(Arquier et al., 2008; Honegger et al., 2008). Most recently, iron-loaded ferritin, produced by the fat body, was shown to have a stimulatory role on imaginal disc cells (Li, 2010). Together, these data indicate that the larval fat body plays an important, but still undefined, role on peripheral tissue homeostasis in *Drosophila*. While less well-studied, the adult fat body may retain some of the roles of the larval fat body. For instance, ovaries in *Imp-L2* knockdown adult females have increased numbers of vitellogenic egg chambers, suggesting increased egg production (Honegger et al., 2008). If so, the role of the fat body factor Imp-L2 on peripheral tissue growth and/or proliferation in conserved between the larval and adult fat bodies.

Based on primary sequence, no adipokine homologs are present in the *Drosophila* genome. Nevertheless, it is possible adipokine-like molecules might be functionally conserved in the absence of primary sequence conservation, making bioinformatics-based identification of adipokine homologs more difficult. Osmotin, a plant antifungal protein has less than 10% sequence identity to adiponectin, but it can bind the mammalian adiponectin receptor in cell culture and activate the same downstream molecules (Narasimhan et al., 2005). The presence of adipokine-like molecules in *Drosophila* is strongly suggested by the existence of an adiponectin receptor homolog, *dAdipoR*, that shares 60% identity with its mammalian homologs (Yamauchi et al., 2003).

Outline and summary

The goal of my thesis project is to better understand the role of insulin signaling in the dietary regulation of *Drosophila* ovarian GSCs and their progeny and to identify additional dietary-sensing pathways that play a role in the ovarian response to diet and

DILPs. In Chapter II, I follow up on my studies as a technician that described a direct role for insulin signaling in the *Drosophila* germline (LaFever and Drummond-Barbosa, 2005). I identify the PI3K branch of the insulin signaling pathway as the transducer of the DILP-stimulated signal and examine the role of the downstream negative regulator FOXO in this pathway. This work also complements the studies on the role of insulin signaling on the GSC cell-cycle, which was performed by Dr. Hsu and published as a co-first author paper (Hsu et al., 2008). Chapter III describes a role for TOR as an additional nutrient-dependent factor that regulates the GSC cell-cycle independently of insulin signaling. I also provide a detailed analysis of TOR-specific roles in the ovarian GSC lineage and the somatic follicle stem cell lineages. These studies demonstrate that the effects of nutrition on the ovary are both cell-type and cell microenvironment-dependent and reveal interesting parallels between *Drosophila* and mammalian follicle growth (LaFever et al., 2010). Studies aimed at understanding the connection between the *Drosophila* fat body and the ovarian response to diet and DILPs is described in Chapter IV. The studies described therein are still unpublished but they suggest that either increasing or decreasing fat body storage levels negatively affects oogenesis. I also describe my preliminary work on the cell-autonomous and non-cell autonomous diet-dependent roles for the *Drosophila* adiponectin receptor (*dAdipoR*) on ovarian stem cells and their progeny. Furthermore, I provide evidence that nutrient-sensing pathways within the adult fat body can stimulate the production/secretion of unidentified factors that regulate specific aspects of oogenesis. Finally, I describe a proteomics/bioinformatics/genetic approach to identifying a potential dAdipoR ligand and additional fat body secreted proteins that act upon the ovary. Taken together these studies implicate the fat body in the dietary regulation of oogenesis. In the final chapter, I will

further discuss the implications of my research and explain how they provide an important contribution to the field of nutritional stem cell regulation.

CHAPTER II

DIET CONTROLS DROSOPHILA GERMLINE STEM CELLS AND THEIR PROGENY VIA INSULIN-DEPENDENT AND –INDEPENDENT MECHANISMS

The studies described in this chapter were published in *Developmental Biology* [Hwei-Jan Hsu, Leesa LaFever, and Daniela Drummond-Barbosa, *Developmental Biology*. 2008; Jan 15;313(2):700-12]. First authorship was shared between me and Dr. Hwei-Jan Hsu. I have modified the title and the text of the published article so only my contribution to the publication is presented here.

Introduction

Stem cells self-renew and give rise to various differentiated cell types within many adult tissues (Potten and Loeffler, 1990; Weissman, 2000). The maintenance of stem cell properties and the precise regulation of their proliferation are therefore crucial to maintain tissue integrity and function. Stem cells reside in a specialized microenvironment, or niche, where they receive local signals, such as bone morphogenetic proteins (BMPs), Hedgehogs, and Wnts that regulate their maintenance and proliferation (Li and Xie, 2005; Spradling et al., 2001). Despite the unquestionable importance of local signals in regulating stem cells, stem cell activity is also influenced by stimuli originating outside of the tissues in which they reside, such as diet, hormones, or physical insults (Drummond-Barbosa, 2005; Narbonne and Roy, 2006). By sensing and responding to external signals, stem cells can tailor the rate of cell production to the ever-changing demands imposed on living organisms by their environment.

The ease of identification and manipulation of germline stem cells (GSCs) in the *Drosophila melanogaster* ovary provides an ideal model system for studying GSC behavior *in vivo* (Wong et al., 2005). Each *Drosophila* ovary is comprised of ovarioles or strings of progressively more developed egg chambers (Spradling, 1993). The production of egg chambers is maintained by small populations of stem cells located within the germarium, the anterior-most region of the ovariole (Kirilly and Xie, 2007). The division of a GSC produces a cystoblast that divides four more times to form 2-, 4-, 8-, and 16-cell cysts. One cell becomes the oocyte; the others become nurse cells. Follicle cells derived from somatic stem cells surround the cyst, generating an egg chamber that goes through fourteen developmental stages to form a mature oocyte.

The effect of diet on stem cells and their descendents has been well documented in the *Drosophila* ovary (Drummond-Barbosa and Spradling, 2001). On a protein-rich diet, germline and somatic stem cells have high division rates, and their progeny also divide and grow fast. On a protein-poor diet, these rates are reduced and vitellogenesis is blocked. The response to diet is rapid and reversible, and it requires insulin signaling. Specifically, insulin-like peptides (DILPs) produced in two clusters of neurosecretory cells in the brain directly regulate GSC division, cyst growth and vitellogenesis, whereas follicle cells receive a secondary signal from the germ line (LaFever and Drummond-Barbosa, 2005). Several questions regarding the direct role of DILPs in mediating the effects of diet on GSC proliferation remain. It is unclear how DILPs impinge on the GSC division cycle, whether DILPs alone mediate the effect of diet on GSCs, and whether GSCs require proximity to niche cells to respond directly to neural DILPs.

The insulin/insulin-like growth factor (IGF) pathway is evolutionarily conserved

and controls many essential processes linked to nutrient sensing, such as metabolism, reproduction, longevity, and cell growth and proliferation (Goberdhan and Wilson, 2003; Hafen, 2004). *Drosophila* has one homolog for each component of the insulin/IGF pathway, including one receptor (*Drosophila insulin receptor*, or *dinr*); one exception, however, is the presence of seven *DILP* genes. Stimulation of cells by insulin-like signals results in activation of the insulin receptor substrate (encoded by the *chico* gene, in *Drosophila*) downstream of the receptor and activation of the Ras/MAPK and phosphoinositide-3 kinase (PI3K) branches of the insulin pathway (Oldham and Hafen, 2003). Activation of PI3K increases the production of phosphatidylinositol (3,4,5)-trisphosphate, which recruits Akt to the plasma membrane, where it becomes activated and phosphorylates several downstream targets. In mammals, the Ras/MAPK pathway is required for cell proliferation in response to IGF-1 (Lu and Campisi, 1992; Tanaka et al., 1996). In contrast, the PI3K pathway is necessary and sufficient to promote DILP-induced growth and proliferation downstream of the insulin receptor substrate-like gene *chico* during *Drosophila* development (Goberdhan and Wilson, 2003; Oldham and Hafen, 2003). The requirement for specific branches of the insulin pathway during GSC proliferation, however, has not been previously examined.

Insulin/IGF-mediated growth is negatively regulated by the transcriptional factor FOXO (Forkhead box, sub-group "O") (Barthel et al., 2005; Puig and Tjian, 2006). Under high insulin signaling, FOXO is phosphorylated by Akt and retained in the cytoplasm. Under low insulin signaling, FOXO translocates from the cytoplasm to the nucleus and activates transcription of its target genes, which have roles in the regulation of cell cycle, protein synthesis, and metabolism. In *Drosophila*, *dFOXO* mediates the decrease of

imaginal disc cell proliferation resulting from reduced insulin signaling, and overexpression of *dFOXO* results in a starvation-like phenotype (Junger et al., 2003; Kramer et al., 2003; Puig and Tjian, 2006).

In this study, we demonstrate that the PI3K branch of the insulin signaling pathway is primarily responsible for mediating the ovarian response to diet and DILPs. We also show that loss of the transcription factor *FOXO*, a downstream negative regulator of the insulin signaling pathway, is not sufficient to rescue the effects of a poor diet on GSC proliferation and cyst growth, which indicates that additional factors are required to suppress GSC proliferation rates when nutrients are limiting.

Materials and methods

Drosophila strains and culture

Drosophila stocks were maintained at 22–25 °C. *yw* was used as a wild-type control. $chico^{1}$ and $dFOXO^{25}$ alleles have been described (Drummond-Barbosa and Spradling, 2001; Junger et al., 2003). Genomic rescue constructs $P\{chico^{WT4.2}\}$, $P\{chico^{Drk2.1}\}$, and $P\{chico^{PI3K9}\}$ have been described and are not expected to affect Chico protein stability (Oldham and Hafen, 2003). We also confirmed by RT-PCR that these transgenes are expressed at similar levels. Other genetic elements are described in Flybase (Ashburner and Drysdale, 1994). Flies were cultured in standard medium with wet yeast paste (protein-rich diet) or in an empty vial containing a Kimwipe soaked in 5% molasses (protein-poor diet).

Generation and analysis of mosaic ovarioles

Genetic mosaics were generated as described (LaFever and Drummond-Barbosa, 2005). For *chico* mosaic analyses, females of the genotype *hs-FLP/+; FRT40A chico1/FRT40A arm-lacZ or hs-FLP/;FRT40A chico1/FRT40A armlacZ; P{chico*}/+* were generated. (*P{chico*}* represents genomic rescue constructs.) To induce FLP-mediated recombination, we heat shocked 0- to 3-day-old females for 1 h at 37 °C twice a day for 3 days and subsequently transferred them to fresh food with dry yeast daily for 10 days before dissection. $chico^{1}$ homozygous clones were identified by the absence of β-galactosidase (β-gal). GSC division and cyst growth rates were determined as described (LaFever and Drummond-Barbosa, 2005). For *dFOXO* mosaic analysis, *hs-FLP/;FRT 82B dFOXO*/FRT82B arm-lacZ* females were generated, heat shocked, and cultured for 10 days as above. (*dFOXO** represents wild-type or $dFOXO^{25}$ alleles.) *dFOXO* and control mosaics were then transferred to either rich or poor diets for 0, 2, 5, and 10 days before dissection and analysis as above. Ten days was chosen as the last time point because by then we would expect a nearly complete turnover of the population of cystoblasts and cysts within the germarium on either diet (Drummond-Barbosa and Spradling, 2001; LaFever and Drummond-Barbosa, 2005), which would be important for the detection of any potential changes in the relative division rate of the GSCs (measured as the relative number of β-gal-negative and β-gal-positive cystoblasts and cysts inside the germaria). Please note that although wild-type GSC division rates are lower on a poor diet (Drummond-Barbosa and Spradling, 2001), the relative division rate remains unchanged if both GSCs within each germarium equally modulate their proliferation upon a dietary switch. Results were subjected to chi-square analysis (for GSC relative division rates) or

Student's t-test (for cyst growth rates).

Immunostaining and fluorescence microscopy

Ovaries were dissected in Grace's insect medium (Cambrex), fixed for 13 min at room temperature in Grace's medium plus 5% formaldehyde (Ted Pella), washed, and stained as described (de Cuevas et al., 1996). The following antibodies were used: mouse monoclonal 1B1 (1:10) (Developmental Studies Hybridoma Bank, DSHB), rabbit polyclonal α-spectrin (de Cuevas et al., 1996) (1:100), mouse monoclonal anti-β-gal (1:500) (Promega), and rabbit polyclonal anti-β-gal (1:1000) (Cappel). Alexa 488-, Alexa 568-, or Alexa 633- conjugated goat anti-mouse and anti-rabbit secondary antibodies (1:400) (Molecular Probes) were used. Samples were incubated in 1 μg/ml DAPI (Sigma) for 8 min. Ovaries were mounted in Vectashield (Vector Laboratories). Samples were examined using a Zeiss LSM 510 confocal microscope.

Results

The PI3K pathway mediates the effects of insulin-like signals on GSC proliferation and cyst growth

To disrupt activation of the PI3K or Ras/MAPK branches, we used *chico* genomic rescue transgenes (Oldham et al., 2002) that carry point mutations in the predicted consensus binding sites for either the p60 ($chico^{PI3K-}$) or Grb2/Drk ($chico^{Drk-}$) adaptor proteins, respectively. We removed the endogenous *chico* function in GSCs expressing these point mutants using the flipase *(FLP)/FLP* recognition target (*FRT*) technique (Figure 2.1A-D) and determined the ratio of mutant to control cystoblasts and cysts within mosaic germaria as a measure of the relative division rates of *chico* mutant GSCs

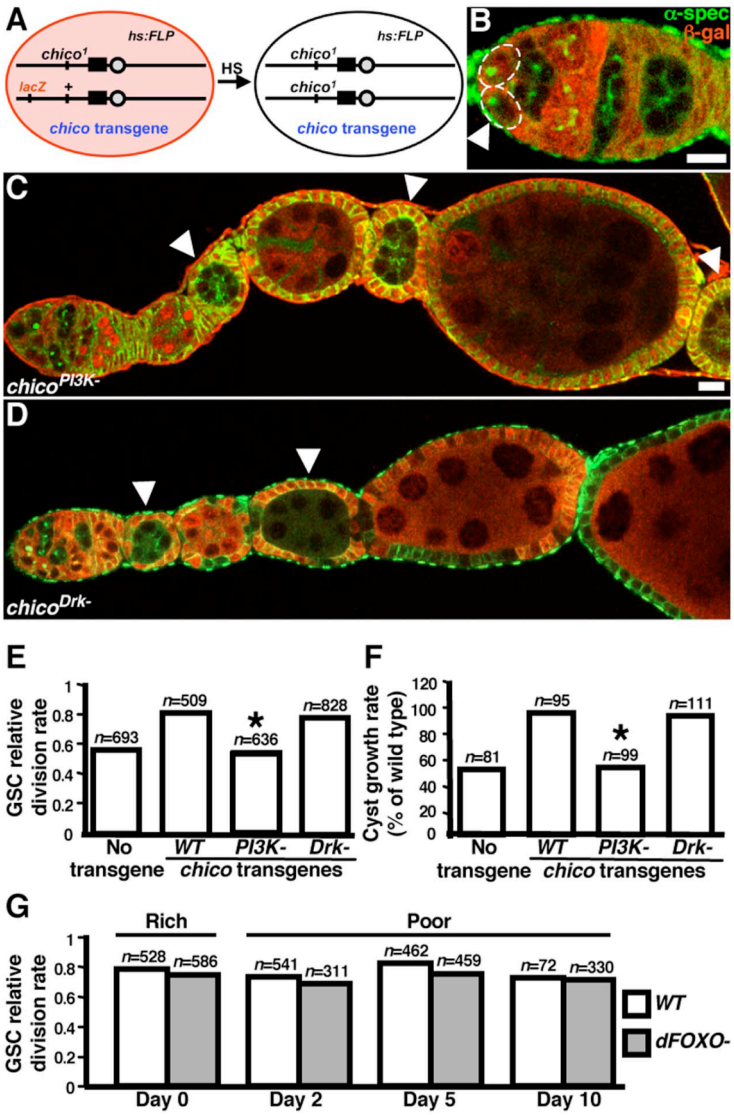

Figure 2.1. DILPs control the rates of GSC division and cyst growth via the PI3K pathway. (A) *FLP/FRT* technique used to generate *chico*^{1} null clones recognized by the absence of β-gal and expressing *chico* transgenes. **(B)** A mosaic germarium used for analysis of GSCs (dashed ovals). Arrowhead, β-gal negative GSC. **(C)** A mosaic ovariole showing delayed *chico*$^{PI3K-}$ mutant cysts (arrowheads). **(D)** Example of *chico*$^{Drk-}$ mutant cysts (arrowheads). **(E)** The relative division rate of *chico*$^{PI3K-}$ GSCs is significantly lower than that of *chico*^{WT} GSCs. **(F)** *chico*$^{PI3K-}$ cysts are severely delayed while *chico*$^{Drk-}$ cysts are comparable to *chico*^{WT} cysts**. (G)** The relative division rates of *dFOXO*^{25} GSCs are not significantly different from those of wild-type GSCs on rich or poor diets. α-spectrin (green) highlights cell membranes and fusomes, whereas β-gal (red) labels control cysts. Ovarioles in C, D are shown at the same magnification. *n*, number of cystoblasts and cysts counted (E,G) or of β-gal-negative cysts analyzed (F). Scale bars, 10 μm. Asterisks, $P<0.001$.

(LaFever and Drummond-Barbosa, 2005; Xie and Spradling, 1998) (Figure 2.1E). The reduced relative division rate of *chico*^{1} mutant GSCs in the absence of a *chico* transgene (*chico*^{1} control) was comparable to that of previously described *dinr* mutant GSCs (LaFever and Drummond-Barbosa, 2005).

Expression of a wild-type *chico* transgene (*chico*^{WT}) restored the GSC relative division rate to wild-type levels. In contrast, expression of the *chico*$^{PI3K-}$ transgene resulted in a GSC relative division rate indistinguishable from that of the *chico*^{1} control, indicating that activation of PI3K downstream of *chico* is absolutely required for the upregulation of GSC proliferation in response to DILPs. The activity of the *chico*$^{Drk-}$ transgene was equivalent to that of *chico*^{WT}, suggesting that the Ras/MAPK branch is dispensable. Similar requirements were found for cyst growth (Figure 2.1C, D, F) and progression through vitellogenesis (0% of fully mutant *chico*^{1} control [n=12] or *chico*$^{PI3K-}$ [n=7] ovarioles showed progression into vitellogenesis instead of degeneration, whereas 100% of *chico*^{WT} [n=7] or *chico*$^{Drk-}$ [n=5] ovarioles contained vitellogenic egg chambers). These results show that the direct effect of DILPs on GSC proliferation, cyst growth, and vitellogenesis are entirely mediated by PI3K during the response to diet. Thus, they reveal a considerable degree of similarity in the control of proliferation by DILPs between growing larval cells and adult GSCs.

dFOXO is not required to maintain the repressed state of GSCs under a poor diet

Although mutation of the *Drosophila* homolog *dFOXO* does not result in any overt phenotype, *dFOXO* is required for the inhibitory effects of low insulin signaling on the proliferation of larval tissues (Puig and Tjian, 2006). Thus, we asked if *dFOXO* is required to maintain the repressed state of GSCs under a poor diet. We generated clones of cells

homozygous for the null *dFOXO*^{25} mutation (Junger et al., 2003) and measured the relative division rates of *dFOXO*^{25} GSCs in mosaic females transferred to a poor diet. We reasoned that if *dFOXO* were required to inhibit GSC proliferation on a poor diet (when insulin signaling is low), *dFOXO*^{25} GSCs would divide faster than control GSCs within mosaic germaria, resulting in a higher relative division rate on a poor diet relative to that on a rich diet (see Materials and methods).

As expected, we found that on a rich diet (when *dFOXO* is normally off), the relative division rate of *dFOXO*^{25} GSCs was comparable to that of wild-type GSCs. Surprisingly, the relative division rates of *dFOXO*^{25} GSCs remained statistically unchanged after 2, 5, and 10 days on a poor diet, similarly to those of wild-type GSCs. *dFOXO*^{25} cyst growth rates and progression through vitellogenesis were also comparable to those of the wild-type control on both rich and poor diets (Table 2.1). These results indicate that *dFOXO*^{25} GSCs reduce their proliferation rates in response to a poor diet to the same extent as wild-type GSCs, and thus that *dFOXO* is not required to maintain the poor diet-induced repressed state of GSCs. It is possible that the effects of low insulin signaling are *dFOXO* independent. Alternatively, other signals may be required to modulate GSC division in response to diet such that activation of the insulin pathway by removal of *dFOXO* is not sufficient to compensate for the effects of a poor diet.

Discussion

Multiple signals mediate the response of GSCs to diet

The environment exerts tremendous pressure during the evolution of biological processes to such a degree that many of these processes themselves can adjust to frequent,

Table 2.1

***dFOXO* is not required for the response to a protein-poor diet.**

Strain	Diet	Days after switch[a]	GSC relative division rate[b]	Cyst growth rate[b]	Vitellogenesis rate[b]
Wild type	Rich	0	0.79 (528)[c]	100% (54)[c]	-
		2	0.72 (453)	100% (52)	100% (3)[c, d]
		5	0.73 (630)	100% (60)	100% (8)
		10	0.82 (426)	100% (73)	100% (6)
	Poor	2	0.73 (541)	100% (21)	0% (2)
		5	0.82 (462)	100% (77)	25% (4)
		10	0.71 (72)	100% (14)	0% (1)
dFOXO^{25}	Rich	0	0.74 (586)	100% (62)	-
		2	0.58 (459)	100% (14)	-
		5	0.76 (603)	100% (61)	100% (9)
		10	0.87 (518)	100% (98)	100% (18)
	Poor	2	0.68 (311)	100% (42)	0% (3)
		5	0.75 (459)	100% (87)	0% (4)
		10	0.72 (330)	100% (38)	0% (8)

[a]Females were maintained for 10 days on a rich diet after generation of clones and subsequently transferred to either rich or poor diets for the indicated number of days.
[b]Cyst growth rates are expressed as a percentage of the wild-type development rate, and vitellogenesis rates represent the percentage of cysts within ovarioles containing fully β-gal-negative germline that initiated vitellogenesis instead of degenerating. The results obtained from *dFOXO*^{25} clonal analysis were not statistically different from those of the wild-type control.
[c]The total number of cystoblasts and cysts, β-gal-negative cysts, and ovarioles containing fully β-gal-negative germline analyzed, respectively, are shown in parentheses.
[d]The small number of fully β-gal-negative ovarioles analyzed reflects the rarity of double GSC recombination events within a single germarium.

short-term external changes. Stem cells often lie at the root of these processes due to their critical role in maintaining the function and integrity of many adult tissues. It is therefore very likely that stem cells in other systems will exhibit responses to environmental stimuli comparable to the response of ovarian stem cells to diet in the *Drosophila* ovary. In fact, parallels can be drawn between the effects of DILPs on GSCs and those of insulin/IGFs in other stem cell systems. For example, reduced insulin signaling results in the decreased proliferation of germline precursors in *Caenorhabditis elegans* during preparation for dauer diapause (Narbonne and Roy, 2006), whereas in adults it inhibits gamete production (Gems et al., 1998). In addition, focal cerebral ischemia results in increased proliferation of adult mammalian neural progenitor cells in the subgranular zone of the dentate gyrus and in the subventricular zone of the lateral ventricles, and this response was shown to require IGF-1 activity in rats (Yan et al., 2006). Similarly, IGF-2 is required for fetal liver cells to support the proliferation of hematopoietic stem cells in culture (Zhang and Lodish, 2004). Finally, insulin normalizes delayed corneal wound healing in diabetic rats (Zagon et al., 2007), although it is unclear whether or not the activity of corneal epithelial stem cells is affected.

Fast and effective stem cell responses to complex stimuli such as diet would be expected to result from multiple signals. Our data provide evidence that in *Drosophila* GSCs, in addition to DILPs, at least one other signal mediates the effect of diet. It is possible that GSC regulation involves the Target of rapamycin (TOR) kinase. TOR integrates many stimuli such as amino acid levels, metabolic status, or signaling inputs, and has a known role in growth control (Oldham and Hafen, 2003). In addition, it has been shown to regulate the cell cycle via the G1 phase (Chan, 2004) and may be required for

normal ovarian function in *Drosophila* (Zhang et al., 2006). Alternatively, the effects of diet may be mediated by microRNAs, which have been reported to regulate GSC division in *Drosophila* (Hatfield et al., 2005).

The control of proliferation by DILPs shows similarities between GSCs and larval somatic cells

The apparently exclusive role that we find for the PI3K branch of the insulin pathway in mediating the effects of DILPs on GSC proliferation and cyst growth has also been demonstrated in proliferating larval cells (Goberdhan and Wilson, 2003; Oldham and Hafen, 2003). The fact that disruption of the predicted consensus binding site for Grb2/Drk, the adaptor protein in the Ras/MAPK branch, in the insulin receptor substrate (IRS) Chico results in no obvious phenotype in this or other studies (Oldham et al., 2002) raises the concern that may not completely abolish Ras/MAPK activation downstream of insulin receptor activation. Indeed, the cytoplasmic region of the *Drosophila* insulin receptor can induce both PI3K and MAPK activation in the absence of the IRS in cultured 32D cells, although it still requires the IRS for mitogenesis (Yenush et al., 1996). Nevertheless, disruption of the consensus binding site for p60, the PI3K adaptor, leads to phenotypes indistinguishable from those resulting from the complete elimination of *chico* function. Furthermore, the Grb2/Drk binding site is conserved in *Drosophila*, suggesting that DILP-mediated Ras/MAPK activation via Chico may have a minor or context specific role undetectable in our experiments. In fact, Ras activates PI3K in *Drosophila* and mammals (Prober and Edgar, 2002; Rodriguez-Viciana et al., 1996), and although Ras-mediated regulation of PI3K is dispensable for viability, it is required for maximal PI3K signaling in specific biological contexts (Orme et al., 2006). It remains unclear whether optimal Ras signaling requires the presence of an intact Grb2/Drk binding site in Chico.

CHAPTER III

SPECIFIC ROLES OF TARGET OF RAPAMYCIN IN THE CONTROL OF STEM CELLS AND THEIR PROGENY IN THE *DROSOPHILA* OVARY

This chapter was published in *Development* [Leesa LaFever, Alexander Feoktistov, Hwei-Jan Hsu, and Daniela Drummond-Barbosa. *Development*. 2010 Jul;137 (13):2117-26] and is reproduced here verbatim.

Contributions to the data appearing in this chapter are as follows: I contributed to all figures and tables; Alexander Feoktistov contributed data on the Tor^{P2293L} mutant and wild-type alleles to Figures 3.4, 3.5, 3.6, and 3.8, and Tables 3.1 and 3.3. Dr. Hwei-Jan Hsu contributed the Tor^{E161K}/Tor^{A948V} cell cycle analysis in Figure 3.2.

Introduction

Stem cells self-renew and produce differentiating progeny for tissue integrity and function (Potten and Loeffler, 1990). Local and intrinsic factors maintain stem cell properties (Li and Xie, 2005), but external and circulating factors also affect stem cells. *Drosophila* intestinal and mammalian neural stem cells increase proliferation upon damage via insulin-like signals (Amcheslavsky et al., 2009; Yan et al., 2006; Zhang et al., 2001). Hormones modulate mammary stem cells (LaMarca and Rosen, 2008). Dietary factors stimulate mouse embryonic and hematopoietic stem cell activity (Hinge et al., 2009; Kim et al., 2009). It remains largely unknown, however, whether stem cells and their progeny respond to systemic changes uniformly or more specifically.

The *Drosophila* ovary houses stem cells in the germarium, the anterior-most portion of each ovariole (Figure 3.1A) (Li and Xie, 2005). Two or three germline stem cells (GSCs) in a specialized niche self-renew and produce cystoblasts, which divide four times with incomplete cytokinesis to form germline cysts containing one oocyte and fifteen nurse cells. Follicle stem cells (FSCs) self-renew and produce follicle cells that envelop each cyst to form an egg chamber, or follicle. After leaving the germarium, each follicle develops through fourteen stages, forming a mature oocyte. As the cyst grows, follicle cells divide mitotically until stage 7, when they begin endoreplicating. Yolk uptake or vitellogenesis initiates at stage 8 (Spradling, 1993). The control of distinct stem cell populations and their differentiating progeny can thus be probed in this system.

Ovarian stem cells and their progeny respond to diet. On a protein-rich diet, GSCs and FSCs proliferate rapidly, and their descendents divide and grow robustly. On a protein-poor diet, proliferation and growth are slowed, early germline cysts die, and vitellogenesis is blocked (Drummond-Barbosa and Spradling, 2001). Insulin signaling is required for all responses, except early cyst viability (Drummond-Barbosa and Spradling, 2001) (L. LaFever and D. Drummond-Barbosa, unpublished results). Insulin-like peptides directly promote GSC division, cyst growth, and vitellogenesis (LaFever and Drummond-Barbosa, 2005), and indirectly control GSC maintenance (Hsu and Drummond-Barbosa, 2009). Insulin-like peptides promote GSC G2 progression through PI3 kinase and FOXO; however, additional diet mediators control both G1 and G2 (Figure 3.1B) (Hsu et al., 2008).

The conserved TOR kinase regulates cell survival, growth and proliferation

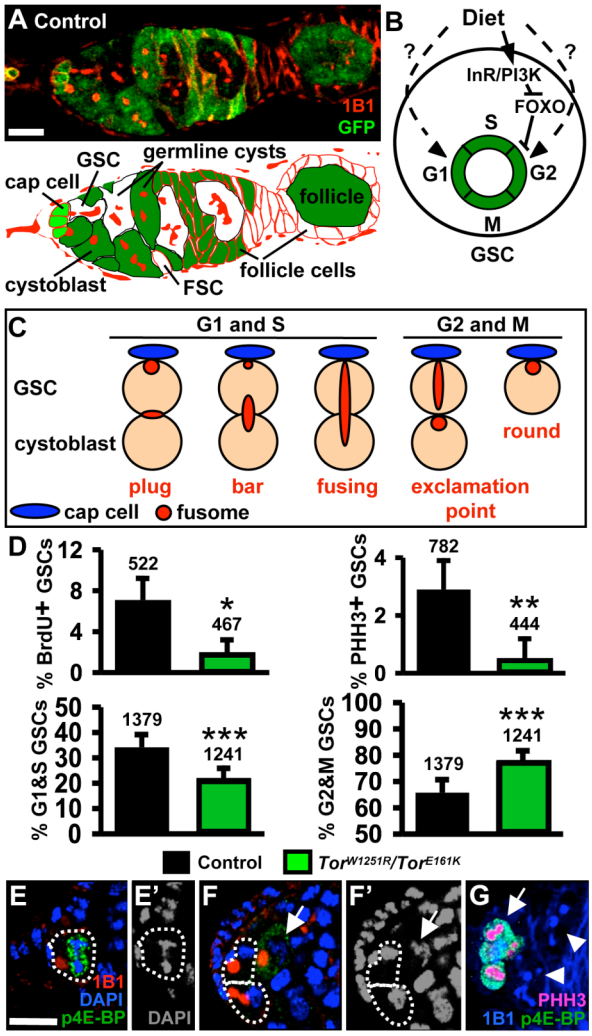

Figure 3.1. TOR controls GSC G2. (**A**) Lineage-traced germarium. Cells are labeled with GFP (green), except for a follicle stem cell (FSC), a germline stem cell (GSC), and their descendents. 1B1 (red) labels fusomes and follicle cell membranes. Cell types are indicated below. GFP-negative GSC and FSC gave rise to GFP-negative cysts and follicle cells, respectively. (**B**) GSC division control by diet. *InR* regulates G2 via PI3 kinase and FOXO, while unknown factors regulate G1 and G2 (Hsu et al. 2008). (**C**) GSC fusome morphology. During G1 and S, fusome has "plug", "bar", or "fusing" morphologies, while in G2 and M, fusome has "exclamation point" or "round" morphologies (de Cuevas and Spradling 1998; Hsu et al. 2008). (**D**) Frequencies of GSCs positive for BrdU (BrdU+, S marker) or PHH3 (PHH3+, M marker), or displaying "G1 and S" (G1&S) or "G2 and M" (G2&M) fusomes. Numbers above bars indicate number of GSCs analyzed. (**E**) Phosphorylated 4E-BP (p4E-BP, green)-positive GSC in M. (**F**) p4E-BP-negative GSCs in interphase. 1B1 (red). DAPI (blue, DNA). DAPI alone is shown in (**E',F'**). Arrow indicates p4E-BP-positive cystoblast in M. (**G**) p4E-BP-positive cysts in M (arrow) and p4E-BP-negative cysts in interphase (arrowheads). PHH3 (pink), M marker. 1B1 (blue). Error bars, s.d. *, $P < 0.03$. **, $P < 0.01$. ***, $P < 0.001$. Scale bars, 10 μm.

downstream of growth factors, amino acids, hormones, and energy status (Wang and Proud, 2009). Tuberous sclerosis complex 1 (Tsc1) and 2 inhibit TOR activity (Pan et al., 2004) and the TOR and insulin pathways cross-talk, but also have independent functions (Hietakangas and Cohen, 2009). *Drosophila* hypomorphic *Tor* mutants have small ovaries with frequent cell death and absent vitellogenic follicles (Zhang et al., 2006), although specific oogenesis processes requiring *Tor* have remained unclear.

This study reveals specific *Tor* roles in *Drosophila* GSCs versus FSCs. Although *Tor* is required for proper proliferation of GSCs and FSCs, it plays a major role in GSC, but not FSC, maintenance. TOR also differentially regulates stem cells versus their progeny. *Tor* is necessary for early cyst proliferation, growth, and survival, by preventing apoptosis. In contrast, TOR does not regulate follicle cell proliferation, and controls follicle cell growth and survival independently of apoptosis or autophagy. Follicle cell TOR activity also affects underlying cyst growth. Finally, TOR regulates these processes via insulin-dependent and –independent mechanisms. These studies uncover specific roles of TOR in the control of stem cells and their differentiating progeny in the *Drosophila* ovary. TOR is a known nutrient sensor in many systems (Wang and Proud, 2009); we therefore speculate that TOR is part of a broadly conserved mechanism that ties stem cell maintenance and function, and the survival, proliferation and growth of their descendents, to diet-dependent factors.

Materials and methods

Drosophila culture and genetic mosaic analyses

Fly stocks were maintained at 22-25°C on standard medium. *y w* is a wild-type control. Tor^{A948V}, Tor^{W1251R}, Tor^{E161K}, Tor^{P2293L}, Tor^{R248X}, $foxo^{21}$, $foxo^{25}$, $Tsc1^{Q87X}$, InR^{E19}, InR^{339}, $Thor^{2,}$ and $Atg7^{d4}$ alleles and other genetic elements are described (Ashburner and Drysdale, 1994; Bernal and Kimbrell, 2000; Hsu et al., 2008; Juhasz et al., 2007; LaFever and Drummond-Barbosa, 2005; Tapon et al., 2001; Zhang et al., 2006).

Mosaic analyses of flipase (FLP)/FLP recognition target (*FRT*)-mediated stem cell-derived clones, including cyst growth and GSC relative division rate measurements, were performed as described (Hsu et al., 2008; LaFever and Drummond-Barbosa, 2005). Many rounds of stem cell division occur prior to our analyses (with the exception of the initial daughter cells from a newly mutant GSCs); therefore, perdurance of wild-type products is not a concern. Early germline cysts were staged based on fusome morphology (de Cuevas and Spradling, 1998). Egg chambers were staged based on size and nuclear morphology (Spradling, 1993). GSC and FSC maintenance was measured as described (Song and Xie, 2003; Xie and Spradling, 1998). The fraction of germaria containing a GFP-negative GSC or FSC relative to total germarium number was measured at different times after heat-shock, starting at four days (T_0). T_0 values were set at 100%, and remaining values normalized to T_0. Results were subjected to a Student's *t*-test or Chi-square analysis.

Immunostaining and microscopy

Ovaries were fixed and stained with 4',6-diamidino-2-phenylindole (DAPI) and

antibodies as described (Hsu et al., 2008). Antibodies used were: mouse anti-β-Gal (Promega, 1:500), rabbit anti-GFP (Torrey Pines, 1:5,000), rabbit anti-phosphohistone H3 (PHH3) (Upstate Biotechnology, 1:250), guinea pig anti-Double-parked (Dup) (gift from T. Orr-Weaver, 1:500), rat anti-BrdU (Accurate Biochemicals, 1:500), rabbit anti-phospho-4E-BP1 (Thr37/46) (Cell Signaling Technology, 1:200), rabbit anti-cleaved Caspase-3 (Cell Signaling Technology, 1:50), mouse anti-Hts (1B1) (Developmental Studies Hybridoma Bank, DSHB, 1:10), mouse α-spectrin (DSHB, 1:50), mouse anti-Cyclin B (CycB) (DSHB, 1:20), mouse anti-Lamin C (LamC) (DSHB, 1:100), mouse anti-fasciclin III (FasIII) (DSHB, 1:25), Alexa 488-, 568- or 633-conjugated goat anti-mouse, -rabbit, -guinea pig, or -rat secondaries (Molecular Probes, 1:400). 5-bromo-2-deoxyuridine (BrdU) incorporation and detection were performed as described (Lilly and Spradling, 1996). ApopTag Fluorescein Direct In Situ Apoptosis Detection Kit (Millipore) was used as described (Drummond-Barbosa and Spradling, 2001). Samples mounted in Vectashield (Vector Lab) were analyzed using a Zeiss Axioplan 2, or Zeiss LSM 510 or LSM 700 confocal microscopes.

Cell cycle analyses

GSC division cycle analyses were performed in zero- to two-day old females maintained for five days on yeasted standard medium as described (Hsu et al., 2008). Briefly, GSCs, identified by fusome morphology and cap cell juxtaposition, were scored using BrdU (S), PHH3 (M), and CycB (G2, M). CycE was not used to mark G1 because it is expressed during most of the GSC cell cycle (Hsu et al., 2008). Experiments were performed at least in triplicate and results subjected to Student's *t*-test.

To measure proliferation of FSCs, optical confocal sections 1.5 μm apart along the Z-axis of germaria containing FSC-derived clones were analyzed. We identified the FSC as the anterior-most, marker-negative follicle cell in the region immediately anterior to the germarium 2A/2B border (Margolis and Spradling, 1995). FSCs and their immediate daughters typically lie just anterior to bright FasIII-staining region (Nystul and Spradling, 2009). Each marker-negative FSC was scored as BrdU-positive or –negative, and percentages of BrdU-positive FSCs relative to total marker-negative FSC number were calculated. Follicle cell cycle in *Tor* mosaics was analyzed using CycB, BrdU, PHH3, and Dup (late G1 and S) (Thomer et al., 2004). Chi-Square statistical analyses were performed.

Follicle cell size analysis

Relative follicle cell size was measured in mosaic follicle cell monolayers at stages when follicle cells normally undergo mitosis (stage 2-6) or endoreplication (stage 7-10). Using ImageJ 1.40g, *Tor* mutant or control GFP-negative follicle cell clones ranging from two to 16 cells were measured in arbitrary area units. For each measured GFP-negative clone, a similar measurement was made for an adjacent wild-type, GFP-positive follicle cell group of equal number, and the ratio between GFP-negative and GFP-positive areas obtained. Average ratios for each mosaic genotype were expressed as a percentage and subjected to Student's *t*-test.

Results

TOR controls GSC proliferation at G2 largely independently of insulin signaling

Insulin-like peptides partially mediate G2 effects of diet, but additional mediators control both G1 and G2 (Hsu et al., 2008). To test if the nutrient-sensor TOR (Wang and Proud, 2009) controls GSC proliferation, we analyzed Tor^{W1251R}/Tor^{E161K} and Tor^{A948V}/Tor^{E161K} hypomorphic females, identifying GSCs by position and fusome morphology (Figure 3.1C). Frequencies of 5-bromo-2-deoxyuridine (BrdU) and phosphohistone H3 (PHH3) labeling were significantly lower in *Tor* mutant GSCs than those of controls (Figure 3.1D; Figure 3.2A), indicating reduced proliferation rates. To determine if *Tor* controls GSCs via a predominant effect on either G1 or G2, we used fusome morphology as a cell cycle marker (Fig. 1C) (de Cuevas and Spradling, 1998; Hsu et al., 2008). *Tor* mutant females had a higher frequency of GSCs with "G2 and M" fusomes, and a lower frequency of GSCs with "G1 and S" fusomes relative to controls (Figure 3.1D, Figure 3.2A). Thus, *Tor* mutant GSCs progress more slowly through G2. Interestingly, wild-type GSCs and dividing cysts display increased levels of 4E-BP phosphorylation, which serves as a TOR activity reporter (Miron et al., 2003), during M but not interphase (Figure 3.1E-G), further suggesting that an increase in TOR activity may be necessary for the G2/M transition.

To determine if TOR is required intrinsically or indirectly (e.g. through the niche) for GSC proliferation, we generated genetic mosaic females in which *Tor* mutant ovarian cells (recognized by the absence of a β-galactosidase [β-gal] or green fluorescent protein [GFP] marker) are present in the context of surrounding control cells. Alleles of increasing severity were used: Tor^{W1251R}, a hypomorph; Tor^{P2293L}, a kinase-dead; Tor^{R248X},

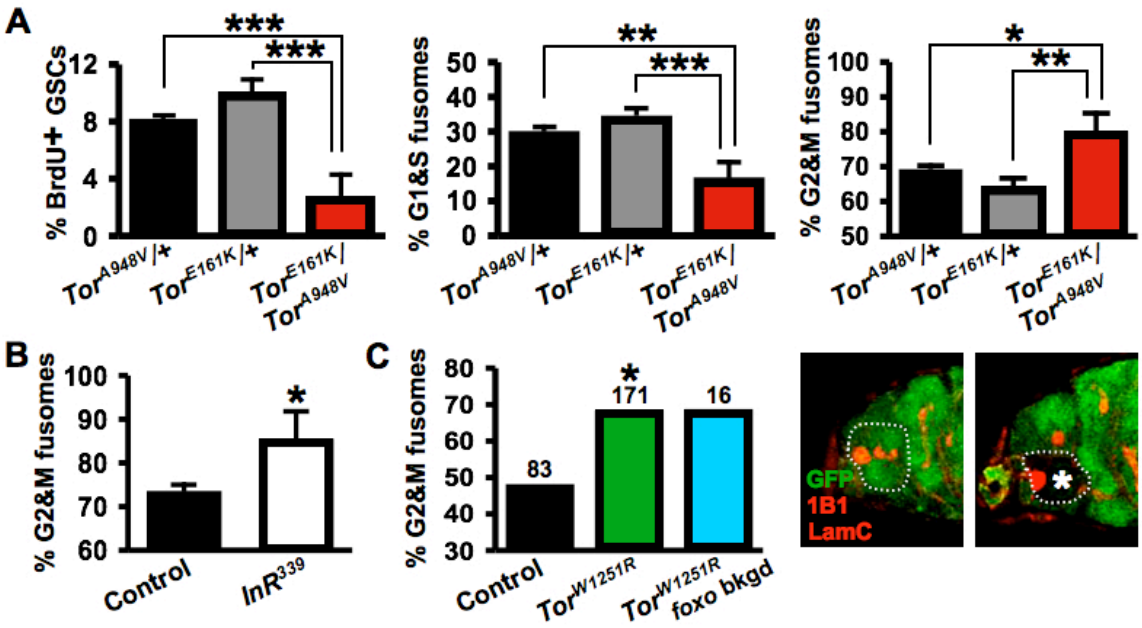

Figure 3.2. TOR and insulin signaling control GSC progression through G2 cell-autonomously. (**A**) Frequencies of BrdU-positive (BrdU+) GSCs or GSCs displaying "G1 and S" (G1&S) or "G2 and M" (G2&M) fusome morphologies in heterozygous control and Tor^{E161K}/Tor^{A948V} hypomorphic females. (**B**) Control experiment showing frequencies of InR^{339} GSCs versus neighboring control GSCs displaying "G2 and M" fusome morphologies within mosaic germaria. (**C**) Frequencies of Tor^{W1251R} GSCs versus neighboring control GSCs displaying "G2 and M" fusome morphologies within mosaic germaria. *foxo* bkgd, Tor^{W1251R} clones generated in $foxo^{21}/foxo^{25}$ background. Example of a mosaic germarium with one control GSC (GFP-positive, "fusing" fusome morphology) and one Tor^{W1251R} mutant GSC (GFP-negative, "round" fusome morphology, marked by an asterisk) is shown to the right. Images represent different optical slices from the same germarium, and GSCs are outlined. 1B1 and LamC (red) stain fusomes and cap cell nuclear membranes respectively. Numbers above bars indicate number of GSCs analyzed. Error bars, s.d. *, $P<0.04$. **, $P<0.006$. ***, $P<0.002$.

a null. In mosaic germaria, the ratio of the number of progeny (i.e. cystoblasts and cysts) from the *Tor* mutant GSC to the number of progeny from the control GSC was markedly reduced relative to the corresponding ratio in mock mosaic germaria (Table 3.1; see Figure 3.4A), consistent with the slower proliferation of *Tor* mutant GSCs.

To directly test for an intrinsic effect of *Tor* on the cell cycle, we analyzed fusome morphology in genetic mosaics. As a control experiment, we analyzed germaria mosaic for an insulin receptor mutation, InR^{339} (Figure 3.2B), and found an increased frequency of "G2 and M" fusomes, in accordance with the known requirement for *InR* in GSC proliferation via G2 (Hsu et al., 2008). Similarly, Tor^{W1251R} GSCs in mosaics had an increased frequency of "G2 and M" fusomes relative to neighboring control GSCs (Figure 3.2C), consistent with an intrinsic requirement for G2 progression. Despite the similar trend, however, the frequencies of "G2 and M" fusomes in Tor^{W1251R} and control GSCs in mosaics were both reduced relative to frequencies in whole *Tor* mutant and control females, respectively, suggesting either communication between GSCs in mosaics, or background differences.

Both the insulin pathway and TOR are intrinsically required for normal GSC G2 progression. Thus, TOR regulation of G2 could be insulin dependent or independent (Figure 3.1B). In *InR* mutants, removal of the downstream negative regulator *foxo* rescues the G2 delay (Hsu et al., 2008). We therefore reasoned that if TOR acts through InR/PI3K/FOXO to regulate G2, *Tor foxo* double mutants should reverse the *Tor* mutant G2 delay. Because $Tor^{W1251R}/Tor^{E161K}; foxo^{21}/foxo^{25}$ flies were inviable, we generated *Tor* mosaics in a $foxo^{21}/foxo^{25}$ background. Still, this genotype exhibited reduced adult viability, precluding GSC cell cycle analyses. Instead, we measured the ratio of *Tor*

Table 3.1
***Tor* is required for germline cyst division, growth, and vitellogenesis**

Strain	Time[a]	Germline Cyst Proportions[b]	% Dying Cysts[c]	Cyst Growth Rate[d]	Progression into Vitellogenesis[e]
Control	6	0.92 (773)[f]	15.9% (69)[g]	100% (29)[h]	Yes (24)[i]
	10	1.02 (396)	18.0% (50)	100% (26)	Yes (14)
Tor^{R248X}	6	0.37 (206)	28.0% (25)	--	No (6)
Tor^{P2293L}	6	0.29 (161)	30.6% (72)	27% (6)	No (15)
	10	0.28 (81)	36.5% (52)	26% (10)	No (5)
Tor^{W1251R}	6	0.35 (115)	14.7% (34)	48% (25)	No (22)
	10	0.41 (453)	37.2% (43)	27% (12)	No (66)
Tor^{W1251R} $Thor^{2}$					
	10	0.29 (162)	--	26% (5)	No (8)
Control*; $FOXO^{j}$*					
	10	0.92 (72)	--	100% (14)	Yes (8)
Tor^{W1251R} ;					
$FOXO^{j}$	10	0.43 (89)	--	56% (3)[k]	No (4)
InR^{E19}	10	0.61 (159)	--	40% (9)	No (6)
InR^{E19} $FOXO^{25}$	10	1.16 (257)	--	50% (25)	No (19)
Control	4	0.74 (318)	--	--	--
$TSC1^{Q87X}$	4	0.64 (329)	--	--	--
	10	N/A	--	160% (15)	Yes (14)
$TSC1^{Q87X}$ InR^{E19}	4	0.39 (225)	--	--	--
	10	N/A	--	160% (37)	Yes (37)

[a]Number of days after heat-shock (AHS).
[b]Cyst proportions are expressed as a ratio of GFP- or β-gal marker-negative cystoblasts and cysts to the total number of marker-positive cysts per germarium.
[c]The percentage of dying cysts is the number of germaria with at least one Apoptag®-positive cyst divided by the total number of germaria analyzed.
[d]See methods for explanation of cyst growth rate measurements.
[e]Percentage of GFP- or β-gal-negative cysts past stage 7 indicate progression through vitellogenesis.
[f]The number of cystoblasts and cysts analyzed are shown in parentheses
[g]The number of germaria analyzed
[h]The number of GFP- or β-gal-negative cysts analyzed
[i]The number of ovarioles analyzed with cysts past vitellogenesis
[j]Wildtype or *Tor* mutant clones were generated in $FOXO^{21}/FOXO^{25}$ mutant females. Small size is due to fewer *ywhsflp; FRT40A* Tor^{W1251R}*/ FRT40A ArmZ;* $FOXO^{21}/FOXO^{25}$ females eclosing in fewer numbers and being more sensitive to heat-shock
[k]Growth rate is not statistically different from that of Tor^{W1251R} mutant cysts.

mutant to control GSC progeny in the $foxo^{21}/foxo^{25}$ background, and found that loss of *foxo* does not rescue the reduced proportions observed in a wild-type background (Table 3.1; see Figure 3.4A). As expected, loss of *foxo* rescues the low *InR* mutant to control GSC progeny ratio of *InR* mosaics (Table 3.1). Cyst death contributes to the low *Tor* cyst proportion ratio (see below); however, the fact that removal of *foxo* does not result in a partial cyst proportion rescue suggests that *Tor* controls GSC proliferation largely independently of the insulin pathway, although insulin signaling upstream of FOXO may provide a minor contribution to TOR activation.

TOR activity is required for GSC maintenance

Five to seven-day old Tor^{W1251R}/Tor^{E161K} females had fewer GSCs per germarium (1.8± 0.7, *n*= 472) than controls (2.8± 0.7, *n*= 557). To test if *Tor* is intrinsically required for GSC maintenance, we performed a relative GSC maintenance assay in *Tor* mosaics (Figure 3.3). Control GSCs were lost slowly (Figure 3.3A,D), as expected (Hsu and Drummond-Barbosa, 2009; Wang and Lin, 2005; Xie and Spradling, 1998). In contrast, Tor^{P2293L} and Tor^{W1251R} GSCs were lost significantly faster (Figure 3.3B,D). No TUNEL-positive GSCs were detected in 226 germaria with mosaic *Tor* germline, suggesting that *Tor* mutant GSCs are not lost by apoptosis. TOR activity is known to control autophagy (Chang et al., 2009), but inactivation of the autophagy pathway by an *Atg7* mutation failed to rescue the *Tor* mutant GSC loss (Table 3.2). Thus, the *Tor* GSC maintenance defect is likely caused by differentiation, although we cannot exclude the possibility that GSCs die by a distinct mechanism.

Given the increased loss of *Tor* mutant GSCs, we reasoned that high TOR activity might promote GSC maintenance. We generated germline clones mutant for *Tsc1*, which

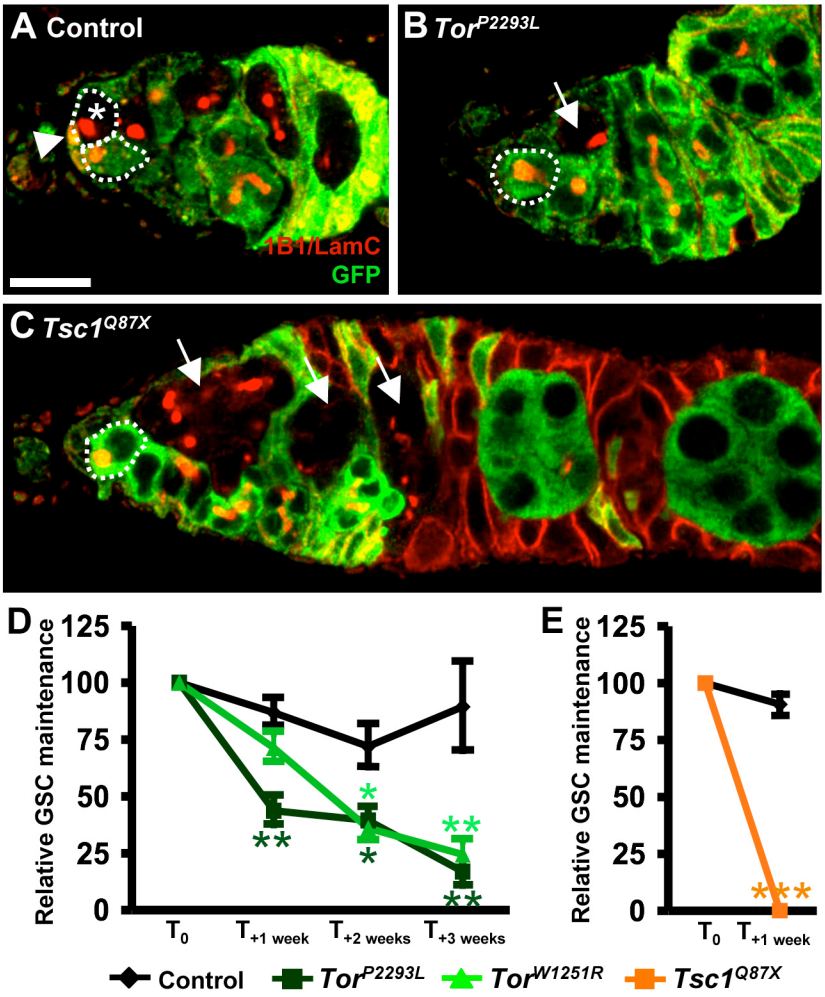

Figure 3.3. Normal TOR activity promotes GSC maintenance. (A-C) Control, *Tor*^{P2293L}, and *Tsc1*^{Q87X} mosaic germaria. GFP (green), control cells. 1B1 (red), fusomes and follicle cell membranes. LamC (red), cap cell nuclear membranes (arrowhead). GSCs are outlined. Asterisk, GFP-negative GSC. Arrows, *Tor*^{P2293L} or *Tsc1*^{Q87X} cysts derived from GSCs subsequently lost. **(D-E)** Quantification of relative GSC maintenance. Fraction of mosaic germaria containing a GFP-negative GSC was arbitrarily set at 100% at time point T_0 (4 days after clone induction), and data from one week ($T_{+1\ week}$), two weeks ($T_{+2\ weeks}$), or three weeks ($T_{+3\ weeks}$) later were normalized to T_0. Error bars, s.e.m. *, $P<0.01$. **, $P<0.005$. ***, $P<0.001$. Scale bar, 10 μm.

Table 3.2
Tor* mosaic GSC loss and low follicle cell numbers are independent of *Atg7

Strain[a]	% GSC loss[b]	% GFP-negative follicle cells[c]
FRT40A control	4.8% (21)[d]	46.2% (4673)[e]
FRT40A control (*Atg7*^{d4} bkgd)[f]	5.0% (20)[g]	42.4% (5565)*[h]
Tor^{W1251R}	27.5% (40)	12.1% (3629)
Tor^{W1251R} (*Atg7*^{d4} bkgd)[f]	20.0% (40)[g]	6.0%[g] (4368)*[h]
Tor^{P2293L}	44.1% (34)	17.1% (6401)
Tor^{P2293L} (*Atg7*^{d4} bkgd)[f]	35.0% (23)[g]	5.0%[g] (2945)*[h]

[a]Clones were analyzed 10 days after clone induction.
[b]Percentage of germaria with GFP-negative cystoblasts/cysts but lacking their GFP-negative GSC mother (which indicates recent GSC loss) relative to the total number of ovarioles with a mosaic germ line.
[c]Percentage of GFP-negative follicle cells relative to the total number of follicle cells analyzed.
[d]Total number of germaria with mosaic germline analyzed is shown in parentheses.
[e]Total number of follicle cells analyzed is shown in parentheses.
[f]Clones were generated in *Atg7*^{d4} homozygous background.
[g]There is no statistically significant difference between results in wild-type versus *Atg7*^{d4} background.
[h]The *Atg7*^{d4} mutation does not rescue of the *Tor* mutant phenotype, but the percentage of GFP-negative follicle cells is significantly smaller in the *Atg7*^{d4} background: *, $P<0.001$.

encodes an upstream negative regulator of TOR (Tapon et al., 2001). Surprisingly, *Tsc1*^{Q87X} GSCs exhibit an even greater loss rate than *Tor* mutant GSCs, such that within a week from the initial measurement, no *Tsc1*^{Q87X} GSC remains in the niche (Figure 3.3C,E). Optimal levels of TOR activity may therefore be required for proper GSC maintenance. Alternatively, TSC1 may be required for GSC maintenance independently of TOR.

TOR controls germline cyst proliferation and survival

As described above, *Tor* mutant GSCs produce markedly fewer progeny relative to control GSCs in mosaics (Figure 3.3A; Table 3.1), partially due to reduced proliferation (Figure 3.1). *Tor*, however, can also regulate cell survival (Chang et al., 2009). Indeed, compared to control mosaics, *Tor* mosaics show increased frequency of TUNEL-positive cysts (Figure 3.4B; Table 3.1), suggesting apoptosis of *Tor* mutant cysts.

To test whether *Tor* mutant cysts die at specific stages, we quantified the frequency of control and *Tor* mutant cystoblasts, and 2-, 4-, 8-, and 16-cell cysts (normalized per GSC). Stages were identified by fusome morphology, which becomes progressively more branched as cyst cell number increases (de Cuevas and Spradling, 1998). While the frequencies of cystoblasts and 2-cell cysts per *Tor* mutant GSC were indistinguishable from those of controls, no *Tor*^{P2293L} 8 or 16-cell cysts were observed in mosaic germaria, and the *Tor*^{W1251R} allele yielded fewer 8-cell cysts and no 16-cell cysts at 10 days after clone induction (Figure 3.4C). Thus, most *Tor* mutant cysts apparently die at the 8- and 16-cell stages. Occasionally, we observe follicles in which *Tor* mutant

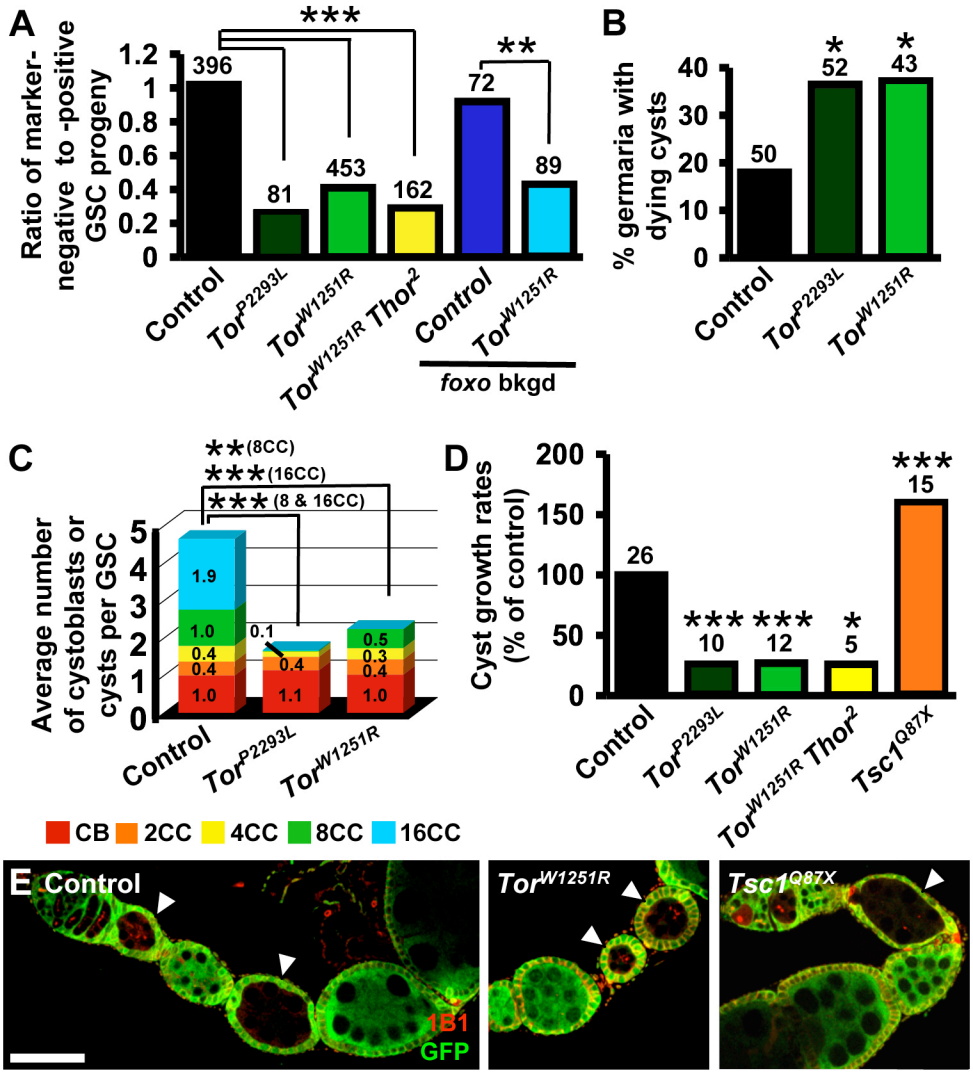

Figure 3.4. TOR regulates germline cyst proliferation, growth, and survival independently of 4E-BP and FOXO. (A) Ratios of marker-negative to -positive GSC progeny in mosaic germaria. *foxo* bkgd indicates clones induced in $foxo^{21}/foxo^{25}$ females. **(B)** Percentage of germaria with TUNEL-marked dying cystoblasts/cysts. **(C)** Average number of marker-negative cystoblasts (CB) or cysts (2CC, 2-cell cyst; 4CC, 4-cell cyst; 8CC, 8-cell cyst; 16CC, 16-cell cyst) normalized per marker-negative GSC in control and *Tor* mosaics. **(D)** Growth rates (normalized to control) for marker-negative cysts in mosaics. Numbers above bars indicate numbers of cystoblasts and cysts (A), mosaic germaria (B), or cysts (D) analyzed. *, $P \leq 0.04$. **, $P \leq 0.02$. ***, $P \leq 0.001$. **(E)** Control, Tor^{W1251R} or $Tsc1^{Q87X}$ cysts (arrowheads) in mosaics. 1B1 (red), cell membranes. GFP (green), wild-type cells. Scale bar, 50 μm.

cysts with fewer than 16 cells are encapsulated with a neighboring wild-type 16-cell cyst, which may contribute to *Tor* mutant cyst reduction. Finally, the number of *Tor* mutant cystoblasts and 2-cell cysts are similar to controls despite reduced *Tor* mutant GSC proliferation rates, suggesting proportionately slowed *Tor* mutant cyst division.

TOR controls germline cyst growth

Although most *Tor* mutant cysts die early, a few of those cysts form a follicle. These are usually 16-cell cysts (or sometimes 8-cell cysts), and are more frequently observed at 6 rather than 10 days after clone induction. *Tor* mutant cysts grow at about 25% of the wild-type rate, suggesting a significant growth delay (Figure 3.4D,E). In fact, follicles of Tor^{P2293L} cysts do not grow past the stage 2 size, while follicles of hypomorphic Tor^{W1251R} cysts reach the stage 3 or 4 size (Figure 3.4E; Table 3.1). It is possible that these rare escaper follicles result from TOR protein perdurance in the initial progeny from a newly mutant GSC. In fact, *Tor* null mutants can develop to larval stage 2 before death, presumably due to perdurance of maternally derived TOR protein for about two to three days (Zhang et al., 2000). Conversely, $Tsc1^{Q87X}$ cysts have increased follicle growth rates (Figure 3.4D,E; Table 3.1), consistent with the increased imaginal cell growth and proliferation observed upon TSC1/2 loss (Gao et al., 2002).

TOR control of cyst proliferation, growth, and survival is 4E-BP-independent

Many of *Tor* functions reflect its role in protein translation control via downstream targets eukaryotic translation initiation factor 4E (eIF4E) binding protein (4E-BP, encoded by *Thor* in *Drosophila*) and S6 kinase (S6K) (Miron and Sonenberg, 2001; Teleman et al.,

2008). 4E-BP is a conserved translational inhibitor that binds eIF4E, a cap-dependent translational activator, and 4E-BP phosphorylation by TOR releases eIF4E inhibition (Hay and Sonenberg, 2004). Accordingly, eIF4E overexpression leads to increased cell size in mammalian cells and *Drosophila* (Lachance et al., 2002; Lazaris-Karatzas et al., 1990). To test if reduced TOR activity affects cyst numbers and growth rates via 4E-BP-mediated translational inhibition, we analyzed Tor^{W1251R} $Thor^{2}$ clones. Neither the proportion of Tor^{W1251R} $Thor^{2}$ to control germline cysts nor the growth rates of Tor^{W1251R} $Thor^{2}$ cysts were statistically different from Tor^{W1251R} mosaics (Figure 3.4A,D; Table 3.1), indicating that *Thor* is dispensable for these effects. Instead, TOR may control translation in the germline primarily via S6K or Myc (Miron and Sonenberg, 2001; Teleman et al., 2008). In fact, mutation of *S6K* in mosaic ovarioles results in similar defects to those caused by *Tor* mutation (L. LaFever and D. Drummond-Barbosa, unpublished results), and Myc has been shown to act downstream of TOR (Teleman et al., 2008) and to control ovarian cell size (Maines et al., 2004).

TOR mediates the effects of insulin signaling on germline cyst growth, but also receives additional inputs

Tor and the insulin pathway are required to control GSC proliferation and cyst growth (this study) (Hsu et al., 2008; LaFever and Drummond-Barbosa, 2005), and several studies showed that insulin signaling is among inputs integrated by TOR (Grewal, 2009; Hay and Sonenberg, 2004). Although the effects of insulin signaling on GSC division are mediated by *foxo* (Hsu et al., 2008), it is unknown whether *foxo* mutation suppresses the slow growth of *InR* mutant cysts, potentially mediated via *Tor* and/or *foxo*. As expected, the low ratio of InR^{E19} to control GSC progeny (which reflects slower proliferation of InR^{E19}

GSCs) is reversed by the *foxo*^{25} mutation, but not by the *Tsc1*^{Q87X} mutation, in double mutant mosaics (Table 3.1). The reverse occurs in cyst growth control. *InR*^{E19} cysts have markedly reduced growth rates (LaFever and Drummond-Barbosa, 2005) (Table 3.1), while *InR*^{E19} *Tsc1*^{Q87X} cysts have higher growth rates than control cysts in mosaic ovarioles (Table 3.1). In contrast, *InR*^{E19} *foxo*^{25} cysts had cyst growth rates comparable to those of *InR*^{E19} cysts in mosaic ovarioles (Table 3.1). Thus, although the insulin pathway controls the proliferation of GSCs via *foxo*, it apparently controls the growth of their differentiating progeny via *Tor*. Nevertheless, null *Tor* mutant cysts have a more severe growth delay relative to null *InR* cysts (LaFever and Drummond-Barbosa, 2005), strongly suggesting that additional dietary factors besides insulin signaling modulate cyst growth via TOR.

TOR is necessary for FSC proliferation, but not maintenance

Tor is intrinsically required for GSC proliferation and maintenance; therefore, we wondered if *Tor* may similarly control FSCs as a mechanism to coordinate the response of both stem cell types to diet-dependent signals. To determine if *Tor* is required for FSC proliferation, we identified FSCs based on lineage tracing and measured S phase frequencies in control versus *Tor* mutant FSCs (Figure 3.5A). Approximately half of control GFP-negative FSCs are BrdU-positive, while this frequency is drastically reduced for *Tor*^{P2293L} or *Tor*^{W1251R} FSCs (Figure 3.5B), indicating that *Tor* is required for normal FSC proliferation.

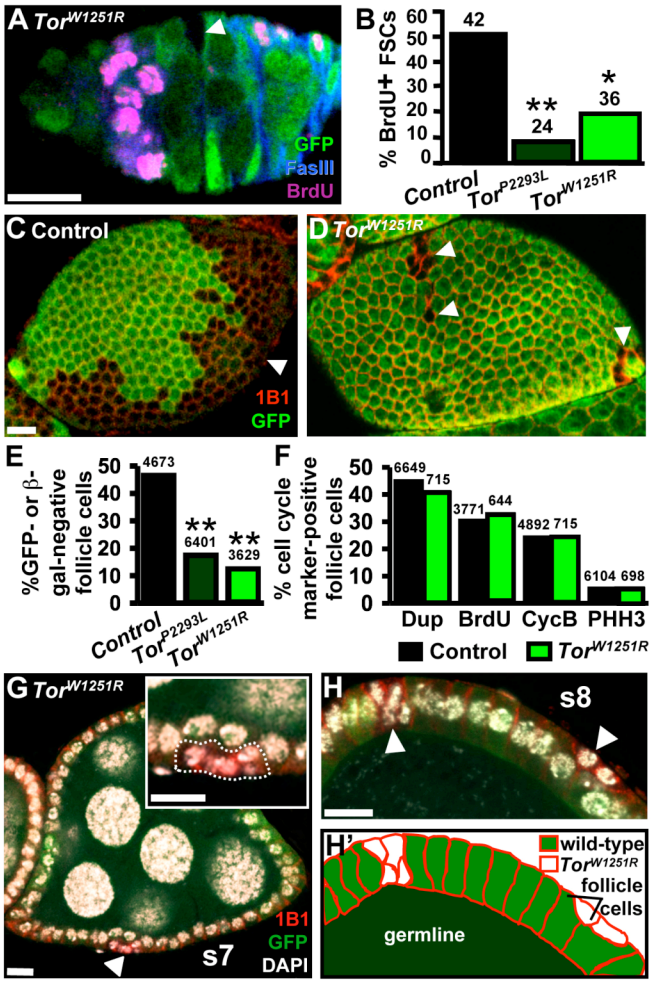

Figure 3.5. TOR controls FSC, but not follicle cell, proliferation. (**A**) GFP-negative *Tor*^{W1251R} FSC (arrowhead) in *Tor*^{W1251R} mosaic germarium. GFP (green) labels heterozygous cells. Fasciclin III (FasIII, blue) labels all but immediate FSC daughters. BrdU (pink, due to mouse and rat secondary antibody cross-reaction) marks cells in S. (**B**) BrdU-positive control, *Tor*^{P2293L}, or *Tor*^{W1251R} FSC frequencies in mosaics. (**C,D**) Control and *Tor*^{W1251R} mosaic follicle cell monolayers 10 days after clone induction. 1B1 (red), follicle cell membranes. Arrowheads, GFP-negative follicle cell clones. (**E**) Percentage of GFP- or β-gal-negative follicle cells relative to total follicle cell number. (**F**) Percentage of GFP- or β-gal-negative follicle cells positive for Dup (G1 and S), BrdU (S), CycB (G2 and M) or PHH3 (M) relative to total marker-negative follicle cell number in stage 2 to 6 follicles. (**G**) Stage 7 follicle containing *Tor*^{W1251R} follicle cells (arrowhead; outlined in inset) that lost contact with underlying germline. DAPI (white) labels DNA. (**H**) Posterior region of stage 8 follicle containing *Tor*^{W1251R} follicle cell clones (arrowheads) and outlined in (**H'**). Numbers above bars indicate total number of GFP-negative FSCs (**B**) or marker-negative follicle cells (**E,F**) analyzed. * $P<0.003$, **, $P<0.001$. Scale bars, 10 μm.

To determine if *Tor* activity controls FSC maintenance, we performed a FSC maintenance assay in mosaic ovarioles analyzed at different times after clone induction (see Materials and Methods). Although there was considerable experimental variability (Table 3.3), *Tor* and *Tsc1* do not appear to play a major role in FSC maintenance.

TOR does not affect follicle cell proliferation

Given that *Tor* controls FSC division, we asked whether *Tor* also regulates proliferation of their progeny. First, we compared *Tor* mutant to control follicle cell numbers in mosaic ovarioles (Figure 3.5C-E). In control mosaics containing wild-type GFP-positive and -negative FSCs, approximately equal numbers of follicle cells derived from each FSC result in a one-to-one ratio of progeny (Figure 3.5C,E) (Margolis, 1995). In contrast, *Tor* mosaics have a significantly reduced ratio of Tor^{P2293L} or Tor^{W1251R} to control follicle cells (Figure 3.5D,E). Similar results were observed for InR^{E19} or InR^{E19} $foxo^{25}$ follicle cells (LaFever and Drummond-Barbosa, unpublished results), suggesting that insulin signaling controls follicle cell numbers independently of *foxo*. Although we had concluded that *InR* is not required cell autonomously in follicle cells (LaFever and Drummond-Barbosa, 2005), retrospective analyses revealed our previous misinterpretation due to weak GFP staining (heterozygous *InR* follicle cells with one copy of GFP mistaken for GFP-negative *InR* mutant follicle cells). These data suggest that *Tor* controls follicle cell survival and/or proliferation, given that the reduced *Tor* mutant FSC proliferation cannot account for the dramatic reduction in *Tor* mutant follicle cell number (Nystul and Spradling, 2009).

Table 3.3

***Tor* does not appear to regulate FSC maintenance**

Strain	4 days[a]	8 days	11 days	12 days	18 days	25 days
			Experiment 1:			
FRT40A control	57%[b] (101)[c]	55% (93)	--	47% (72)	--	--
Tor^{P2293L}	95% (93)	70% (98)	--	69% (75)	--	--
Tor^{W1251R}	87% (195)	54% (214)	--	39% (198)	--	--
FRT82B control	92% (100)	71% (108)	--	61% (81)	--	--
$Tsc1^{Q87X}$	81% (99)	84% (115)	--	66% (76)	--	--
			Experiment 2:			
FRT40A control	--	--	40% (67)	--	33% (57)	13% (62)
Tor^{P2293L}	--	--	43% (28)	--	24% (51)	5.0% (40)
Tor^{W1251R}	--	--	30% (77)	--	20% (50)	5.5% (55)
			Experiment 3:			
FRT40A control	--	--	25% (67)	--	41% (63)	9.1% (55)
Tor^{P2293L}	--	--	40% (35)	--	21% (67)	1.6% (61)
Tor^{W1251R}	--	--	20% (70)	--	3.4% (87)	13% (55)
			Experiment 4:			
FRT40A control	--	--	46% (50)	--	37% (49)	11% (56)
Tor^{P2293L}	--	--	15% (47)	--	31% (51)	17% (41)
Tor^{W1251R}	--	--	41% (56)	--	16% (70)	14% (50)
			Experiment 5:			
FRT40A control	62% (183)	--	--	45% (121)	--	--
Tor^{P2293L}	66% (67)	--	--	58% (139)	--	--
Tor^{W1251R}	41% (119)	--	--	23% (141)	--	--

[a]Number of days after clone induction.
[b]Percentage of germaria containing at least one GFP-negative FSC.
[c]Total number of germaria analyzed is shown in parentheses.

To directly test if *Tor* mutant follicle cells have reduced proliferation, we analyzed Tor^{W1251R} follicle cells using Cyclin B (G2 and M), BrdU (S), PHH3 (M) and Double parked (Dup, late G1 and S) (Thomer et al., 2004; Whittaker et al., 2000). Surprisingly, the frequencies of cells positive for these cell cycle markers were indistinguishable between control and *Tor* mutant follicle cells (Figure 3.5F), indicating that *Tor* does not modulate follicle cell proliferation, unlike for FSCs. Thus, *Tor* controls follicle cell numbers by modulating their survival.

TOR promotes follicle cell survival independently of suppression of apoptotic or autophagic cell death

Tor modulates apoptosis and autophagy in many systems (Chang et al., 2009; Diaz-Troya et al., 2008). We therefore examined apoptosis incidence in control versus *Tor* mutant follicle cells in mosaics using TUNEL labeling and activated Caspase-3 antibody staining. Negligible numbers of either TUNEL-positive or activated Caspase-3-positive follicle cells were observed in either control or Tor^{W1251R} mosaics (9 to 41 mosaic ovarioles analyzed for each genotype/condition), suggesting that *Tor* mutant follicle cells are not eliminated by apoptosis.

If *Tor* mutant follicle cell number reduction is a result of autophagic death, then blocking autophagy in *Tor* mosaics should increase *Tor* mutant follicle cell numbers to wild-type levels. Null mutations in *Atg7* result in 85-95% reduction in autophagy at the ultrastructural level, but homozygous females are still viable and fertile (Juhasz et al., 2007; Juhasz and Neufeld, 2008). We therefore analyzed Tor^{W1251R} mosaic follicle cells in $Atg7^{d4}$ homozygotes. Well-fed $Atg7^{d4}$ females exhibited vitellogenic follicle degeneration and stage 14 oocyte accumulation, which normally occur under starvation and are

consistent with impaired autophagy-dependent nutrient mobilization from the fat body (a storage tissue) (Drummond-Barbosa and Spradling, 2001; Grewal and Saucedo, 2004; Hsu et al., 2008). Furthermore, degenerating follicles accumulate, in agreement with autophagy being required for clearance of dying follicles (Pritchett et al., 2009). Despite these clear indications that autophagy is disrupted in $Atg7^{d4}$ females, the ratio of Tor^{P2293L} or Tor^{W1251R} to control follicle cells remained unchanged in the $Atg7^{d4}$ background (Table 3.2), suggesting that reduction in *Tor* mutant follicle cell numbers does not require autophagic death.

Alternative mechanisms may explain the reduced survival of *Tor* mutant follicle cells. When the entire follicle cell monolayer is homozygous for Tor^{W1251R}, follicle development is supported through stage 9 (see Fig. 3.9), suggesting that surrounding wild-type cells may contribute to the reduced *Tor* mutant follicle cell numbers. Intriguingly, *Tor* mutant follicle cells surrounded by wild-type follicle cells often appeared to be undergoing extrusion from the mosaic follicle cell layer. Approximately 65% of mosaic ovarioles containing *Tor* mutant follicle cells (15 out of 22 for Tor^{P2293L} mosaics, and 14 out of 22 for Tor^{W1251R} mosaics) displayed at least one mutant cell above or below the wild-type monolayer, which was never observed in control mosaics (Figure 3.5G,H). As described above, extruded *Tor* mutant follicle cells were negative for activated Caspase 3. These results suggest that wild-type neighbors eliminate *Tor* mutant follicle cells without apparent apoptosis.

TOR regulates follicle cell size and timely exit from the follicle cell mitotic program

We also examined whether *Tor* controls follicle cell size. Follicle cells undergo mitotic cell divisions until stage 6, then transition to an endoreplicative program and

greatly increase in size (Royzman and Orr-Weaver, 1998). During mitotic stages, Tor^{P2293L} or Tor^{W1251R} follicle cells are significantly smaller than neighboring control cells, while in endoreplicative stages, this difference is more pronounced (Figure 3.6), demonstrating that *Tor* controls not only follicle cell number, but also size.

The more pronounced difference in *Tor* mutant follicle cell size in endoreplicative stages led us to hypothesize that *Tor* may control the mitosis to endoreplication transition. Mitotic follicle cells go through G1, S, G2 and M, while endoreplicating follicle cells alternate between G1 and S (Lee and Orr-Weaver, 2003; Wu et al., 2008). To directly determine whether *Tor* mutant follicle cells continue to divide mitotically beyond stage 6, we examined the PHH3 (M) and CycB (G2 and M) markers in *Tor* mutant follicle cells (Figure 3.7A-C). We analyzed BrdU-incorporation as a control (S-phase present in both programs), and no significant difference was observed between control and Tor^{W1251R} follicle cells (Figure 3.7C). As expected, neighboring control follicle cells at stages 7 and 8 were all negative for PHH3 and CycB (Figure 3.7A-C), unlike earlier mitotic follicle cells (see Figure 3.5F). In contrast, some of the Tor^{W1251R} follicle cells at stages 7 and 8 were positive for PHH3 (4.4%) and CycB (26%) (Figure 3.7A-C), suggesting that Tor^{W1251R} follicle cells divide mitotically past stage 6.

The occurrence of PHH3- and CycB-positive Tor^{W1251R} follicle cells at stages 7 and 8 could reflect a consistent defect of Tor^{W1251R} follicle cell mitotic exit, or a defect in a subset of Tor^{W1251R} follicle cells. We therefore analyzed expression of Dup, a conserved pre-replicative complex component (Thomer et al., 2004; Whittaker et al., 2000), in mosaic follicle cell layers. Dup has a robust and dynamic G1 and S pattern in mitotic follicle cells, but becomes more diffuse during endoreplication, when it is confined to G1

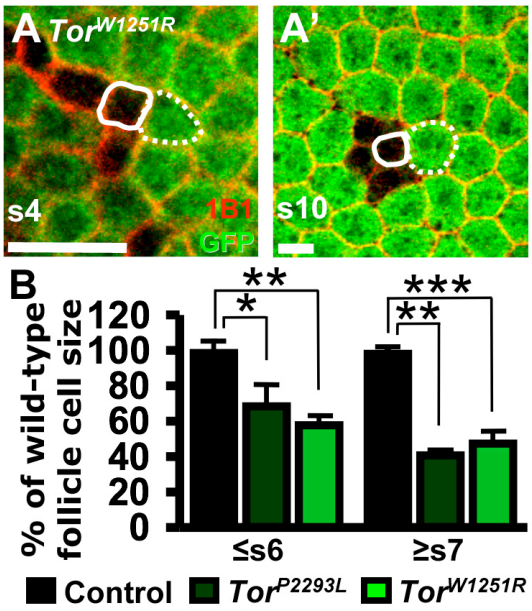

Figure 3.6. TOR controls follicle cell growth. (**A,A'**) Tor^{W1251R} follicle cells in stage 4 (s4) and stage 10 (s10) mosaic follicles. GFP (green) labels control cells. 1B1 (red) labels cell membranes. Solid and dashed outlines indicate a Tor^{W1251R} or control follicle cell, respectively. Scale bar, 10 μm. (**B**) GFP-negative Tor^{P2293L} or Tor^{W1251R} follicle cell size as a percentage of GFP-positive neighboring control follicle cell size in stages 6 and younger (≤ s6) or stages 7 and older (≥ s7). Error bars, s.d. *, $P<0.01$. **, $P<0.002$. ***, $P<0.0001$.

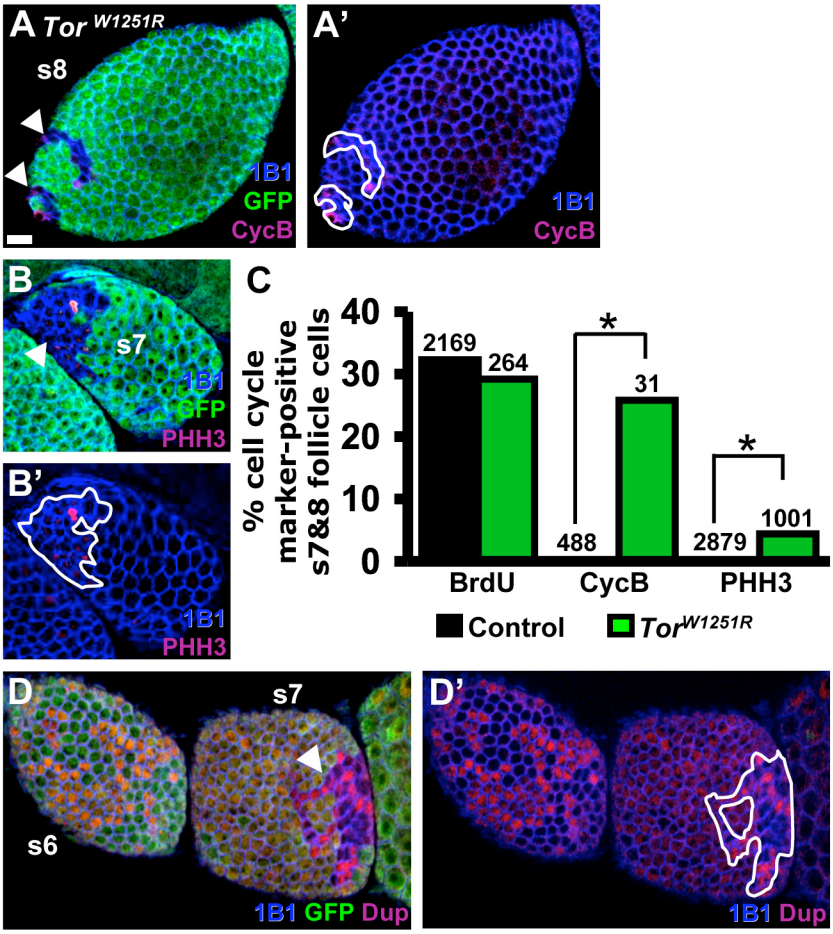

Figure 3.7. *Tor* promotes timely follicle cell mitosis-to-endoreplication transition. (**A,B**) Tor^{W1251R} follicle cells in stage 7 and 8 mosaic follicles. GFP (green) labels control cells. 1B1 (blue) labels cell membranes. CycB (red) marks G2 or M. PHH3 (red) marks M. Tor^{W1251R} follicle cell clones are indicated by arrowheads (**A,B**) and outlined (**A',B'**). (**C**) Frequencies of BrdU-, CycB- or PHH3-positive Tor^{W1251R} follicle cells and neighboring control cells in stages 7 and 8. Total number of control or Tor^{W1251R} follicle cells analyzed is indicated above bars. *, $P<0.0001$. (**D,D'**) Double parked (Dup, red) expression in stage 6 and 7 Tor^{W1251R} mosaic follicles. Tor^{W1251R} follicle cell clone is indicated by an arrowhead (**D**) and outlined (**D'**). Scale bar, 10 μm.

(Thomer et al., 2004). *Tor*^{W1251R} follicle cells in stages 6 and later exhibit the dynamic Dup pattern characteristic of a mitotic cell cycle in contrast to the diffuse pattern of neighboring control follicle cells (Figure 3.7D,D'), suggesting that all *Tor*^{W1251R} follicle cells have a defect in endoreplication entry. We could not determine if *Tor*^{W1251R} follicle cells eventually endoreplicate due to prohibitively low frequencies of *Tor* mutant follicle cell clones beyond stage 8. Thus, reduced *Tor* activity leads to either a delay or a block in the mitosis to endoreplication switch.

Follicle cell TOR activity influences underlying cyst growth and vitellogenesis

Germline cyst growth and surrounding follicle cell proliferation are coordinated (LaFever and Drummond-Barbosa, 2005; Maines et al., 2004; Wang and Riechmann, 2007). Since *Tor* intrinsically controls follicle cell number, we asked whether *Tor* mutant follicle cells influence underlying wild-type cyst growth. If *Tor*^{P2293L} or *Tor*^{W1251R} follicle cells cover at least one-third of a wild-type cyst, there is a significant growth delay, evident by larger wild-type follicles positioned anteriorly (Figure 3.8A-C; Table 3.4). Conversely, wild-type cysts surrounded by *Tsc1*^{Q87X} follicle cells have accelerated growth (Figure 3.8D; Table 3.4). These results indicate that, although *Tor* does not control follicle cell proliferation, follicle cell TOR activity affects growth of the underlying germline, presumably via effects on follicle cell number and/or growth.

Follicle cell *Tor* activity also influences vitellogenesis progression of underlying oocytes. We rarely found mosaic ovarioles with a fully *Tor* mutant follicle cell monolayer and wild-type germline. Vitellogenesis was supported in only 2 out of 12 examples of such ovarioles containing *Tor*^{W1251R} follicle cells, which could reach a small stage 10 follicle before degenerating (Figure 3.9). For *Tor*^{P2293L} follicle cells, no vitellogenic

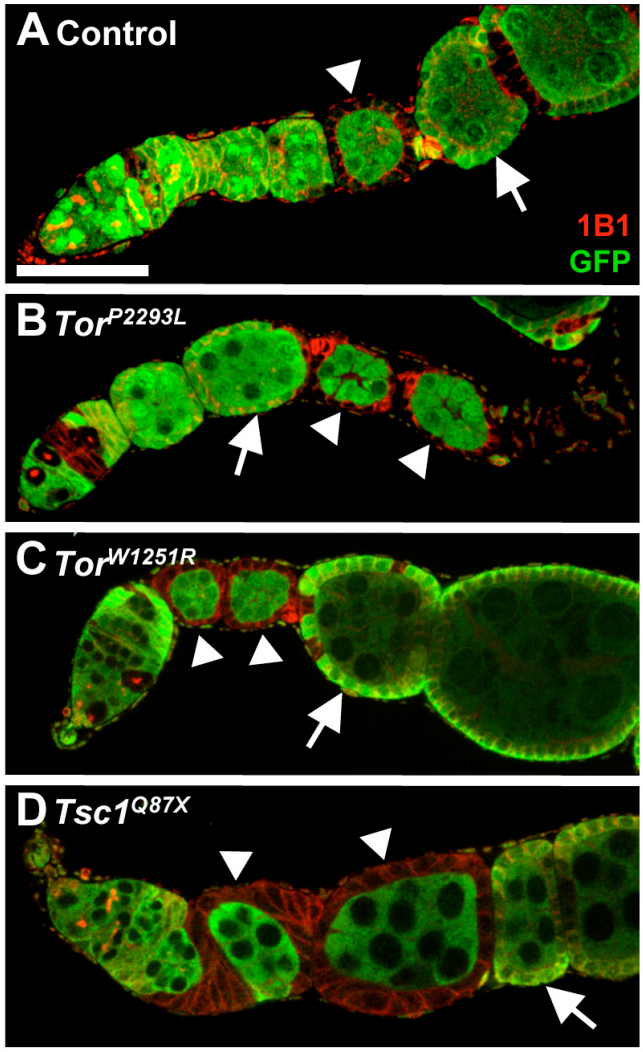

Figure 3.8. Follicle cell TOR activity influences germline growth. (**A-D**) Wild-type germline cysts completely surrounded by control, Tor^{P2293L}, Tor^{W1251R}, and $Tsc1^{Q87X}$ GFP-negative follicle cells (arrowheads). Arrows, neighboring control follicles. GFP (green), heterozygous cells. 1B1 (red), follicle cell membranes. Scale bar, 50 μm.

Table 3.4
***Tor* activity in follicle cells controls the growth of underlying germline cysts**

Strain	Time[a]	% of wild-type cysts with altered growth[b]
FRT40A control	6	delayed-0% (15)[c]
	10	delayed-0% (13)
Tor^{R248X}	6	delayed-75% (4)
Tor^{P2293L}	6	delayed-85.7% (23)
	10	delayed-93% (15)
Tor^{W1251R}	6	delayed-50% (2)
	10	delayed-95% (19)
Tor^{W1251R} $Thor^{2}$	10	delayed-100% (7)
$Tsc1^{Q87X}$	10	accelerated-80% (5)
$Tsc1^{Q87X}$ InR^{E19}	10	accelerated-80% (5)

[a]Number of days after clone induction.
[b]Percentage of wild-type germline cysts surrounded by at least one-third GFP-negative follicle
cells showing either delayed or accelerated growth (see Materials and Methods).
[c]Number of wild-type cysts surrounded by at least one-third GFP-negative follicle cells analyzed.

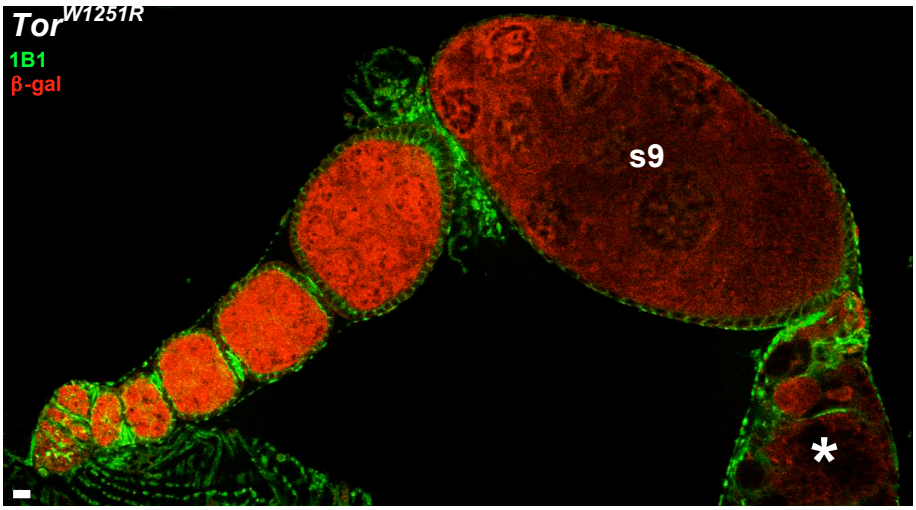

Figure 3.9. *Tor* mutant follicle cells do not support wild-type cyst growth past stage 9. *Tor* mosaic ovariole with fully mutant follicle cells and wild-type germline cysts. A degenerating follicle posterior to a stage 9 (s9) follicle is marked by an asterisk. β-gal (red, wild-type cells). 1B1 (green, follicle cell membranes). Scale bar, 10 μm.

follicles were observed in 14 ovarioles examined. These data suggest that follicle cells communicate with germ cells downstream of TOR to regulate vitellogenesis. Among plausible mechanisms would be an effect of *Tor* on the production of yolk proteins by follicle cells (Hansen et al., 2004; Hansen et al., 2005) or a more indirect effect involving the coordination between follicle cell number and germ cell development.

Discussion

Stem cells support multiple adult tissues, and they also respond to external and physiological inputs (Drummond-Barbosa, 2008). Our recent studies uncovered dietary effects on *Drosophila* ovarian stem cells (Drummond-Barbosa and Spradling, 2001; Hsu and Drummond-Barbosa, 2009; Hsu et al., 2008; LaFever and Drummond-Barbosa, 2005). Insulin signals control GSCs, their niche, and differentiating progeny; however, additional dietary mediators remain obscure. Here, we reveal strikingly specific effects of *Tor* on GSCs, FSCs, and their progeny. Coupled to studies showing the conserved role of TOR as a nutrient sensor (Wang and Proud, 2009), these results address how specific effects of a nutrient-responsive factor may contribute to the coordination between different stem cell populations and their descendents.

G2 is a major point of GSC proliferation control by diet-dependent pathways

Both insulin signals and TOR are nutrient-sensing factors (Wang and Proud, 2009) that converge on G2 to regulate *Drosophila* GSC proliferation (Hsu et al., 2008) (this study). G2 regulation in response to diet/insulin signals also occurs in *Drosophila* male GSCs and in *Caenorhabditis elegans* germline precursors (Narbonne and Roy, 2006;

Ueishi et al., 2009). Starvation promotes deleterious mutations during *Saccharomyces cerevisae* division (Marini et al., 1999), and cancer cells form repair foci during a delayed G2 upon DNA damage (Kao et al., 2001). The multitude of GSC G2 regulators may reflect a mechanism to ensure genomic integrity under poor dietary conditions.

Although TOR regulates the G1/S transition, it also modulates G2/M in *S. cerevisae*, *Schizosaccharomyces pombe*, and mammalian cells (Wang and Proud, 2009). Combined with the *Tor* role in GSC G2, the increased phosphorylation of 4E-BP specifically during M suggests that a TOR activity increase may precede the G2/M transition. Interestingly, activated TOR is highly enriched at the mitotic spindles of rat ovarian granulosa cells, and TOR inhibition by rapamycin impairs their proliferation (Yaba et al., 2008). Marked increases in S6K activity and 4E-BP1 phosphorylation in M occur in HeLa cells (Boyer et al., 2008; Heesom et al., 2001), further suggesting TOR activity cell cycle regulation as part of a conserved mechanism to tie G2/M to nutrient availability.

Specific effects of TOR on stem cell populations

Although both GSCs and FSCs require *Tor* for normal proliferation, only GSC maintenance requires optimal TOR activity. These distinctions do not reflect a fundamental difference between germline and somatic stem cells because TOR appears to control the maintenance of several, although likely not all, mammalian somatic stem cell types. In hematopoietic stem cells, *Tsc1* or *PTEN* loss results in increased TOR signaling, short-term expansion, but progressive stem cell depletion (Gan et al., 2008; Yilmaz et al., 2006). TOR activation downstream of Wnt1 overexpression leads to transiently increased

hair follicle proliferation followed by stem cell loss (Castilho et al., 2009). In contrast, *PTEN* mutant ovarian granulosa cells do not become depleted (Fan et al., 2008), despite elevated TOR activity (Adhikari et al., 2009). Because granulosa cells may derive from stem cells (Lavranos et al., 1999), it is tempting to speculate that maintenance of these stem cells may not require precise TOR regulation, similarly to *Drosophila* FSCs.

TOR differentially regulates stem cells and their progeny

Ovarian stem cells and their progeny respond to TOR differently. Reduced *Tor* activity leads to apoptosis of 8- and 16-cell cysts, but *Tor* mutant GSCs do not appear to undergo apoptotic or autophagic death. The niche may conceivably prevent GSC death. Indeed, we find no reports of GSC cell death within their *in vivo* niche. Consistent with the niche promoting GSC survival, GSCs die at higher rates when separated from somatic cells in culture (Niki, 2009). Laser ablation of the single apical niche cell causes death of *Locusta migratoria* male GSCs (Zahn et al., 2007). This model, however, does not account for normal number of *Tor* mutant cystoblasts and 2-cell cysts. Perhaps a combination of niche displacement and growth defects leads to *Tor* mutant 8- and 16-cell cyst death.

Reduced *Tor* activity slows FSC proliferation, but has no effect on the cell cycle of follicle cells. This striking difference suggests that follicle cell proliferation may be largely insensitive to direct effects of diet. Follicle cells may instead receive their primary cue to divide from the underlying germline, perhaps via the actomyosin cytoskeleton, as recently suggested (Wang and Riechmann, 2007). Consistent with this idea, when germline cyst growth is slowed down by *InR* or *Myc* mutation, surrounding wild-type

follicle cells adjust their numbers accordingly (LaFever and Drummond-Barbosa, 2005; Maines et al., 2004), although it remains to be determined if this reflects changes in follicle cell proliferation *per se*.

Tor mutant follicle cells are extruded in a competitive environment

Cell competition can occur when cell populations with different growth capacities coexist. It has been proposed that a cell senses the translational capacity of their neighbors and thus distinguishes "winner" versus "loser" cells. The "losers" undergo apoptosis and secrete factors that stimulate "winner" proliferation (Johnston, 2009). Although *Tor* regulates growth and translation (Wang and Proud, 2009), *Tor* mutant follicle cells do not exhibit apoptosis, but are instead extruded from mosaic monolayers. Apoptosis-independent extrusion of cells with compromised Decapentaplegic (Dpp, a bone morphogenetic protein family member) signaling has been reported in mosaic *Drosophila* wing disc epithelia (Gibson and Perrimon, 2005; Shen and Dahmann, 2005). This similarity suggests a possible connection between Dpp signaling and TOR.

Insulin-dependent and independent roles of TOR in cell growth and proliferation

TOR can be activated downstream of insulin signaling, but also receives additional inputs (Grewal, 2009). Insulin signaling controls germline growth via TOR, while insulin (via FOXO) and TOR signaling regulate GSC proliferation in parallel. *Tor* null ovarian cell defects are also more severe than *InR* null defects (see also LaFever and Drummond-Barbosa, 2005), implying that TOR receives additional inputs during oogenesis.

Amino acid transport activates TOR signaling in *Drosophila* and mammals (Avruch et al., 2009; Hietakangas and Cohen, 2009). The *Drosophila* genome predicts approximately 40 amino acid transporters (www.flybase.org), and recent evidence suggests that methionine is a key dietary amino acid for oogenesis in *Drosophila* (Grandison et al., 2009). Further studies should investigate how various classes of amino acid transporters affect ovarian TOR signaling, and amino acid requirements for specific oogenesis processes.

4E-BP and translational control downstream of TOR

4E-BP, encoded by *Thor*, represses cap-dependent translation via eIF4E inhibition. TOR phosphorylates and inhibits 4E-BP, leading to translation de-repression (Fingar et al., 2002). 4E-BP, however, does not mediate *Tor* ovarian phenotypes, suggesting that TOR likely acts through S6K or Myc (Grewal, 2009; Hay and Sonenberg, 2004; Li et al.). Indeed, S6K overexpression partially restores *Tor* mutant growth, viability and fertility (Zhang et al., 2000), while Myc loss causes germline growth phenotypes similar to *Tor* defects (Maines et al., 2004).

Whether or not 4E-BP is required in any other tissues to mediate the effects of reduced TOR activity remains unclear. Although overexpression of eIF4E increases cell growth rates while overexpression of 4EBP results in smaller cell size, loss of 4E-BP does not phenocopy eIF4E overexpression (Fingar et al., 2002; Teleman et al., 2005a). Furthermore, *Thor* mutation has no obvious phenotype in *Drosophila* except for increased sensitivity to stress and impaired innate immunity (Bernal and Kimbrell, 2000; Teleman et

al., 2005a). Although *Thor* is required for dietary restriction effects on lifespan (Zid et al., 2009), we found no reports of *Tor Thor* double mutants in the literature.

Parallels between the role of TOR in Drosophila and mammalian ovaries

Our results bring to light interesting parallels between the role of TOR in *Drosophila* and mammalian ovaries. Insulin and TOR signaling are active in mammalian ovaries (Adhikari et al., 2009; Yaba et al., 2008), and rapamycin inhibits follicle growth in cultured mouse ovaries (Yaba et al., 2008), suggesting similar regulation of oocyte growth and follicle cell proliferation between *Drosophila* and mammals. Although adult mammalian ovaries do not contain GSCs, overexpression of either insulin or TOR signaling in mouse primordial germ cells leads to premature ovarian failure caused by the hyperactivation and subsequent depletion of the primordial germ cell pool (Adhikari et al., 2009; Reddy et al., 2008), a phenotype that is arguably reminiscent of the rapid loss of *TSC1* mutant GSCs.

CHAPTER IV

ROLES FOR THE FAT BODY IN THE REGULATION OF OVARIAN STEM CELLS AND THEIR PROGENY

Introduction

It is recognized in mammalian systems that obesity and Type II Diabetes can increase the risk of both infertility and certain types of cancers (Budak et al., 2006; Delort et al., 2009; Mitchell et al., 2005; Pasquali, 2006; Percik and Stumvoll, 2009). While adipokinetic regulation, insulin signaling, and lipid signaling defect are all potential links between these disorders, adipokinetic regulation is of particular interest (Mitchell et al., 2005; Pasquali, 2006; Qatanani and Lazar, 2007). Adipokines are adipocyte-secreted molecules with roles in insulin sensitivity and metabolic homeostasis, providing adipose tissue with an endocrine role in addition to its role as a lipid-storage depot (Budak et al., 2006; Mitchell et al., 2005; Scherer, 2006; Staiger and Haring, 2005). A myriad of mammalian studies have been published in recent years, suggesting links between adipokine signaling and infertility, cancer, and stem cell activity; however, many of these reports contain inconclusive or conflicting data, potentially due to some level of functional redundancy both within families of adipokines and between different adipokines (Chiarugi and Fiaschi, 2010; Mitchell et al., 2005; Wong et al., 2004).

The *Drosophila* fat body is largely analogous to mammalian adipose tissue (adipocytes) and liver (oenocytes) and plays both nutrient storage and endocrine roles (Liu et al., 2009). As in mammals, *Drosophila* adipocytes store energy in the form of

triglycerides, or TAG. These lipid molecules are packaged into droplets surrounded by lipid storage droplet proteins (Lsd1 and 2), which serve to both support the lipid droplet structurally and restrict the access of lipases. The *Drosophila* TAG lipases, Brummer and CG8552, break down lipid droplets when nutrients are limiting (Arrese and Soulages, 2010). Oenocytes uptake lipids for further processing (Gutierrez et al., 2007). While it is evident that the *Drosophila* fat body has roles outside of fat storage and mobilization (Liu et al., 2009) (see Chapter I), it is unclear whether adipokines are present in insects, and, if so, whether they are functionally conserved.

Our laboratory has demonstrated that past nutritional environments can affect the proliferation rates of ovarian cells in adult females for at least one day, suggesting fat storage levels are sensed by peripheral tissues (Drummond-Barbosa and Spradling, 2001). Others have demonstrated that imaginal disc cell culture must be supplemented with larval fat bodies for both imaginal disc cell-cycle activation and maintenance (Britton and Edgar, 1998). The larval fat body has also been implicated in regulating insulin-like peptide secretion from the brain by an unknown signal secreted downstream of TOR signaling (Geminard et al., 2009). Additionally, studies have demonstrated that the fat body secretes DILPs that regulate feeding, Imp-L2 that regulates peripheral tissue growth and proliferation, larval serum proteins (LSPs) that store amino-acids for cellular processes in the hemolymph, and iron-bound ferritin that provides a source of iron necessary for cell proliferation (Honegger et al., 2008; Li, 2010; Liu et al., 2009; Slaidina et al., 2009). Several of these fat body secreted factors are produced downstream of nutrient-sensing pathways in the fat body (Geminard et al., 2009; Slaidina et al., 2009), much like adipokine secretion in mammals (Marshall, 2006).

Based on primary sequence alignment, no mammalian adipokine homologs have been identified in *Drosophila*, but insects do have a highly conserved adiponectin receptor, or *dAdipoR* (Yamauchi et al., 2003). These receptors are conserved from yeast to humans and activate the same downstream signaling pathways when substituted for one another in either yeast or in the mammalian C2C12 muscle cell line (Garitaonandia et al., 2009; Narasimhan et al., 2005). While dAdipoR is currently an orphan receptor, it is possible that the ligand is conserved not at the primary sequence level, but at the tertiary level. Evidence in support of this possibility is that adiponectin and the anti-fungal protein osmotin can both bind and activate adiponectin receptor signaling. These two protein share less than 10% sequence identity, but have similar protein folds at the tertiary level (Narasimhan et al., 2005).

The unpublished studies described in this chapter suggest that genetic alteration of *Drosophila* fat body storage levels and manipulation of nutrient signaling pathways, including the *Drosophila* adiponectin receptor, *dAdipoR*, within the adult ovary and fat body affects oogenesis, by an unknown mechanism(s). As a first step towards understanding how the fat body and ovary communicate, I took a proteomics-based strategy to identify fat body secreted proteins. These studies are still incomplete, but they may provide clues to the mechanistic links between the fat body and stem cell regulation.

Materials and methods

Drosophila strains and culture

Fly stocks were maintained at 22-25°C on standard medium. *FB-Gal4* (Gronke et al., 2005), *Adh-Gal4* (Fischer et al., 1988), *3.1 Lsp2-Gal4* (Cherbas et al., 2003), Adp^{60}

(Hader et al., 2003), *Bmm*^{1} (Gronke et al., 2005), *Lsd2*^{51} (Gronke et al., 2003), *UAS-DILP2* (Ikeya et al., 2002), *UAS-Imp-L2*^{RNAi} (Honegger et al., 2008), *dALS* RNAi *(dALSi)* (Arquier et al., 2008) and other genetic elements are described in FlyBase (Ashburner and Drysdale, 1994). *UAS-CG5315*^{RNAi} (VDRC# 40936) and other RNAi lines are listed in Table 4.2.

Adult specific RNAi expression was performed by crossing flies carrying a *UAS*-inducible RNAi transgene to flies carrying a fat body specific *Gal4* driver and *tubP-Gal80*^{ts}. The cross was cultured at 18°C (*Gal80*^{ts} active, *Gal4* off) and the resulting 0-5 day old female progeny carrying all three transgenes were transferred to 29°C (*Gal80*^{ts} inactive, Gal4 on) for five days on a rich diet in the presence of sibling males. The *Gal4/Gal80*^{ts} technique is described in (McGuire et al., 2003).

Genetic mosaics were generated as described in Chapters II and III. For *dAdipoR*^{27} mutant mosaic analysis, females of the genotype *hsFLP/+; FRT82B dAdipoR*^{27}*/FRT82B Ubi-GFP* were generated by standard crosses. To induce FLP-mediated recombination, 0-5 day old females were heat-shocked for 1 hour at 37°C twice a day for 3 days and subsequently transferred to a rich diet (standard medium with wet yeast paste) for 7 days then maintained on a rich diet or switched to a poor diet (molasses and agar) for an additional 3 days. *dAdipoR*^{27} mosaic clones were identified by the absence of green fluorescent protein (GFP). Relative GSC division rates were determined as described (LaFever and Drummond-Barbosa, 2005). Germline stem cell loss was also determined as described (LaFever and Drummond-Barbosa, 2005). Cyst growth rates and progression through vitellogenesis, were qualitatively analyzed by comparison to GFP-positive wild-type clones within the same tissue.

Lineage-labeling with LacZ

To generate mitotic fat body clones, females of the genotype *hsflp/+; X-15-29/X-15-33* were obtained by standard crosses as described (Drummond-Barbosa and Spradling, 2001; Margolis and Spradling, 1995). Mitotic clones were induced by a one hour heat-shock at 37°C at different time-points throughout larval development or as early adults. Flies were then fed on a rich diet for either five days post eclosion or an additional five days post heat-shock. To preserve fat body tissue, abdomens were removed from the body and dissected open in Grace's medium by a single lateral incision. Intestine and ovaries were removed, leaving behind fat body attached to the abdominal wall. Abdomens were fixed in 0.5% gluteraldehyde in PBS for eight minutes at room temperature, then washed for 30 mins in PBS with 0.1% Tween 20 (PBT). Mitotic fat body clones that express β-galactosidase were identified by X-gal staining (Margolis and Spradling, 1995). Abdomens were incubated at 37°C for two hours in 10 mM NaH_2PO_4-Na_2HPO_4 (pH 7.2), 150 mM NaCl, 1 mM $MgCl_2 \cdot 6H_20$, 3 mM $K_4[FeII(CN)_6]$, 3 mM $K_3[FeIII(CN)_6]$, 0.5% Triton X-100, and 0.2% X-Gal (5-bromo-4-chloro-3-indolyl-β-D-galactopyranoside). The staining reaction was stopped by washing ovaries in PBT for 30 minutes. Fat body tissue was then scraped from the abdominal wall and mounted in a 50% glycerol/PBS mounting solution. Fat body X-gal-positive clones were visualized by bright field microscopy using a Zeiss Axioplan 2 microscope.

Ovarian proliferation assays

Egg production was measured essentially as described (Drummond-Barbosa and Spradling, 2001) with the following modifications. Five pairs of flies were placed in

bottles with plates containing either a rich diet (agar, molasses, and wet yeast paste) or a poor diet (agar and molasses). Food plates were changed daily and egg production was analyzed in triplicate every 24 hours for 4-7 days. Data is graphically represented as the average number of eggs laid per female per 24 hours. Error bars represent the standard deviation between the three replicates. Follicle cell mitotic index was performed as described (LaFever and Drummond-Barbosa, 2005; LaFever et al., 2010). Ovarioles stained with Phosphohistone H3 (PHH3) and a follicle cell membrane marker (1B1 or α-spectrin) were imaged by confocal microscopy on both the top and bottom focal planes to visualize the basal surface of the follicle cells. A minimum of 15 ovarioles were analyzed per genotype and the total number of PHH3-positive follicle cells was divided by the total number of follicle cells within the mitotic region to obtain the mitotic index.

Reverse Transcriptase (RT)-PCR

For analysis of sex-specific and nutritional regulation of *dAdipoR* isoforms, total RNA was extracted from either 10 females or 16 males fed either a rich or poor diet for 3 days. For tissue-specific isoform expression of *dAdipoR*, 10 heads, carcasses, or ovaries from females were collected for RNA extraction. All flies were 3-6 days old. RNA extracted using TRIzol® Reagent (Invitrogen) was reverse transcribed using Superscript™ II RT (Invitrogen). *dAdipoR* transcripts were amplified with EconoTaq PLUS green (Lucigen) using transcript specific primers: *dAdipoR* isoform A/C (forward primer DDB 210, 5'GATTCGGCCACTAATCTCCTC, and reverse primer DDB 211, 5'GATGCAGCCAAGAAGATGTG), *dAdipoR* isoform B (forward primer DDB 221, 5'CCCAAAACCCTGACACAGT and reverse primer DDB 211), or all *dAdipoR* isoforms

(forward primer DDB 250, 5'CATGATCAGCAGCGCAATTC and reverse primer DDB 251, 5'GAGCAGGCAGAGGAGTTTG).

Development of *dAdipoR* mutant alleles by piggyBac *FLP/FRT* recombination

Flies containing two piggyBac elements flanking *CG5315* (*dAdipoR*) and a heat-shock inducible flipase were generated by standard crosses. Females were crossed to balancer stock males and their resulting progeny, from egg to pupal stages, were heat-shocked to induce *FLP/FRT* mediated recombination between the *FRT* sequences contained within the piggyBac elements. Recombination events occurring in the germline are inherited by the progeny, which were collected and crossed to balancer stocks to isolate single recombination events (see Figure 4.7B). A more detailed description of this technique can be found in (Thibault et al., 2004).

To screen for deletion of *CG5315* by piggyBac-mediated recombination, genomic DNA was extracted from five flies for each potential recombinant line. Flies were homogenized in 66.8 μl of Buffer A (100mM Tris-Cl, pH 7.5; 100 mM EDTA; 100 mM NaCl; 0.5% SDS) and incubated at 65°C for 30 min. 133.4 μl ice cold LiCl/KAc solution was added and incubated on ice for 10 min. Samples were spun at 13,000 rpm for 15 minutes at room temperature and 166.7 μl supernatant was transferred to a new tube. 100 μl isopropanol was added, mixed well, and spun for 15 min at 13,000 rpm at room temperature. Supernatant was removed and the resulting pellet was washed with cold 70% ethanol twice, then dried and resuspended in 25 μl 10 mM Tris pH 8.0. A PCR-based screen for recombinants was developed as described (Thibault et al., 2004). Primers used to identify recombination events between piggyBac elements $CG5315^{F05395}$ and

CG5315^{c02150} (resulting in the *CG5315*$^{\Delta 27}$ mutant allele) were DDB201, 5'CAACGTATGACCGCATTTCC and DDB205, 5'CCTCGATATACAGACCGATAA AAC and DDB203, 5'TAAAACCCCTGCAATCGC. Positive recombination events were identified by two bands corresponding to 338 bp and 664 bp. Primers used to identify recombination events between piggyBac elements *CG5315*^{F05395} and *CG5315*^{e01762} (resulting in the *Df(3R)CG5315*^{38} allele) were DDB201 and DDB205 and DDB199, 5'CAATCGCCGGATAGTAGAGCAT. Recombination events were identified by two bands corresponding to 338 bp and 574 bp.

Plasmid constructs and generation of *CG5315* (*dAdipoR*) transgenic flies

UASpI- and *hsp70-CG5315 isoform (iso) A/C* constructs were generated by excising *CG5315 isoform A/C* cDNA from the *Drosophila* Geneomics Resource Center (DGRC) from the *pOT2* vector with EcoRI and HindIII enzymes, then partial digesting using XhoI. The insert was gel-purified and subcloned into the *UAST* vector linearized with EcoRI and XhoI enzymes. *CG5315 isoA/C* insert was then excised from the *UAST* vector using EcoRI and XbaI enzymes and directionally subcloned into *UASpI-* and *pCasper-hsp70* vectors linearized with EcoRI and Xba1 enzymes. Transgenic lines listed in Table 4.1 were generated by germline transformation as described (Rubin and Spradling, 1983).

Analysis of fat storage levels in *Drosophila*

Visualization of the *Drosophila* adult fat body was performed by incubating fixed flies [30 minutes in 5% formaldehyde (Ted Pella)] cut sagittally at the midline in Oil Red

O staining solution (6 ml of 0.1% Oil Red O in isopropanol and 4 ml distilled water, prepared fresh and passed through a 0.2-μm syringe filter) for 10 minutes at room temperature, then rinsing in 70% isopropanol for 5 minutes. Fat tissue was imaged by digital photography under a dissecting microscope.

To quantify whole body fat storage levels, samples were prepared from a modified version of a protocol obtained from Ronald Kühnlein (Gronke et al., 2005) and triglyceride levels were measured by the Serum Triglyceride Determination Kit (Sigma, TR0100). 3 whole flies or 7 individual ovaries or carcasses were homogenized in 1 ml 0.05% Tween 20 in a BioPrep homogenizer on level 4.0 for 20 seconds, incubated at 70°C for 5 minutes, and centrifuged for 1 min at 5000 rpm. 500 μl of the supernatant was placed in a new tube and centrifuged again for 3 min at 13000 rpm. 50 μl of sample was used for each enzymatic reaction (all at 37°C). Sample was first incubated with 160 μl glycerol reagent. The enzymatic reaction was allowed to develop for 20 min and absorbance at 540 nm was measured as a readout of total free glycerol. Next, 40 μl of triglyceride reagent was added and reaction was allowed to develop for an additional 20 min with shaking, and absorbance at 540 nm was measured to obtain total glycerol levels (including that from TAG). The absorbance from free glycerol was subtracted from the absorbance from total glycerol, resulting in a measurement of total TAG. Total TAG concentration per sample was then determined by comparison to a protein standard curve and presented as total concentration of TAG/protein.

Immunostaining and fluorescence microscopy

Ovarian staining was performed as described in Chapter II and III Material and Methods. Antibodies used that were not described in previous chapters: mouse monoclonal OO18 RNA-binding (orb) (1:20) (Developmental Studies Hybridoma Bank, DSHB). hu-li tai shao ring canal (hts-RC) (1:50) (DSHB). Samples were examined using a Zeiss LSM 510 or LSM 700 confocal microscope.

GSC cell-cycle analysis

GSC cell-cycle analysis was performed as described in Chapter III Materials and Methods with the exception that EdU (5-ethynyl-2'-deoxyuridine) (Invitrogen) was used as an alterative for BrdU as an S-phase GSC marker. EdU allows simultaneous immunostaining with other antibodies so percentages of GSCs in different cell-cycle phases can be directly calculated. The number of EdU-positive GSCs was quantified and subtracted from the total number of GSCs with a G1/S fusome morphology to obtain the total number of GSCs in G1. The number of PHH3-positive GSCs (M-phase) were subtracted from the total number of GSCs with G2/M fusome morphologies, resulting in the total number of GSCs in G2. Frequencies of GSCs in different cell-cycle stages were presented in a circular pie chart to represent the relative length of time for each cell-cycle stage.

Adult fat body sample preparation for MudPIT and iTRAQ proteomics analysis

Offline 2D LC-MS/MS: Abdominal fat was manually scraped from the abdomens of 75 females and head fat body was manually scraped from the heads of 10 females into ice

cold PBS, transferred to sample buffer (Invitrogen, NP0004), then flash frozen. After completion of collections, samples were thawed on ice and reducing agent (Invitrogen, NP0007) at 1:10 and PMSF to 1 mM were added. Tissue was homogenized for 1 minute, boiled 10 minutes, and spun at 13000 rpm for 2 minutes. Samples were run about 2 cm into a 10% SDS Bis/Tris gel from Invitrogen (NP0301) at 200V for 5 minutes using the Invitrogen NuPAGE gel system. The gel was fixed for 10 min in 40 ml H_20, 50 ml methanol, and 10 ml acetic acid. The gel was stained according to protocol with a Colloidal Blue Staining Kit (Invitrogen, LC6025). In short, the fixed gel was incubated in staining solution for 5 min in 55 ml H_20, 20 ml methanol, and 20 ml Stainer A. 5 ml of Stainer B was then added to the staining solution and incubated over night at room temperature. The gel was de-stained by several washes in H_20. In the Vanderbilt Proteomics Core Lab, samples were cut from gel and one abdominal fat body sample and the head fat body sample were in-gel digested with trypsin while a second abdominal sample was digested with chymotrypsin.

Gel-C-MS/MS: Abdominal fat bodies from about 10-15 females were prepared as described for offline 2D LC-MS/MS. 20 μl of sample was run into a 10% SDS Bis/Tris gel at 200V for 30 mins. Resulting gel bands were divided into 11 regions by the Vanderbilt Proteomics Core, in-gel digested with trypsin and subjected to LC-MS/MS.

Online 2D LC-MS/MS: Abdominal fat bodies from 4 females were prepared as described above with the exception that PMSF was not added. 20 μl sample was run 2 cm into a 10% Bis-Tris gel, and the resulting band was excised and in-gel digested with trypsin.

iTRAQ (isobaric Tags for Relative and Absolute Quantitation): Abdominal fat was manually scraped from either 60 females fed a rich diet or 90 females fed a poor diet in

quadruplicate. Fat bodies were placed in equal volume of 2X Sample Buffer and brought up to 50 μl volume with additional 1X Sample Buffer. Samples were prepared without PMSF. Quantitation of protein amounts were determined using an EZQ Protein Quantitation Kit (Invitrogen #R33200). Samples were diluted and TCA precipitated so each contained 83 μg of fat body protein. Samples were submitted for iTRAQ preparation and analysis by the Johns Hopkins Proteomics Core Laboratory. See (Wiese et al., 2007) for further details on iTRAQ labeling and procedures.

Analysis of fat body proteomics data

MS/MS spectra from the first three mass spectrometry trials (online and offline 2D LC-MS/MS and Gel-C-MS/MS) were searched using the Seaquest algorithm (Yates et al., 1995) and the *Drosophila* database from the Uniref100 database. Reverse sequences were included for estimation of false positives and found to be below 2%. Protein matches were identified using CHIPS (Complete Hierarchical Integration of Protein Searches). Protein identifications from the first three mass spectrometry trials were converted to a list of corresponding genes and analyzed for overlap between datasets (www.flymine.org). Protein identifications from all three mass spectrometry trials were compiled and bioinformatics analysis was performed using pSORT and TargetP to identify secreted proteins. Protein sequences with a pSORT confidence score of ≥10.0 or a TargetP confidence score of ≥70% were considered predicted extracellular proteins. Known extracellular matrix proteins, including laminins and collagens, were removed from the final candidate list. Candidates with a mammalian homolog and an available RNAi line from the VDRC with no predicted off-targets were selected for further screening.

MS/MS spectra from the iTRAQ quantitative proteomic comparison were searched against the *Drosophila melanogaster* RefSeq 40 database using Mascot (Matrix Science) through Proteome Discoverer software (v1.2, Thermo Scientific). Parameters specified were: species, trypsin used as enzyme (allowing for one missed cleavage), fixed cysteine methylthiolation and 8-plex-iTRAQ labeling of N-termini, and variable methionine oxidation and 8-plex-iTRAQ labeling of lysine and tyrosine. Peptides were identified with a confidence threshold of 1% False Discovery Rate. Ratios between samples are the median ratio of all unique peptides that identify a particular protein. Technical variation was less than 20% (i.e., ratios outside of a 20% confidence interval is considered a significant difference). Proteins with significant differences in levels between a rich and poor diets were compiled and bioinformatics analysis was performed using pSORT and TargetP to identify extracellular proteins. Protein sequences with either a pSORT confidence score of ≥10 or a TargetP confidence score of ≥4 were considered predicted extracellular proteins. The list of predicted secreted proteins was then subjected to TMHMM, which predicts transmembrane helices in proteins, as pSORT and TargetP cannot differentiate between extracellular and membrane-bound proteins. pSORT, TargetP, and TMHMM are all available through the ExPASy (Expert Protein Analysis System) proteomics server (http://ca.expasy.org). The final list of candidates all have RNAi lines available from the Vienna Drosophila RNAi Center for subsequent secondary screening for functionality. Mammalian homologs/orthologs for *Drosophila* genes are reported with individual gene information at Flymine.org.

Results

Altering *Drosophila* fat body mass by targeted cell ablation results in larval lethality

As a first step in establishing a connection between the fat body and the ovary in the adult female, we asked whether manipulation of fat body mass or storage levels perturbs oogenesis. To alter fat body cell mass I attempted to partially ablate fat tissue in the adult by expressing cell death genes using the *UAS/Gal4* system. Complete ablation of the adult fat body results in death (J. Agulia, personal communication), so it is important to identify parameters that reduce fat body cell numbers while still producing viable adults. I gathered a collection of fat body Gal4 drivers (*FB-Gal4*, *CG-Gal4*, *Adh-Gal4*, and *3.1 Lsp2-Gal4*), all of which have been previously characterized (see Materials and Methods). I crossed each driver to a fly strain carrying *UAS-reaper*, which can induce cell death in *Drosophila* by binding to and antagonizing inhibitor of apoptosis proteins (DIAPs), which in turn inhibit caspases (Steller, 2008). Progeny were then analyzed for signs of reduced fat body levels. First, I asked if the progeny eclosed in the proper Mendelian ratios. Second, I analyzed lipid levels both qualitatively by Oil Red O staining, a neutral lipid dye, and quantitatively by an enzymatic assay that measures triacylglyceride (TAG) levels, the major form of energy storage. Third, I assayed progeny for stress sensitivity, including reduced life span under starvation conditions, which would be suggestive of reduced fat body tissue. Finally, flies with lower fat levels were assayed for ovarian defects, including those associated with starvation, such as increased levels of cell death, reduced proliferation rates, and retention of mature staged 14 follicles.

Expression of *UAS-reaper* with *FB-Gal4*, *CG-Gal4*, or *Adh-Gal4* resulted in no viable progeny, but the *3.1 Lsp2>reaper* progeny were viable, normal in size, and eclosed

in expected Mendelian ratios. A starvation assay did not uncover a major difference between *3.1 Lsp2>reaper* and controls as both strains died between one and two days (data not shown). Ratios of [TAG]/[total protein] were not significantly different between *3.1Lsp2>reaper* and controls (0.79 ±0.1 and 0.78 ±0.07, respectively). Finally, egg production was comparatively unchanged on either a rich or poor diet (data not shown). Together these data suggest that fat body tissue levels in *3.1 Lsp2>reaper* females are unchanged.

In order to determine the effects of reducing fat cell mass on oogenesis, additional techniques may be utilized that could restrict the level of cell death and result in viable adults. For instance, other cell death-inducing genes and toxins in addition to *reaper* are available, including *UAS-Grim*, *UAS-Hid*, *UAS-DTA* (diphtheria toxin A), and *UAS-ricin*. I can use the *UAS/Gal4* system combined with a *tubPGal80^{ts}* transgene (see Figure 4.11) or a mosaic ablation approach to induce cell death in a fraction of the adipocyte population while leaving the rest unaffected. An additional method would be to use a Flp-out technique (Sun and Tower, 1999). Heat-shock induction of flipase mediates the excision of a "flp-out" cassette within a fat body specific Gal4 driver (such as *FB>"stop">Gal4*) resulting in its activation. Cells can be genetically modified so they will express both a cell death gene and GFP when the Gal4 driver is activated. This technique allows an additional level of control since cells that should undergo apoptosis will be GFP-positive. Direct observation will allow determination of a properly functioning system since no GFP-positive cells should remain if cell-death is induced at an appropriate level.

Genetically altering *Drosophila* fat body mass has a negative impact on oogenesis

A collection of fat storage mutant strains having either altered lipid levels compared to wild-type provided us with the means to investigate the effects of changes in fat body storage levels on oogenesis. Fat body storage mutants have been identified and characterized in *Drosophila* and include *adipose (adp)*, *brummer (bmm)*, and *lipid storage droplet-2 (lsd2)*. adp^{60} and bmm^{1} mutants have increased fat storage levels, while $lsd2^{51}$ mutants have reduced levels (Gronke et al., 2003; Gronke et al., 2005; Hader et al., 2003) (Figure 4.1A). Lsd2, or the homolog of human Perilipin, surrounds lipid droplets and restricts access to lipases such as Bmm, the homolog of human adipocyte triglyceride lipase (ATGL) (Gronke et al., 2003; Gronke et al., 2005). The human homolog of *Drosophila* Adp is WD and tetratricopeptide repeats 1 (WDTC1), which is proposed to elicit anti-adipogenic functions by regulation of chromatin dynamics and transcription (Suh et al., 2007).

To determine if oogenesis is affected by changes in fat body mass, I first analyzed egg production in each fat storage mutant. $lsd2^{51}$ mutants exhibited a 75% reduction in egg production compared to heterozygous controls ($lsd2^{51}/FM7c$) (Fig. 4.1B). The eggs laid by $lsd2^{51}$ mutants while fewer in number are also abnormal—they are smaller than wild-type eggs and are clear in color and/or collapsed, suggestive of a defect in yolk/lipid deposition or egg shell formation. While this result agrees with a reported cell-autonomous role for *lsd2* in lipid storage in ovarian nurse cells (Vereshchagina and Wilson, 2006), an additional non-cell autonomous role for *lsd2* on the ovary via the fat body cannot be ruled out. Both bmm^{1} and adp^{60} mutants produce about 50% fewer eggs than heterozygous siblings ($bmm^{1}/TM3$ and adp^{60}/Cyo) (Fig. 4.1C,D), and their eggs are phenotypically

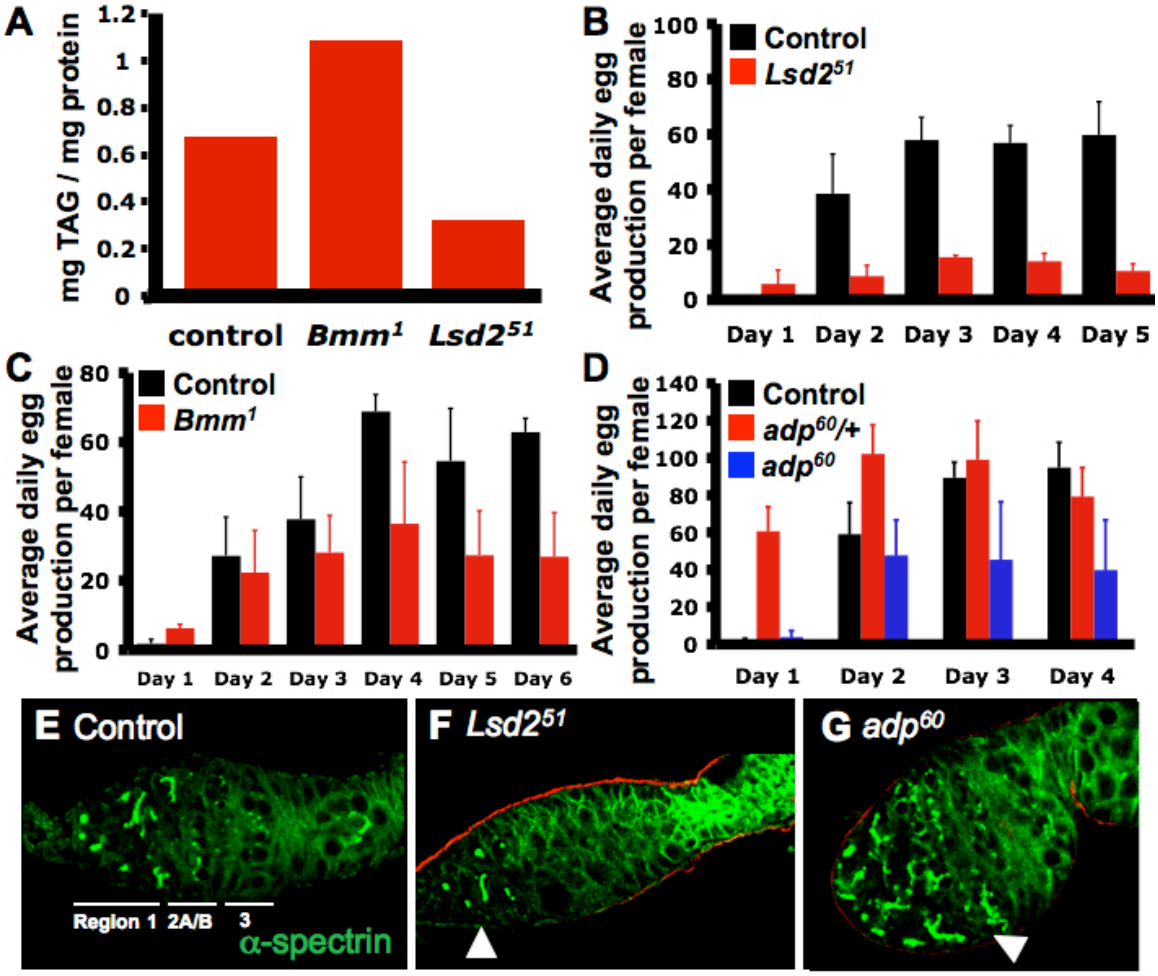

Figure 4.1. Fat storage mutants produce fewer eggs. (A) Standardized triglyceride (TAG) levels in control, *Bmm*^{1}, and *Lsd2*^{51} mutant males. Control genotype is *yw*. **(B)** Average daily egg production per control or *Lsd2*^{51} mutant female over five days on a rich diet. Control genotype is *Lsd2*^{51}*/FM7***. (C)** Average daily egg production per control or *Bmm*^{1} mutant female over six days on a rich diet. Control genotype is *Bmm*^{1}*/TM3***. (D)** Average daily egg production per control, *adp*^{60}/+ or *adp*^{60} mutant female over four days on a rich diet. Control genotype is *yw*. **(E)** Control germarium. α-spectrin (green), fusome and follicle cell membranes. Different regions of the germarium (Regions 1, 2A/2B, and 3) corresponding to progressively more highly branched fusome morphologies are indicated. **(F)** *Lsd2*^{51} mutant germarium. Arrowhead, fusome morphologies corresponding to region 1 are present. **(G)** *adp*^{60} mutant germarium. Arrowhead, highly branched fusomes corresponding to regions 2/B or 3 at the anterior-most tip of the germarium (region 1 location). All germaria are shown at same magnification.

normal. Based on these data, I conclude that changes in fat storage levels have a negative impact on oogenesis; however, I cannot rule out additional roles for these fat storage genes in tissues outside the fat body or even potential developmental defects that later affect oogenesis in the adult. Experiments using spatially and temporally restricted RNAi knock-down of each fat storage gene in the adult female fat body should provide stronger evidence for an effect of fat body mass on oogenesis.

Further analysis of *lsd2*^{51} and *adp*^{60} was performed as part of a Vanderbilt Summer Science Academy project with Hala Zein-Sabbato. We screened for defects in germarium morphology that might explain the previously observed reduction in egg production. Fusome morphology, marked by α-spectrin staining, becomes progressively more branched as cyst cell number increases (de Cuevas and Spradling, 1998). Interestingly, we noticed that *lsd2*^{51} mutant germaria contained qualitatively fewer highly branched fusome morphologies within the region of the germarium that corresponds to older cyst stages (4- to 16-cell cysts) compared to controls (Figure 4.1E,F). The *adp*^{60} mutants, however, exhibited more highly branched fusomes compared to wild-type controls (Figure 4.1E and G). A lack of older cyst stages in *lsd2*^{51} mutant germaria is consistent with reduced egg production, but *adp*^{60} mutants produce fewer eggs and have more older cyst stages, suggesting that this strain may have additional defects at later stages of oogenesis. These preliminary results suggest fat body-derived signals may impinge upon oogenesis to regulate early cyst development.

DILPs regulate fat body mass and egg production rates

Our laboratory has previously demonstrated that overexpression of *dilp2* increases egg production on a rich diet compared to controls, indicating that DILPs are normally limiting under optimal nutritional conditions (see Figure 1.9). One way that the fat body could impinge upon oogenesis is via changes in fat cell mass due to elevated systemic insulin signaling levels. Increased fat cell mass may result in the secretion of adipokine-like factors that act in a stimulatory manner on the ovary. In support of this hypothesis, elevated levels of circulating insulin can increase adiposity in mammals, and the secretion of some adipokines, including leptin and adiponectin, correlate with adiposity (Cancello et al., 2004; Mitchell et al., 2005). Furthermore, elevated insulin signaling activity increases fat body mass in *Drosophila* larvae, suggesting the effect of insulin signaling on fat tissue function may be conserved (DiAngelo and Birnbaum, 2009). Finally, evidence from our lab suggests the fat storage levels can be sensed by the ovary (see Figure 1.9C,D)

To determine if adult females overexpressing *dilp2* have increased fat body cell mass, I performed a triacylglyceride (TAG) assay to measure the total levels of stored fat, which correlate with total fat body mass (see Materials and Methods). I generated four genotypes by standard crosses that overexpress *dilp2* under the control of Gal4 drivers varying both in strength and location of *dilp2* expression (Figure 4.2). To my surprise, I discovered that TAG levels are not higher, but comparatively lower in females expressing *dilp2* with the stronger fat body drivers, *c323* and *FB-Gal4*. TAG levels were unchanged in flies expressing *dilp2* with the pan-neural driver *elav-Gal4* and TAG levels appeared elevated in *c587>dilp*2 flies, but this difference is due to an increased whole body size of the *c587* strain alone compared to our wild-type *yw* strain (data not shown). The *c587*

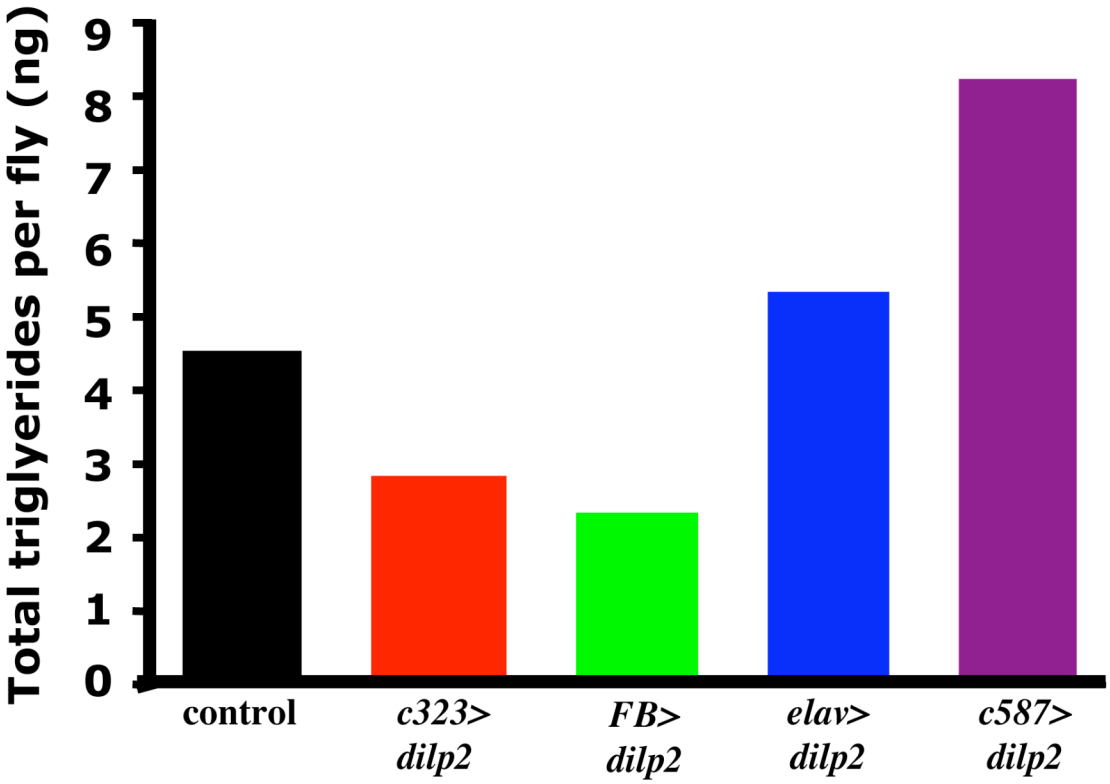

Figure 4.2. *dilp2* overexpression affects fat storage levels. Average total ng of triglycerides (TAG) per rich diet fed female for four days. Ovaries were removed before analyzing TAG content of whole flies. Control is *UAS-dilp2* alone.

Gal4 driver expresses in somatic cells of the ovary and in the fat body. These results suggest that adult-specific elevated insulin signaling does not increase fat body mass as previously observed in larvae, but does increase ovarian activity.

Insulin signaling controls body size in *Drosophila* by modulating both cell size and number during development (Goberdhan and Wilson, 2003) and higher rates of cellular growth and proliferation should require greater nutrient intake/utilization (Conlon and Raff, 1999; Puig and Tjian, 2006). I questioned whether elevated insulin signaling in the adult female results in the reallocation of fat body energy resources into egg production, suggesting insulin signaling levels may set an optimal balance between fat storage mass and reproductive capacity—a balance that optimizes both longevity and fecundity. It is known that increased insulin signaling increases egg production, but shortens lifespan in flies (Honegger et al., 2008) (L. LaFever, data not shown). It is also well-established that insulin signaling pathway mutants are sterile and have increased lifespan (Piper et al., 2008). Flies with decreased fat mass are sensitive to starvation, while those with higher levels are more resistant (Gronke et al., 2003; Gronke et al., 2005; Hader et al., 2003). I questioned whether flies overexpressing *dilps* can maintain higher rates of egg production over long periods of time, or whether increased insulin signaling would eventually have detrimental effects on oogenesis. For instance, in humans increased circulating insulin can eventually lead to insulin-resistance and metabolic syndrome (Duvnjak and Duvnjak, 2009). One symptom of metabolic syndrome in females of reproductive age is polycystic ovarian syndrome, which results in infertility (Barber et al., 2006).

Interestingly, I found that while flies overexpressing *dilp2* as adults can produce comparatively more eggs than wild-type controls for two to three days, egg production

later drops (Figure 4.3A), suggesting that, as in humans, increased circulating insulin levels have a detrimental effect on fertility. To further examine why egg production is decreased in flies overexpressing *dilp2*, I examined ovarian proliferation at time points when egg production is comparatively high (day two) and comparatively low (day seven) (see Figure 4.3A). The proliferation rate (or mitotic index) of follicle cells surrounding germline cysts provides an indirect measure of follicle growth rates since follicle cells divide to keep pace with underlying germline cyst growth (Drummond-Barbosa and Spradling, 2001; LaFever and Drummond-Barbosa, 2005). Unexpectedly, follicle cell mitotic indexes were not reduced, but perhaps even increased in *dilp2* overexpressing flies between day two (2.1%) and day seven (3.3%). Furthermore, there was no significant difference in follicle cell mitotic index between controls and *dilp2* overexpressing flies at either day two (2.5% and 2.1%, respectively) or day seven (3.0% and 3.5%, respectively) (Figure 4.3B). These results indicate that early stages of oogenesis are still responsive to insulin signaling.

I analyzed ovarian morphology at days five and seven (see Figure 4.3A), to determine the stage(s) of oogenesis responsive to elevated insulin signaling levels. I observed that *dilp2* overexpressing females exhibited about three times more stage fourteen egg chambers in their ovaries compared to controls, a phenotype previously associated with reduced nutrient intake (Drummond-Barbosa and Spradling, 2001). Furthermore, a percentage of follicles in those females had 32- as opposed to 16-cells (7% compared to 2% in controls) (Figure 4.3C,D), a phenotype I have found to be associated with perturbation of nutrient-sensing pathways within the fat body (discussed in detail later). These results suggest two possibilities that may not be mutually exclusive. One,

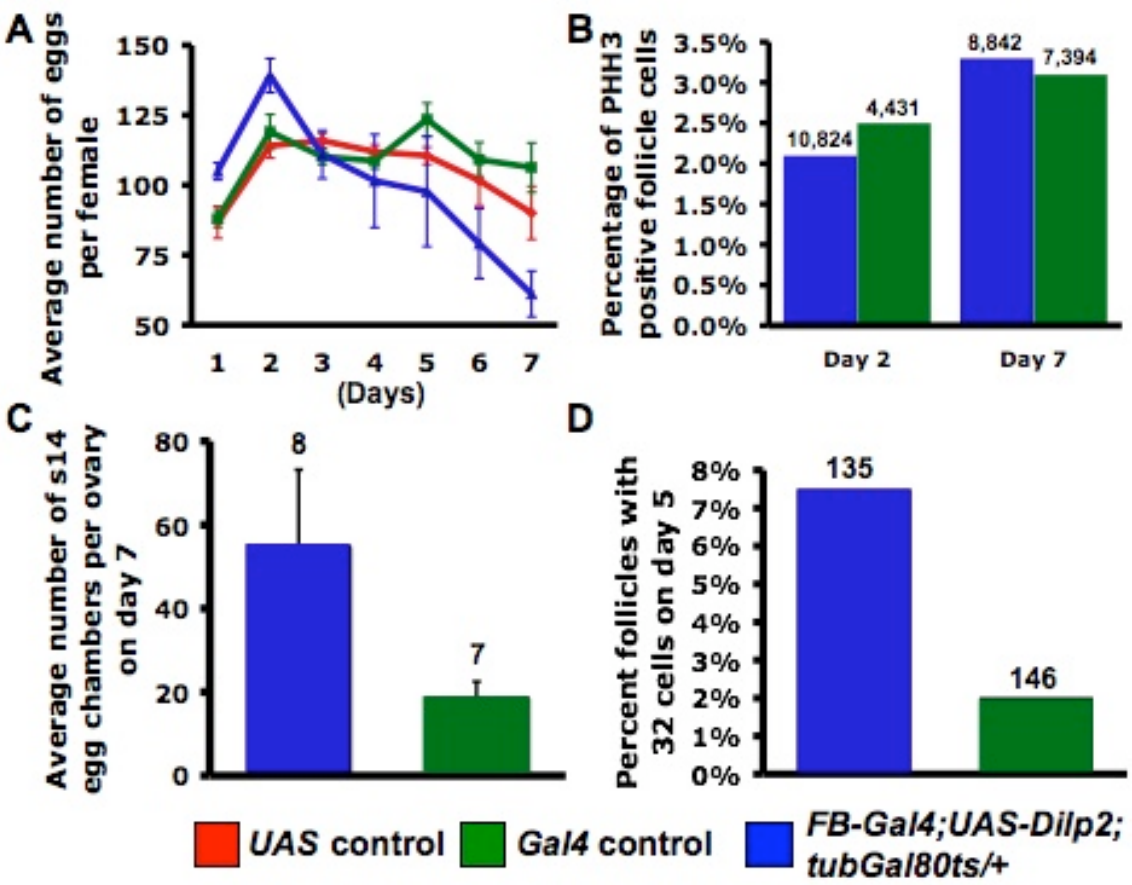

Figure 4.3. Fat body expression of *dilp2* reduces egg production over time. (A) Average number of eggs laid per female per day. **(B)** Mitotic index of follicle cells surrounding previtellogenic follicles at day 2 and 7 (from A). Numbers above bars, total number of follicle cells analyzed. **(C)** Average number of mature, stage 14 eggs present per ovary on day 7 (from A). Numbers above bars, total number of ovaries analyzed. **(D)** Percentage of follicles with 32-cells as opposed to 16 cells on day 5 (from A). Numbers above bars, total number of follicles analyzed. *UAS* control (*yw;UAS-DILP2/+)*. Gal4 control (*FB-Gal4/+; tubPGal80^{ts}/+)*. Scale bars, s.d.

that the ovary may sense the reduced fat body mass caused by *dilp2* overexpression and trigger a starvation-like response, such as reduced egg-deposition, even under rich dietary conditions. Or, two, that fat body-specific nutrient-sensing may be perturbed and the fat body becomes insulin-resistant leading to an improper ovarian response based on the organism's nutritional environment.

A fat body secreted protein, Imp-L2, limits egg production in *Drosophila*

In addition to changes in fat body mass, the fat body might regulate the ovary by modulating systemic insulin signaling since ovarian stem cells and their progeny respond directly to DILPs (LaFever and Drummond-Barbosa, 2005). Potential mechanisms by which this could occur are as follows: the fat body could produce factors that act at the level of DILP secretion, DILP protein stability, or that modulate ovarian sensitivity to DILPs. In *Drosophila* larvae, at least two of these mechanisms are known to occur. An unknown fat body factor secreted downstream of TOR kinase activation modulates DILP secretion from the brain insulin producing cells (IPCs) (Geminard et al., 2009). In addition, fat body secretion of Imp-L2 and ALS, both of which function as a mammalian insulin growth factor binding proteins, leads to downregulation of systemic insulin signaling by binding and sequestering DILPs in the hemolymph (Honegger et al., 2008). It has also been demonstrated in larvae that *dALS* (also known as *CG8561*) and *Imp-L2* expression levels are increased in poor dietary conditions, presumably to quickly modulate systemic insulin signaling levels (Arquier et al., 2008; Honegger et al., 2008). I questioned whether modulation of insulin signaling by *Imp-L2* is conserved in the adult as a mechanism by which the fat body could regulate ovarian stem cells and their progeny.

It is published that adult females with global or fat body-specific *Imp-L2* knockdown have ovaries with increased numbers of vitellogenenic egg chambers, but further details were not provided (Honegger et al., 2008). To determine if *Imp-L2* modulates insulin signaling and thus limits egg production, I induced *Imp-L2* RNAi using two different fat body Gal4 drivers. Similar to the phenotype observed with *dilp2* overexpression, knockdown of *Imp-L2* with the *CG-Gal4* driver significantly increases egg production on a nutrient-rich diet (about 50-60% increase), but not on a poor diet, indicating other factors must also act to limit egg production on a poor diet (Figure 4.4). Knockdown of *Imp-L2* with *FB-Gal4*, compared to controls, also increases egg production, but the phenotype is not as strong as those with CG-Gal4. Differences in Gal4 driver induction strength, expression patterns (*CG-Gal4* also expresses in late stage follicle cells) or genetic backgrounds may explain the observed difference. This result, combined with the previous studies in larvae, indicates that the adult fat body can regulate oogenesis via modulation of the amount of available DILPs in the hemolymph.

I also examined the effect of ALS on egg production, but perturbation of ALS levels in the adult fat body had no effect on fecundity (data not shown). ALS forms a complex with DILPs indirectly through Imp-L2 binding. One potential reason for lack of an adult ovarian phenotype is that ALS may have a larval-specific role. Additionally, it may be that ALS knockdown was not effective with the Gal4 drivers I tested. The previously published study used a larval-specific fat body driver, *pumpless-Gal4* (Arquier et al., 2008).

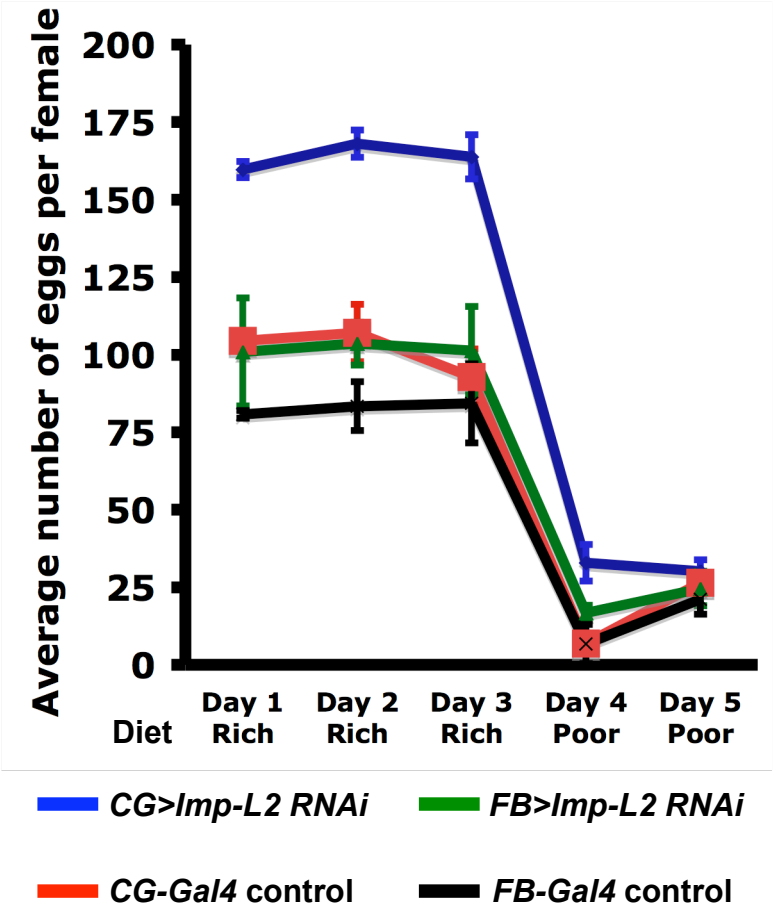

Figure 4.4. *Imp-L2* knockdown increases egg production on a rich diet. Average number of eggs produced per female per day. Error bars, s.d.

The *Drosophila* adiponectin receptor, *dAdipoR*, is expressed in a tissue and isoform specific manner

To obtain further evidence for a potential connection between the fat body and ovary via modulation of insulin sensitivity, I examined the role of the *Drosophila* adiponectin receptor (dAdipoR) in oogenesis. In mammals, adiponectin signaling has a well-known role in sensitizing peripheral tissues to insulin via a feedback mechanism that alleviates TOR kinase activated S6 kinase-mediated suppression of the insulin receptor substrate (Wang et al., 2007). Due to the high level of conservation between nutrient-sensing pathways in insects and mammals, it may be possible that the *Drosophila* adult fat body secretes an adipokine-like factor in response to diet that can activate adiponectin receptor signaling in the ovary and thus sensitize the tissue to circulating levels of DILPs.

While the primary sequences of known mammalian adipokines are not conserved in *Drosophila*, the adiponectin receptor is highly conserved from yeast to humans (Figure 4.5). The *Drosophila* adiponectin receptor, *dAdipoR*, also known as *CG5315*, produces three isoforms and shares 65% similarity with the mammalian receptors, *mAdipoR1* and *mAdipoR2*. *dAdipoR* isoforms A and C have the same protein sequence, but are slightly different in the 5' untranslated mRNA region (Figure 4.6A), which suggests differential regulation at the mRNA level. The *dAdipoR* B isoform encodes a smaller protein. In mice, *mAdipoR1* is ubiquitously expressed while *mAdiopR2* is predominantly expressed in the liver (Yamauchi et al., 2003). A recent study, however, reported that human *AdipoR2* is also highly expressed in adipose tissue (Kos et al., 2010). As a first step in the characterization of the role of *dAdipoR* in *Drosophila*, I examined the expression pattern of *dAdipoR* isoforms in *Drosophila* tissues. Joshua Clanton, a former rotation student in our laboratory, and I found that *dAdipoR* isoforms A and C appear to be ubiquitously

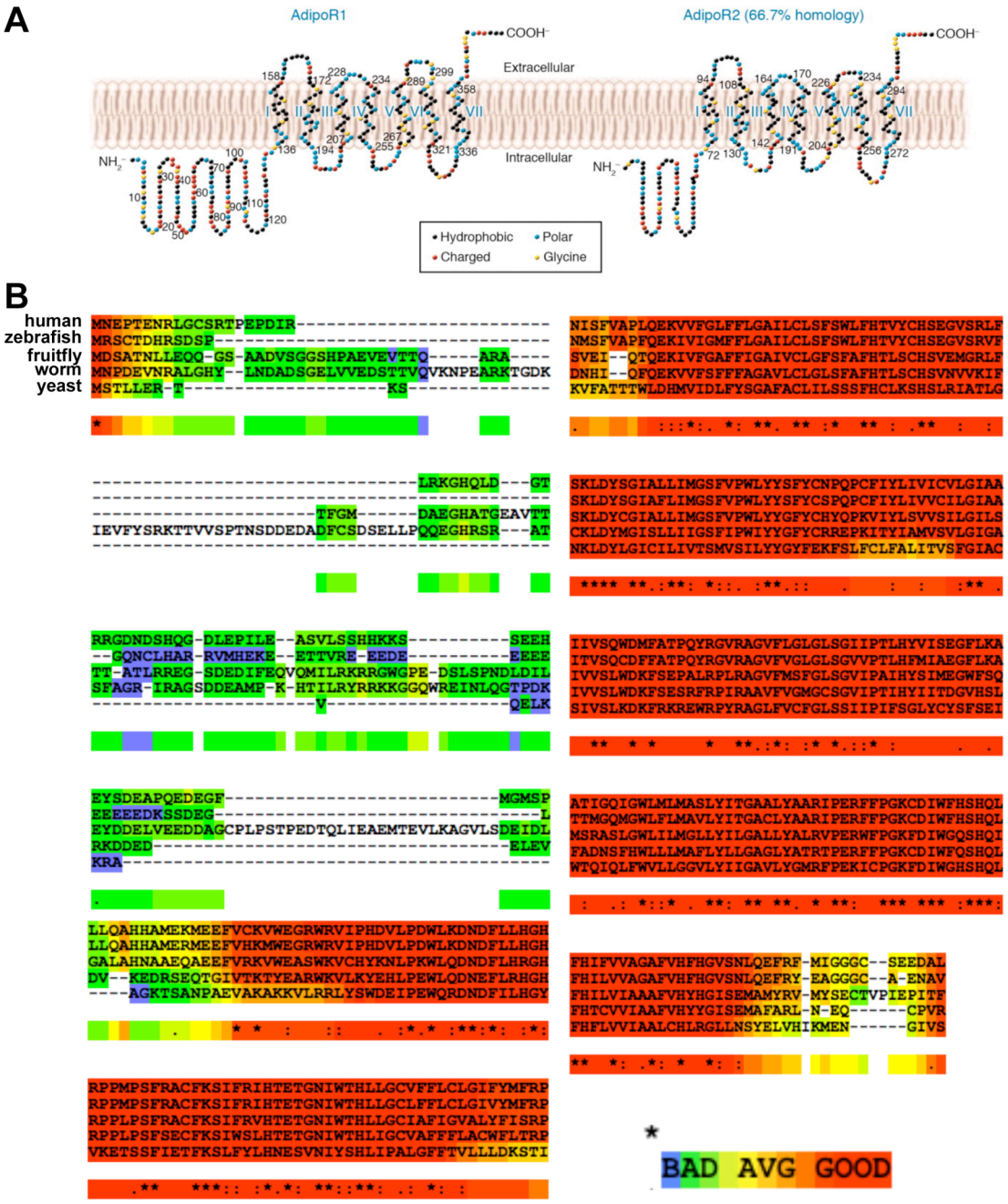

Figure 4.5. The adiponectin receptor (*AdipoR*) is highly conserved from yeast to humans. **(A)** AdipoR is a seven-transmembrane domain protein with an internal N-terminus and external C-terminus (from Kadowaki et al., 2006). **(B)** *dAdipoR* shares 65% similarity to *mAdipoR2*. Alignment by T-COFFEE Version 7.71.

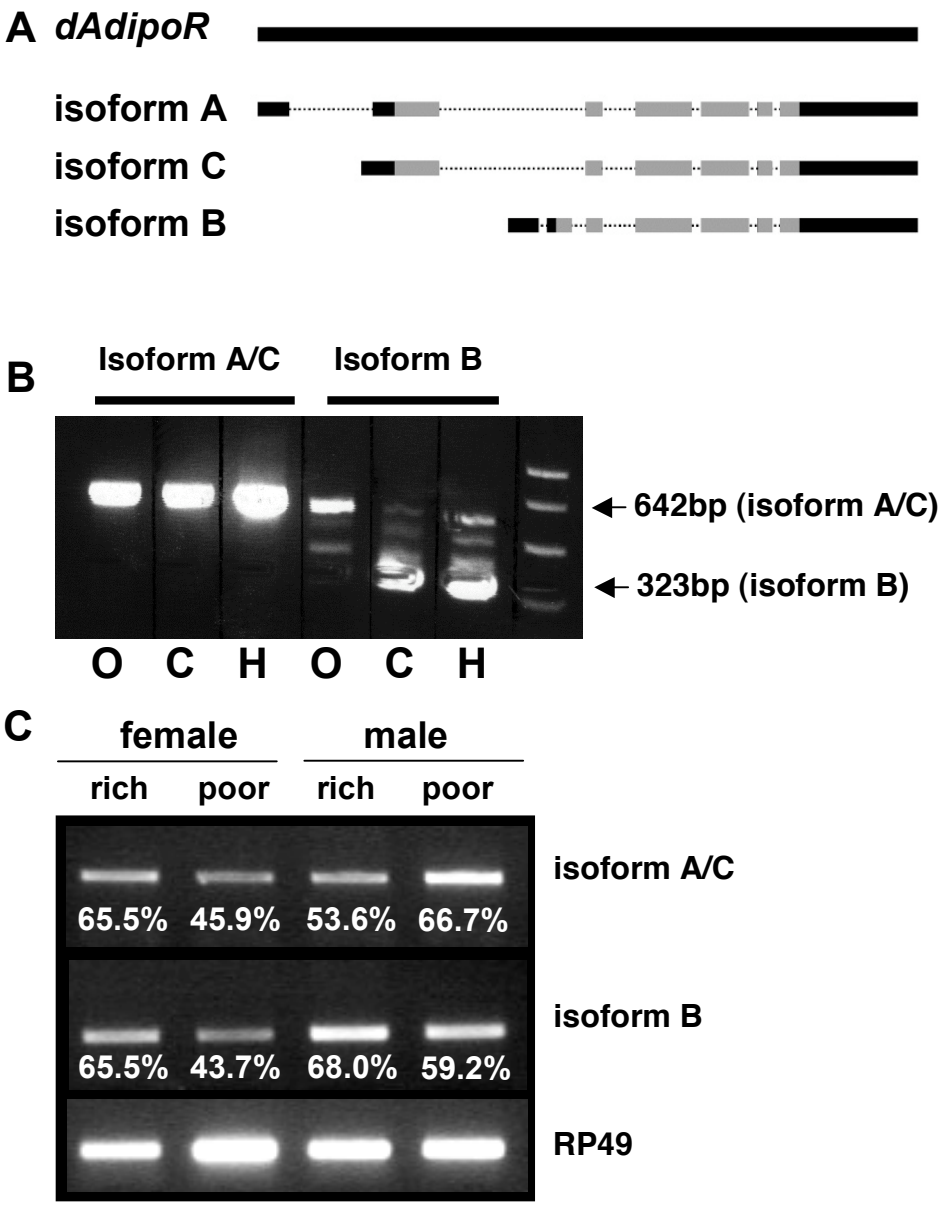

Figure 4.6. *dAdipoR* isoform expression analysis. (A) *dAdipoR* encodes three isoforms. A and C have the same protein sequence. B encodes a shorter protein. **(B)** Primers specific for *dAdipoR* isoforms A and C (642 bp PCR product) detect transcript in ovaries (O), carcasses (C), and head (H). Isoform B (323 bp PCR product) is not detected in the ovaries (DNA band present may be background amplification of isoform A/C), but is present in the carcass and head. RT-PCR was performed by Joshua Clanton as a rotation student. **(C)** RT-PCR of *dAdipoR* isoforms in male versus female and rich versus poor diet. Numbers below bands indicate intensity levels relative to *RP49* control.

expressed in all tissues examined, which include the ovary, head, and the carcass (includes the fat body). The B isoform, while expressed in both the head and carcass, is either absent or below the level of detection in the ovary (Figure 4.6B).

Insulin signaling has been demonstrated to negatively regulate *mAdipoR* transcription via a *PI3K/Foxo1* dependent pathway (Tsuchida et al., 2004). To determine if this level of regulation is conserved in *Drosophila*, I examined expression of *dAdipoR* isoforms in males and females fed either a rich or poor diet. If *dAdipoR* transcription is regulated via *PI3K/dFOXO* in *Drosophila*, I would expect *dAdipoR* expression to be down when the transcription factor dFOXO is repressed on a rich diet, and up when dFOXO is active on a poor diet. My results do not support the model since all *dAdipoR* isoforms decrease relative to an *RP49* internal control from about 65% on a rich diet to about 45% on a poor diet in females (Figure 4.6C). Together these results suggest that *dAdipoR* isoforms are expressed in a tissue-specific manner and that they may be transcriptionally regulated in response to diet, but perhaps not by the same mechanism as reported for mammals. Further analysis will be needed to confirm these finding and to verify whether *dAdipoR* is a target of dFOXO.

Development and characterization of *dAdipoR* null alleles

I next examined the effects of *dAdipoR* loss of function in the ovary. Based on mammalian studies, I hypothesized that loss of *dAdipoR* may reduce insulin sensitivity in the ovary, resulting in comparatively reduced rates of oogenesis when nutrients are limiting. Since no mutant alleles of *dAdipoR* are available, I generated a null allele by piggyBac-mediated recombination between piggyBac transposable elements located in the

5' (*CG5315*^{f05395}) and 3' (*CG5315*^{c02150}) untranslated regions of *dAdipoR* (*CG5315*), resulting in the *dAdipoR*^{27} null allele (Figure 4.7A) (see Materials and Methods for further details on piggyBac-mediated recombination). A large deletion, named *dAdipoR*$^{\Delta 37}$, was also generated by inducing FLP/*FRT*-mediated recombination between flies carrying *CG5315*^{f05395} and *CG5315*^{e01762}, removing *dAdipoR* and an additional three uncharacterized genes (*CG5326*, *CG3393*, and *CG33099*) (Figure 4.7A). Both resulting mutant lines were out-crossed in a wild-type background to remove potential background mutations, then balanced and confirmed by PCR and sequencing.

Neither *dAdipoR* mutant line produced viable homozygous mutant adults, indicating *dAdipoR* is essential for development. To ascertain if the observed lethality is due to loss of *dAdipoR* function and not a background mutation in the parental strain since *dAdipoR*^{f05395} is also lethal, I performed a series of complementation tests between the original parental strains, the *dAdipoR* null alleles, and a set of deficiencies predicted to remove the *dAdipoR* gene region (cytogenetic map region 94B3) (Figure 4.8A). The *dAdipoR*$^{\Delta 37}$ deficiency allele failed to complement six of seven deficiency lines tested, the *dAdipoR*^{27} null allele failed to complement five of seven, and the *dAdipoR*^{f05395} parental strain failed to complement four of seven (Figure 4.8B). Since the three deficiencies in question that complemented the *dAdipoR* mutant alleles should have completely removed the gene region encoding *CG5315*, it is likely that I failed to recognize a marker associated with the wild-type balancer chromosome and mistakenly identified some flies as homozygous when, in fact, they were heterozygous. Since the majority of the deficiencies uncovering *CG5315* failed to complement, however, it is likely that *dAdipoR* loss of function lethality is not due to a background mutation.

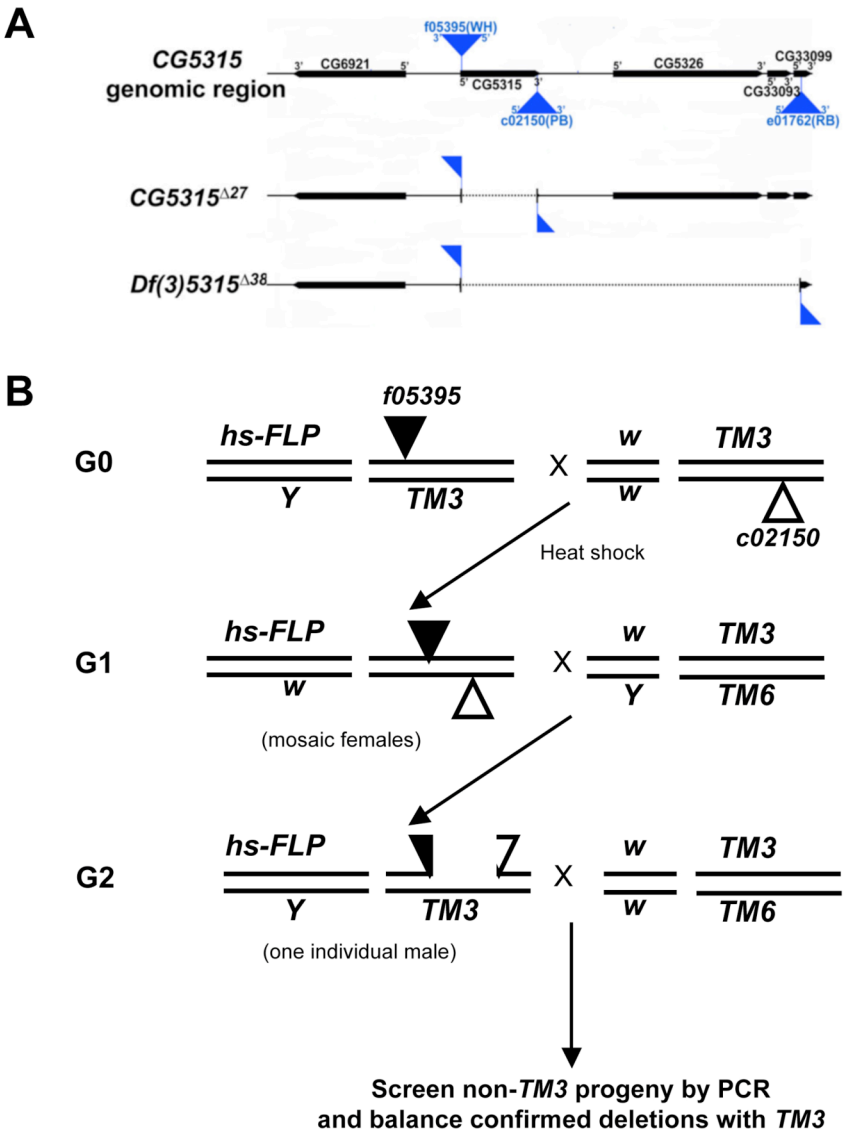

Figure 4.7. Generation of *dAdipoR* null alleles by *FLP*/*FRT* mediated recombination. (A) *dAdipoR* (*CG5315*) genomic region map. piggyBac transposable elements are noted by blue triangles. Regions removed by FLP/*FRT* mediated recombination between piggybac elements are noted by light grey lines between remaining partial piggybac sequences (blue flags). **(B)** Strategy for generation of alleles shown in (A). Further details in Materials and Methods.

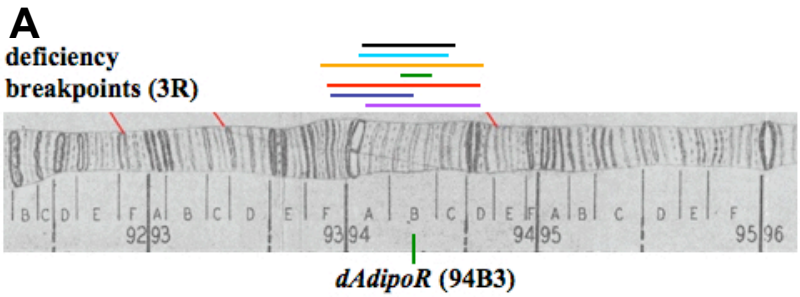

B

	$dAdipoR^{c02150}$	$dAdipoR^{f05395}$	$dAdipoR^{27}$	$dAdipoR^{\Delta 38}$
$dAdipoR^{c02150}$				
$dAdipoR^{f05395}$		✝	✝	✝
$dAdipoR^{27}$		✝	✝	✝
$dAdipoR^{\Delta 38}$		✝	✝	✝
94A3-94D4				✝
93F14-94B5		✝	✝	✝
93F13-94D2				
94B2-94B11		✝	✝	✝
93F11-94D13		✝	✝	✝
94A1-94C1			✝	✝
94A2-94C4		✝	✝	✝

Figure 4.8. *dAdipoR* mutant alleles are homozygous lethal. (A) Cytogenetic map for chromosome containing *dAdipoR* gene region 94B3. Estimated or confirmed area removed by deficiencies (listed in B) are indicated by colored lines. **(B)** Complementation table showing results between crosses of various *dAdipoR* mutant alleles and deficiencies. Combinations that fail to complement *dAdipoR* mutant lethality are indicated by a cross.

Developmental lethality of the *dAdipoR* null allele is not rescued by transgenic expression of isoform A/C

Both to confirm my results that *dAdipoR* loss of function results in lethality and to obtain a source of adult homozygous mutant *dAdipoR* females for ovarian analysis, I prepared a series of *UASp*- and *HS-dAdipoR* transgenic strains (Table 4.1) (see also Materials and Methods). The two inducible expression vectors were generated by placing the *CG5315* isoform A/C cDNA from the *Drosophila* Genomics Resource Center (DGRC) *Drosophila* Gene Collection Release 1 in either a Heat-shock (*hsp70*) or Gal4 inducible upstream activating sequence (*UASp*)-construct.

To rescue the developmental lethality of $dAdipoR^{27}$, I crossed *UASp-*$dAdipoR^{A/C}$ (transgenic line #7)*/Cyo;* $dAdipoR^{27}$*/ TM3* flies to a panel of Gal4 drivers combined with $dAdipoR^{27}$*/ TM3*, including: *Act5c-Gal4*, a ubiquitous driver; *elav-Gal4*, a pan-neural driver; *FB-Gal4*, a fat body specific driver; and *CG-Gal4*, a fat body and late follicle cell driver. In parallel to attempted rescue with *Act5c-Gal4*, I tested if *dAdipoR* expression in either the nervous system or fat body could rescue lethality. Flies were cultured at both 25°C and 29°C to obtain further control of expression levels since the *UAS/Gal4* system is temperature sensitive (higher temperatures can results in higher induction levels) (Duffy, 2002). Progeny were analyzed for absence of the TM3 balancer, which would indicate homozygosity of $dAdipoR^{27}$. No $dAdipoR^{27}$ homozygous progeny were present, indicating transgenic line #7 *UASp-*$dAdipoR^{A/C}$ expression fails to rescue $dAdipoR^{27}$ mutants to adulthood under the control of any of the Gal4 drivers tested. *HS-*$dAdipoR^{A/C}$ was also unable to rescue $dAdipoR^{27}$ loss of function lethality. Females and males of the genotype *HS-*$dAdipoR^{A/C}$*/Cyo;* $dAdipoR^{27}$*/ TM3* were allowed to lay eggs for 24 hours. Those

Table 4.1

***dAdipoR* isoform A/C transgenic lines**

***dAdipoR* transgenic line**	**Insertion location[a]**
pUASpI-CG5315$^{A/C}$ #9	X
pUASpI-CG5315$^{A/C}$ #7	II
hsp70-CG5315$^{A/C}$ #11	II
hsp70-CG5315$^{A/C}$ #14	II
hsp70-CG5315$^{A/C}$ #6	II

[a] Chromosomal location of the transgene

progeny were either raised at 29°C until eclosion or heat-shocked at 37°C to induce *dAdipoR*$^{A/C}$ expression twice a day throughout development. Neither induction condition resulted in viable homozygous *dAdipoR* mutant progeny.

dAdipoR has a diet-dependent role in GSC maintenance and proliferation

Since the effect of *dAdipoR*^{27} loss of function cannot be analyzed in *dAdipoR* mutant adult females, I placed the *dAdipoR*^{27} null allele on a *FRT82B* chromosome arm to examine its role in ovarian stem cells and their progeny by mutant mosaic analysis. *dAdipoR*^{27} mosaic flies were fed a rich diet for seven days post clone-induction, then continued on a rich diet or switched to a poor diet for an additional three days. I hypothesized that loss of *dAdipoR* may reduce ovarian cell proliferation and/or growth rates on a poor diet if its role is to sensitize ovarian tissue to insulin signaling as proposed for the role of *mAdipoR* on peripheral tissues (Wang et al., 2007). First, I examined the effect of *dAdipoR*^{27} loss on GSC division rates by comparing the total number of GFP-positive (wild-type) GSC progeny to the total number of GFP-negative (*dAdipoR* mutant) GSC progeny to obtain a relative division rate as previously described (LaFever and Drummond-Barbosa, 2005). A relative division rate of 1.0 in mosaic germaria with one wild-type and one mutant GSC indicates that both are producing progeny at equal rates. A reduced relative division rates indicates a comparatively slower rate of division in the mutant GSC. Our laboratory has shown that GSC division rates slow when flies are fed a poor diet, when components of the insulin signaling pathway are mutated, or when TOR activity is reduced (Hsu et al., 2008; LaFever and Drummond-Barbosa, 2005; LaFever et al., 2010). As expected, *dAdipoR*^{27} mutant GSCs appear to proliferate more slowly than

their wildtype neighbors when flies were maintained on a poor diet (0.77, n=155), but do not proliferate more slowly on a rich diet (0.95, n=367) (Figure 4.9D), suggesting that loss of *dAdipoR* may render GSCs less sensitive to insulin when nutrients are limiting. While these data have not yet reached significance, if the current trend remains true, an increased sample number should result in a significantly reduced GSC proliferation rates on a poor diet.

While $dAdipoR^{27}$ mutant GSC proliferation rates appear relatively unchanged on a rich diet, they are not maintained in their niche as well as controls (38% $dAdipoR^{27}$ GSC loss, n=69) compared to about 20% GSC loss in controls, but on a poor diet preliminary data suggests the $dAdipoR^{27}$ GSC maintenance defect is rescued (20% GSC loss, n=18) (Figure 4.9A-C). The current model for how mAdipoR signaling regulates insulin sensitivity in muscle is that by adiponectin stimulation of AdipoR leads to AMPK-mediated suppression of TOR activity, thus releasing the feedback suppression of the insulin signaling pathway at the level of the IRS (*chico* in flies). It is therefore reasonable to suggest that loss of *dAdipoR* may result in hyperactive TOR activity on a rich diet and lead to GSC loss (see Chapter III). The fact that the GSC loss defect is rescued on a poor diet further implicates a role for TOR in regulating GSC maintenance downstream of *dAdipoR* since TOR activity is know to be suppressed under nutrient-poor conditions (see Chapter III).

Loss of $dAdipoR^{27}$ does not appear to have a major role on germline cyst growth rates, but fewer $dAdipoR^{27}$ mutant germline cysts are present outside of the germarium compared to mock mosaic controls (data not shown), suggesting that *dAdipoR* may have a

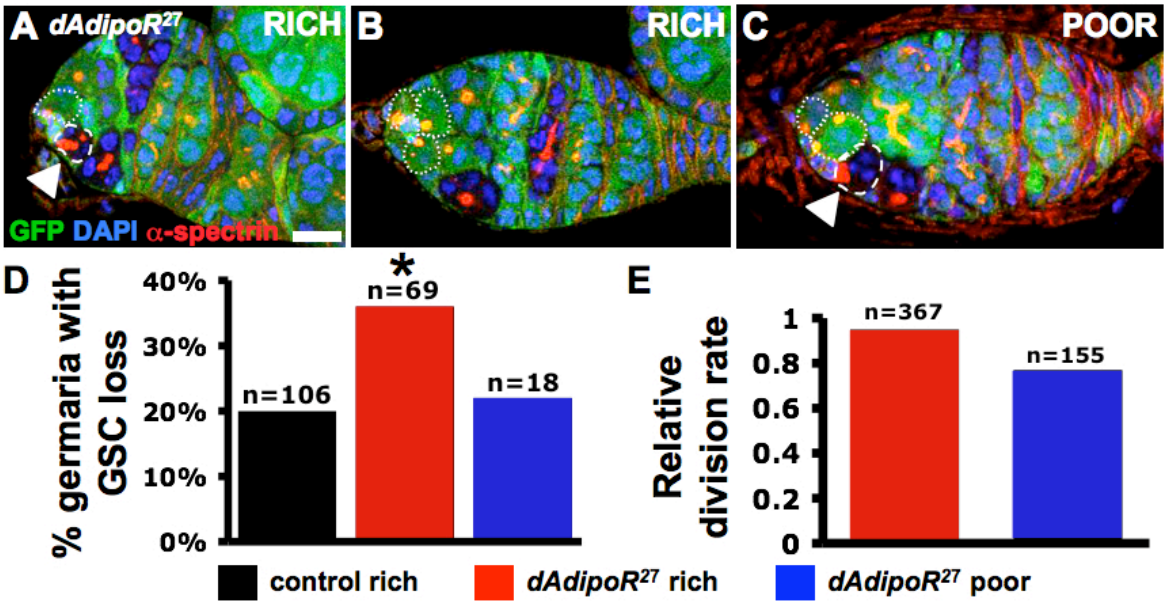

Figure 4.9. *dAdipoR* cell-autonomously regulates GSC maintenance and proliferation in a diet-dependent manner. (A-C) *dAdipoR*^{27} mosaic germaria. Dotted lines, GSCs. Arrowheads, *dAdipoR*^{27} mutant (GFP-negative) GSC. GFP, green (wild-type cells). DAPI, blue (DNA). α-spectrin, red (fusomes and cap and follicle cell membranes). **(D)** The percentage of *dAdipoR*^{27} mosaic germaria with GSC loss is increased on a rich diet. *n*, number of germaria analyzed. **(E)** *dAdipoR*^{27} mutant GSCs proliferate more slowly than wild-type GSCs on a poor diet, but not on a rich diet. *n*, number of cystoblasts and cysts analyzed. *, *P* =0.016. Scale bar, 10 μm.

role in regulating the survival of germline cysts. Future experiments will test for elevated levels of cell death in *dAdipoR*^{27} mosaic germaria compared to mock mosaic control germaria. *dAdipoR* may also have a role in regulating progression through vitellogenesis as fewer vitellogenic *dAdipoR*^{27} mutant germline cysts are present compared to wildtype controls, but a comparative analysis to a mock mosaic control is necessary to validate these data.

dAdipoR may also have a functional role in the follicle cell lineage. Ovarioles with one *dAdipoR*^{27} mutant FSC and one wildtype FSC exhibit a reduced progeny ratio of 30% *dAdipoR*^{27} to 70% wildtype follicle cells on either a rich or poor diet, while mock mosaic ovarioles have on average 50% unmarked (GFP-negative) to 50% marked (GFP-positive) follicle cells (see Chapter III). A role for *dAdipoR* in FSC maintenance has not yet been tested, but the high degree of variability in follicle cell ratios in *dAdipoR*^{27} mosaics (standard deviation of *dAdipoR*^{27} follicle cell number is about ± 17% on either a rich or poor diet) suggests loss of FSCs may also play a role in the observed follicle cell ratios.

These preliminary data indicate that *dAdipoR* may have a diet-dependent role in the GSCs for the regulation of both their maintenance and proliferation, potentially via modulation of the insulin and TOR kinase nutrient-sensing pathways. DILPs, in addition to being directly received by the germline and soma, also activate the insulin signaling pathway in the niche cap cells to modulate GSC maintenance (Hsu and Drummond-Barbosa, 2009). It is possible, therefore, that *dAdipoR* is required in cap cells to regulate GSC activity non-cell autonomously. Experiments to test of knockdown of *dAdipoR* in the niche affects GSC maintenance non-cell autonomously are in progress.

dAdipoR is required in the fat body to regulate rates of egg production

In humans, both *mAdipoR1* and *mAdipoR2* are highly expressed in adipose tissue (Kos et al., 2010) and signaling via adipocyte adiponectin receptors feeds into to multiple nutrient-sensing pathways that regulate a myriad of metabolic functions (Marshall, 2006). The *Drosophila* fat body is insulin sensitive (Bauer et al., 2007) and larval nutrient-sensing pathways (including TOR kinase) regulate peripheral tissue growth and proliferation via secretion of unknown mitogenic factors (Colombani et al., 2003). To determine if adiponectin receptor signaling acts via the adult fat body to regulate the secretion of factors that act on peripheral tissues such as the ovary, I attempted to remove or knockdown *dAdipoR* expression specifically in the adult fat body by fat body mosaic analysis and RNAi, respectively.

Previous studies have utilized larval fat body mosaic analysis techniques, but generation of adult fat body mosaic tissue has not been demonstrated. This is likely due to insufficient knowledge regarding when the adult fat body is proliferative--a requirement to induce mitotic clones via heat-shock induction of flipase. I attempted to generate adult fat body cell clones using the heat-shock inducible *X15-29/X15-33* LacZ knock-in system, which has been previously used to label cell lineages throughout development (Drummond-Barbosa and Spradling, 2001) (Figure 4.10). Unlike the ovarian mosaic analysis technique I previously described, in which the unlabeled cells arose from the mutant progenitor, the LacZ knock-in system positively marks clones of a mitotically-dividing progenitor. X-gal staining (see Materials and Methods) turns the LacZ-positive cells bright blue, allowing for easy identification of even a small number of clonal cells within a tissue.

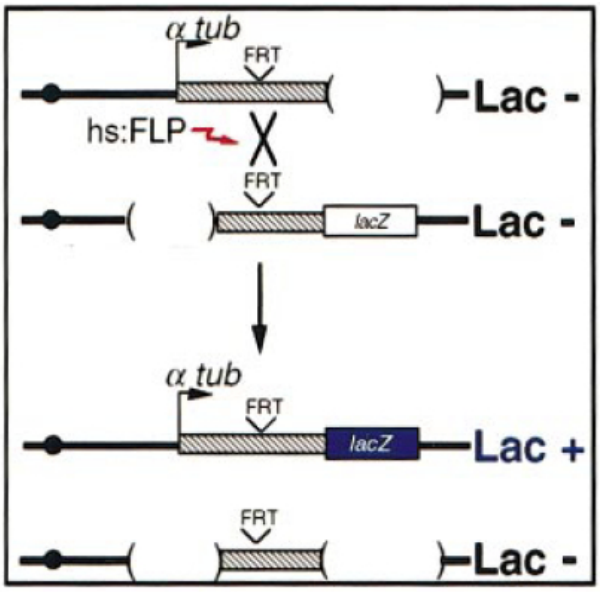

Figure 4.10. A *LacZ* knock-in system for lineage labeling.
A subset of mitotically-dividing cells in flies carrying two inactive transgenes with complementing components (a tubulin promotor and *LacZ*) can be induced to express LacZ by heat-shock induction of flipase, which mediates recombination between the FRT sites and generates an active *tubulin-LacZ* transgene (from Drummond-Barbosa and Spradling, 2001).

Using this lineage-labeling technique, I attempted to identify the time frame in which adult fat cells are mitotically active. It has been proposed that most larval fat body breaks down during pupation and then the adult fat body arises from an unidentified progenitor population to replace the larval fat body during the first few days post-eclosion (Aguila et al., 2007). This would suggest that the adult fat body is proliferative within the first few days after adult eclosion. I tested for fat body cell proliferation by heat-shocking flies carrying the lineage labeling transgenes 0-1 days after eclosion to induce mitotic clones; however, no LacZ-positive fat body cells were observed. LacZ-positive clones were observed throughout the ovary, indicating the lineage-labeling system is functioning properly since ovarian cells are highly mitotically active. Another hypothesis is that the adult fat body could form from a subset of precursor cells established at even earlier developmental stages. I tested this possibility by inducing mitotic clones throughout the 3rd instar larvae stage when the imaginal discs, which give rise to the adult structures, are proliferative. Interestingly, I observed a very low level of LacZ-positive fat body cells (one to two positive cells, but the vast majority were unmarked), indicating a very low level of mitotic activity occurs in adult fat body tissue during the last larval stage, perhaps only for refinement of final fat body cell numbers. These results suggest the adult fat body progenitors are proliferating at an even earlier stage such as the embryonic stage or the first or second larval instar. These possibilities remain untested, due to a change in project focus. Further experiments aimed at identifying the fat body cell lineage will be performed by a new lab member, Kate Laws.

An additional potential technique for generating mutant adult fat body cells is to drive flipase expression under the control of a Gal4 driver instead of by heat-shock

induction. This method does not require knowing when the fat body cells are proliferative, but does require a Gal4 driver that is induced in the earliest fat body progenitor population. Several fat body Gal4 drivers are available to test for the ability to produce fat body clones, including *FB-Gal4*, *CG-Gal4*, *Adh-Gal4*, and *R4-Gal4*, but these experiments have yet to be performed.

The recent development of a collection of RNAi lines for almost every gene in the *Drosophila* genome provides another option for reducing *dAdipoR* expression specifically in the adult fat body (Dietzl et al., 2007). An *dAdipoR* RNAi line predicted to target *dAdipoR* isoforms A and C was obtained from the Vienna *Drosophila* RNAi Center. Ubiquitous expression of $dAdipoR^{RNAi}$ with *Act5C-Gal4* phenocopies the lethality of the *dAdipoR* null alleles, suggesting *dAdipoR* gene expression may be reduced by *dAdipoR* RNAi expression. The level and specificity of *dAdipoR* knock-down by this *RNAi* line, however, remains untested.

I expressed $dAdipoR^{RNAi}$ in the adult fat body using the *FB-Gal4* and $tubulin\text{-}Gal80^{ts}$ transgenes used for adult specific fat body expression ($FB{>}dAdipoR^{RNAi}$) (Figure 4.11) (see also Materials and Methods) and performed a basic egg count fertility assay. Egg production was significantly reduced by about 50% ($P > 0.05$) in $FB{>}dAdipoR^{RNAi}$ files compared to controls on either a rich or poor diet (Figure 4.12). Egg production was also significantly reduced in flies expressing $dAdipoR^{RNAi}$ in the fat body with the *CG-Gal4* driver (data not shown).

To examine potential causes for reduced egg production in these fat body *dAdipoR* mutant females, I performed a GSC cell-cycle analysis (see Materials and Methods) in $FB{>}dAdipoR^{RNAi}$ knockdown females fed a rich diet for six days at the permissive

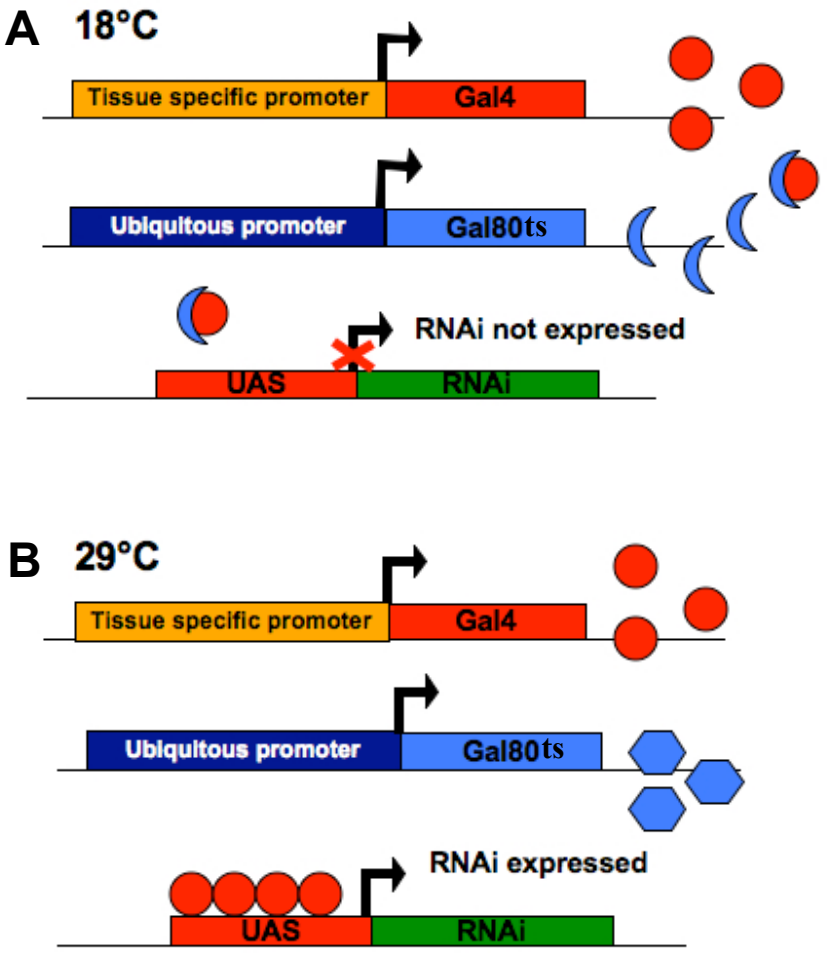

Figure 4.11. A *UAS/Gal4/Gal80^{ts}* technique for tissue-specific and temporally-controlled transgene expression. (A) At 18°C *RNAi* expression is suppressed in flies carrying the *UAS*, *Gal4*, and *Gal80^{ts}* transgenes by Gal80 (represented by blue cresents), which binds and renders Gal4 (red circles) unable to bind and activate *UAS*. **(B)** At 29°C, Gal80 undergoes a conformational change (blue hexagons) and can no longer inhibit Gal4. Gal4 then can bind and activate *UAS* and induce *RNAi* expression.

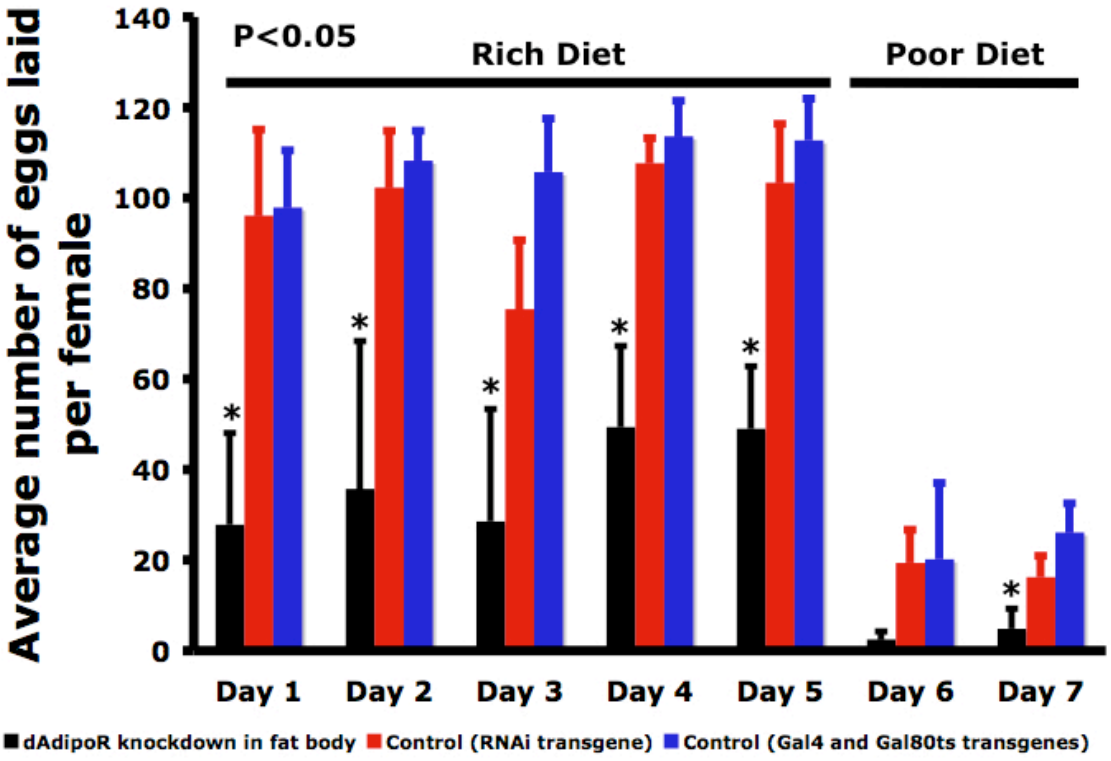

Figure 4.12. Knockdown of *dAdipoR* in the adult fat body reduces rates of egg production. Average number of eggs laid per female per day for five days on a rich diet followed by two days on a poor diet. Genotypes: *dAdipoR* knockdown (*FB-Gal4/+; dAdipoR^{RNAi}/tubP-Gal80^{ts}*), RNAi control (*dAdipoR^{RNAi}/+)*, Gal4/Gal80 control (*FB-Gal4/+; tubP-Gal80^{ts}*/+). Asterisks, $P < 0.05$. Error bars, *s.d.*

temperature of 29°C, which provides more than ample time for *FB>dAdipoR*^{RNAi} expression to affect proliferation rates in the GSCs. Surprisingly, GSC proliferation rates and cell-cycle profiles were unchanged in *FB>dAdipoR*^{RNAi} females compared to controls (Figure 4.13), indicating that the negative effects of fat body *dAdipoR* knockdown on egg laying rates must occur at a later stage of development.

Fat body expression of *dAdipoR* is necessary for proper ovarian cyst cell number

I examined *FB>dAdipoR*^{RNAi} ovarian morphology by DAPI (DNA) staining and ascertained that 15-20% (n=858 cysts) of the germline cysts had elevated cyst cell numbers compared to 0-2% (n=1052 cysts) in controls (Figure 4.14A,B). Germline cysts normally exit mitotic cell-cycles at the 16-cell stage (15 nurse cells and one oocyte) (Spradling, 1993), but many *FB>dAdipoR*^{RNAi} germline cysts contained 32 cells (Figure 4.14A). An increase in germline cyst cell number might be explained by either an additional mitotic division (31 nurse cells and 1 oocyte) or mis-packaging of two separate germline cysts into a single follicle (30 nurse cells and 2 oocytes). To differentiate between these possibilities, I performed immunostaining on ovaries from *FB>dAdipoR*^{RNAi} flies with an antibody against OO15 RNA-binding (Orb), a oocyte- specific protein (Lantz et al., 1992).

In 19/20 of the 32-cell cysts in *FB>dAdipoR*^{RNAi} ovaries, Orb labels a single oocyte, suggesting the majority of germline cysts underwent an additional mitotic division (Figure 4.15A,B). To further verify these data, I stained ovaries from *FB>dAdipoR*^{RNAi} flies with a ring canal antibody, Hts-RC, which would label five ring canals at the oocyte if the germline cyst underwent an additional mitotic division (Yue and Spradling, 1992).

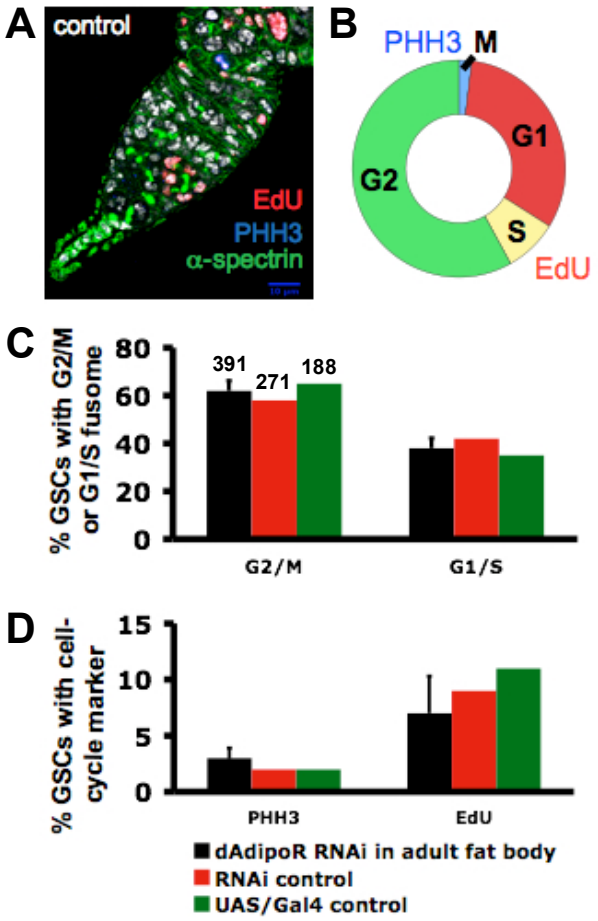

Figure 4.13. Fat body knockdown of *dAdipoR* does not affect GSC proliferation. (A) Control germarium stained with markers for different stages of the GSC cell-cycle. Edu, red, S-phase. PHH3, blue, M-phase. α-spectrin, green, fusome. Scale bar, 10μm. **(B)** Cell cycle profile of GSCs from flies from either controls or *dAdiopR* fat body knockdown females (generated from data shown in C and D). **(C)** % GSCs with either a G2/M or G1/S fusome morphology (see material and methods). Numbers above bars indicate number of GSCs analyzed for each genotype. **(D)** % PHH3-positive or % EdU-positive GSCs (M and S-phases respectively). Error bars, *s.d.*

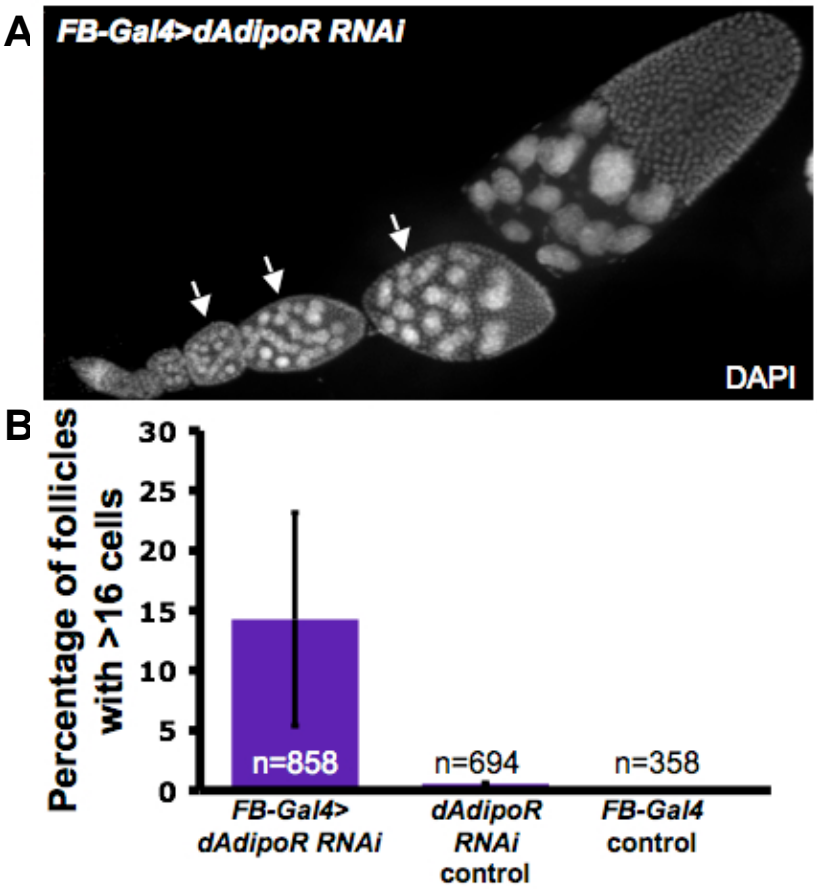

Figure 4.14. Fat body specific knockdown of *dAdipoR* results in 32-cell germline cysts. (A) Ovariole from *FB>dAdipoR* RNAi knock-down females (*FB-Gal4/+;UAS-dAdipoR^{RNAi}/tubPGal80ts*). DAPI, grey, DNA. Arrows indicate 32-cell cysts. **(B)** Quantification of total cysts with more than 16 cells. n, total number of cysts analyzed for each genotype. Error bars, s.d.

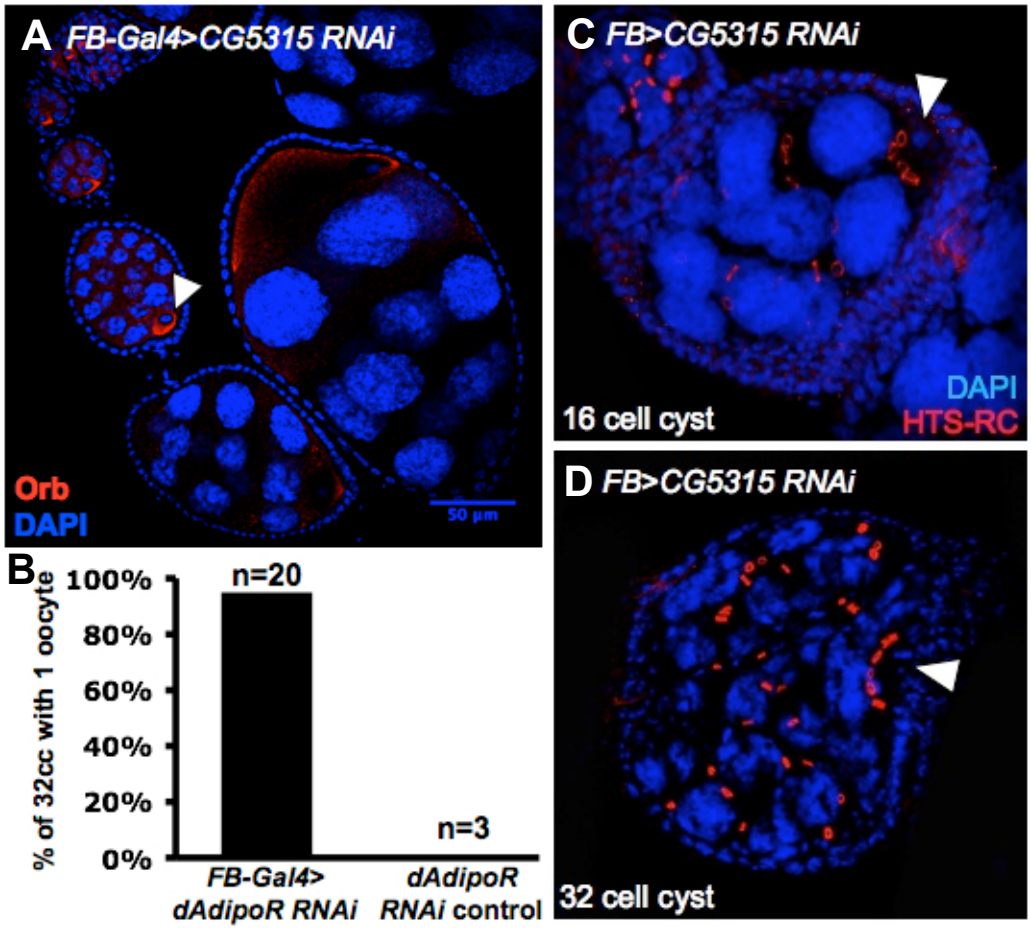

Figure 4.15. Fat body knockdown of *dAdipoR* affects germline cyst division number. (A) Ovariole from adult specific *dAdipoR* knockdown (*FB-Gal4/+;UAS-dAdipoR^{RNAi}/tubPGal80ts*). Orb, red, marks the oocyte. DAPI, blue, marks DNA. Arrowhead indicates a single oocyte in a 32-cell cyst. Scale bar, 50µm. **(B)** Quantification of total number of 32-cell cysts observed that have a single oocyte. n, total number of 32-cell cysts analyzed. **(C)** Z-stack projection of a 16-cell cust from an adult specific *dAdipoR* knockdown (*FB-Gal4/+;UAS-dAdipoR RNAi/tubPGal80ts*). Arrowhead indicates a single oocyte with four ring canals **(D)** Z-stack projection of a 32-cell cyst from same genotype. Arrowhead indicates a single oocyte with five ring canals. HTS-RC, red, marks ring canals. DAPI, blue, marks DNA.

Indeed, 32-cell cysts contained five ring canals at the oocyte, compared to four in controls (Figure 4.15C,D), again indicating that knockdown of *dAdipoR* in the adult fat body has a non-cell autonomous effect on germline cyst mitotic division.

Knockdown of genes involved in nutrient-sensing or fat storage can also result in an additional germline cyst division

Since *AdipoR* is proposed to act via the TOR, insulin, and AMPK signaling pathways to regulate peripheral tissue insulin sensitivity in mammals (Wang et al., 2007), I tested if fat body knockdown of components of these nutrient sensing pathway components also result in a 32-cell ovarian cyst phenotype. For example, I previously demonstrated that overexpression of *dilp2* leads to about 7% 32-cell cysts compared to about 2% in controls (see Figure 4.3D), suggesting that elevated insulin signaling can indeed lead to an extranumerary germline cyst division. To test if dAdipoR acts via nutrient-signaling pathways in the fat body and, if so, how insulin signaling activity may be affected, I obtained a panel of RNAi lines to screen genes that have been either demonstrated or proposed to affect nutrient-sensing pathways or fat storage levels (Table 4.2). RNAi against each gene listed in Table 4.2 was induced in the adult fat body and then ovaries from those flies were analyzed for aberrant germline cyst cell number. Surprisingly, many exhibited cysts with increased cell number, including genes affecting TOR activity such as *Tor* itself, *raptor*, and amino-acid transporters, as well as genes that regulate fat storage levels such as the *Drosophila* TAG lipases, *bmm* and *CG8552* (Table 4.2). These data suggest *dAdipoR* may be acting via nutrient-sensing pathways within the fat body to regulate oogenesis. Interestingly, knockdown of several genes, such as *Tor*, *raptor*, *bmm*, and *InR*, in the fat body resulted in ovarian cell death at distinct stages of

Table 4.2

RNAi lines screened from a non-cell autonomous role on the ovary via the fat body

Gene	Rationale: proposed knock-down effect	RNAi line identification[a]	% 32-cell cysts[b] (number of ovarioles)
w	control: no effect	Bloomington 28980	0% (24)
adp	fat storage up	VDRC 22008	1% (69)
bmm[c]	fat storage up	VDRC 37880	47% (19)
lsd2	fat storage down	VDRC 40735	0% (52)
CG8552	fat storage up	VDRC 35956	33% (12)
Imp-L2	insulin signaling up	VDRC 30931	36% (33)
ALS	insulin signaling up	P. Leopold	4% (51)
Tsc1	TOR activity up	VDRC 22252	18% (33)
InR	insulin signaling down	VDRC 991	0% (55)
Slif	TOR activity down	P. Leopold	35% (23)
Tor	TOR activity down	P. Leopold	38% (8)
raptor	TOR activity down	VDRC 13112	12% (26)
CG16700[d]	?	VDRC 45188	0% (34)
CG13384[d]	?	VDRC 44245	0% (36)
hoe2[d]	?	VDRC 7858	2% (58)
kcc[d]	?	VDRC 10278	35% (40)
CG13646[d]	?	VDRC 1571	41% (32)
VGlut[d]	?	VDRC 2574	47% (45)
CG32079[d]	?	VDRC 39496	0% (39)
dAdipoR	?	VDRC 40936	27% (26)

[a] VDRC, Vienna *Drosophila* RNAi Center

[b] % of 32-cell cysts was determined as the number of ovarioles with at least one 32-cell cyst.

[c] Genes and percentages in red indicate lines considered as positive for a 32-cell cyst phenotype (10% or higher frequency).

[d] Genes with gene ontology listed as amino-acid transporter activity (may reduce TOR activity, but not experimentally tested).

oogenesis (data not shown), providing further evidence that nutrient-sensing in the fat body affects oogenesis.

Based on these data, I am unable to conclude how *dAdipoR* knockdown affects fat body insulin signaling. Neither the levels of RNAi induction or the specificity of the RNAi lines are known, so levels of RNA knockdown in the fat body should be examined by RT-PCR. Furthermore, due to the high level of feedback mechanisms between nutrient-sensing pathways, it is difficult to propose the effect of knockdown of a specific gene on the insulin signaling pathway without performing additional experiments such as pAkt immunostaining, tGPH localization, or FOXO localization, all of which can serve as *in vivo* read-outs of insulin signaling activity (Britton et al., 2002; Kockel et al., 2010; Van Der Heide et al., 2004). Studies are underway to determine if insulin signaling is affected in the fat body of $FB>dAdipoR^{RNAi}$ flies. We also want to understand if modulation of fat body insulin signaling has an effect on oogenesis, and if so, how. Experiments designed to alter insulin signaling levels in the fat body using a series of transgenes that either knockdown or overexpress *InR,* or that produce an InR that is constitutively active or inactive, are currently in progress as part of a rotation student project with Christa Wagner..

***dAdipoR* knockdown in the fat body may affect Cyclin E levels in the germarium**

During early oogenesis, 16-cell germline cysts within the germarium exit the mitotic cell cycle after four mitotic divisions with incomplete cytokinesis. The oocyte then enters meiosis while the remaining 15 cells undergo endoreplication in preparation for their role as nurse cells (Spradling, 1993). The mechanism that triggers mitotic exit at the

16-cell stage is not completely understood, but it is known that the expression patterns of cell-cycle regulators and differentiation genes undergo dynamic changes during the process. Levels of the G1/S regulator, Cyclin E, are normally downregulated after the last mitotic division between an 8- and 16-cell cyst and Cyclin E overexpression leads to an extra mitotic cyst division (Ohlmeyer and Schupbach, 2003). Overexpression of the G2 cyclins, such as Cyclin A and B, can also promote a fifth cyst division—a phenotype suppressed by *Bam*, a gene that produces a protein product required for cyst formation found in the cytoplasm of dividing cysts. *Bam*, *Cyclin A*, *Cyclin B*, and *Cyclin E* are all normally downregulated after the fourth mitotic cyst division (Lilly et al., 2000).

Previous studies have identified genes [such as *encore*, *sine prol*e, *fused*, and *Ataxin 2-binding protein 1* (*A2BP1*)] that have cell-autonomous roles in germline cyst mitotic exit. Encore is a member of a novel family of proteins involved in RNA regulation (Van Buskirk et al., 2000). *sine prole* was identified as a locus in region 45A of chromosome II that is required for fertility (Mohr and Boswell, 2002). Fused is a serine-threonine kinases that acts as a positive regulator of Hedgehog signaling (Narbonne-Reveau et al., 2006). A2BP1 is a protein proposed to have multiple functions relating to RNA metabolism (Tastan et al., 2010). Alterations in the expression level or patterns of these genes leads to improper germline cyst cell number likely due to misregulation of the cyclins and/or *Bam* expression (Lilly et al., 2000; Mohr and Boswell, 2002; Narbonne-Reveau et al., 2006; Ohlmeyer and Schupbach, 2003; Tastan et al., 2010). Cyclin A, Cyclin E, and Bam protein levels are not down-regulated properly in *encore* and *sine prole* mutants (Mohr and Boswell, 2002; Ohlmeyer and Schupbach, 2003) and A2BP1 and fused mutants exhibit expanded Bam expression through the 16-cell cyst stage (Narbonne-

Reveau et al., 2006; Tastan et al., 2010). It has been proposed that the additional cyst division in *encore* mutants may be caused by inefficient proteolysis machinery, which could lead to high cyclin levels and failure to exit mitosis in a timely manner (Ohlmeyer and Schupbach, 2003).

As a first step in determining how an extra germline cyst division occurs in *FB>dAdipoR*^{RNAi} females, I examined the Cyclin E expression pattern in these ovaries. Cyclin E is normally expressed in germarium region 1 (which contains GSCs, cystoblasts, 2-, 4-, and 8-cell cysts), is downregulated in region 2A/2B (which contains 16-cell cysts), and becomes upregulated in region 3 (when 16-cell cysts enter endoreplication) (Ohlmeyer and Schupbach, 2003) (Figure 4.16A). While Cyclin E expression in germaria of *dAdipoR* fat body knockdown females appears mostly normal (13/15) (Figure 4.16B), some have expanded Cyclin E expression into region 2A/2B or higher overall Cyclin E expression levels (2/15, or about 13%) (Figure 4.16C). Since only 15-20% of follicles in *FB>dAdipoR*^{RNAi} ovaries exhibit increased cyst cell numbers (see Figure 4.14), it is not surprising that only a subset of germaria from *FB>dAdipoR*^{RNAi} females would exhibit altered Cyclin E levels and/or expression patterns. I also have evidence that raising *FB>dAdipoR*^{RNAi} flies at lower temperatures can suppress the additional cyst division (data not shown), which is also true for *encore* mutants (Ohlmeyer and Schupbach, 2003). At higher temperatures, the rate of ubiquitin-proteasome dependent proteolysis decreases (Kuckelkorn et al., 2000), so knockdown of *dAdipoR* in the fat body may have a non-cell autonomous effect on ovarian rates of proteolysis, but additional evidence is necessary to confirm these preliminary data.

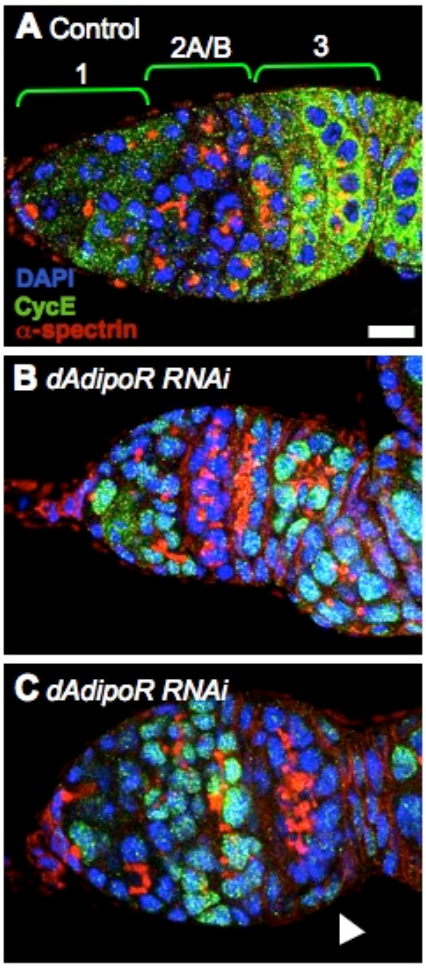

Figure 4.16. Cyclin E expression pattern is altered in the germarium of *dAdipoR* fat body knockdown females. (A) Control germaria (*white-RNAi*) with Cyclin E (CycE) antibody staining. CycE expression is up in region 1, down in 2A/B, and up in region 3 as previously described (Ohlmeyer, 2003). **(B-C)** Two examples of germaria from flies with *dAdipoR* fat body knockdown. CycE expression appears normal in (B), but expression is down in region 3 in (C, arrowhead). DAPI, DNA, blue. CycE, green. α-spectrin marks fusomes and niche and follicle cell membranes in red. Scale bar, 10μm.

It is still untested whether the expression patterns of Cyclin A or Bam are expanded in *FB>dAdipoR*^{RNAi} ovaries. The next step in this analysis would be to determine if weak loss-of-function alleles or partial knockdown of Cyclin E in the germarium can suppress the 32-cell cyst phenotype in *FB>dAdipoR*^{RNAi} ovaries.

A proteomics approach to identify fat body secreted proteins

My studies suggest that oogenesis is regulated in part via the fat body, potentially involving fat body *dAdipoR* signaling. Evidence from our labs and others suggest the fat body releases systemic signals that are received by the ovary (see Figure 1.9). I took a proteomics approach to attempt to identify fat body cell secreted molecules. I collected and submitted female abdominal fat body tissue samples to the Vanderbilt Proteomics Core Lab for shotgun proteomics analysis by Amy Ham and Salisha Hill (see Materials and Methods). Offline 2-dimensional liquid chromatography tandem mass spectrometry (2D LC-MS/MS) identified 435 proteins produced from 420 genes (Figure 4.17B). I categorized the fat body proteome by gene ontology and identified a large number of the genes linked to metabolism (>50%), which agrees with the central role of the fat body in metabolism (Figure 4.17A). Known fat body proteins were present, including the three yolk proteins (YP1, 2, and 3), lipid storage droplet-2, (Lsd2) and an imaginal disc growth factor-4 (IDGF4). The abdominal fat body proteome also overlaps with 70% of a previously published larval lipid droplet proteome (Beller et al., 2006). These results indicate my method of fat body extraction enriches for fat body proteins; however, several known fat body proteins were not identified, suggesting the level of sensitivity could be improved.

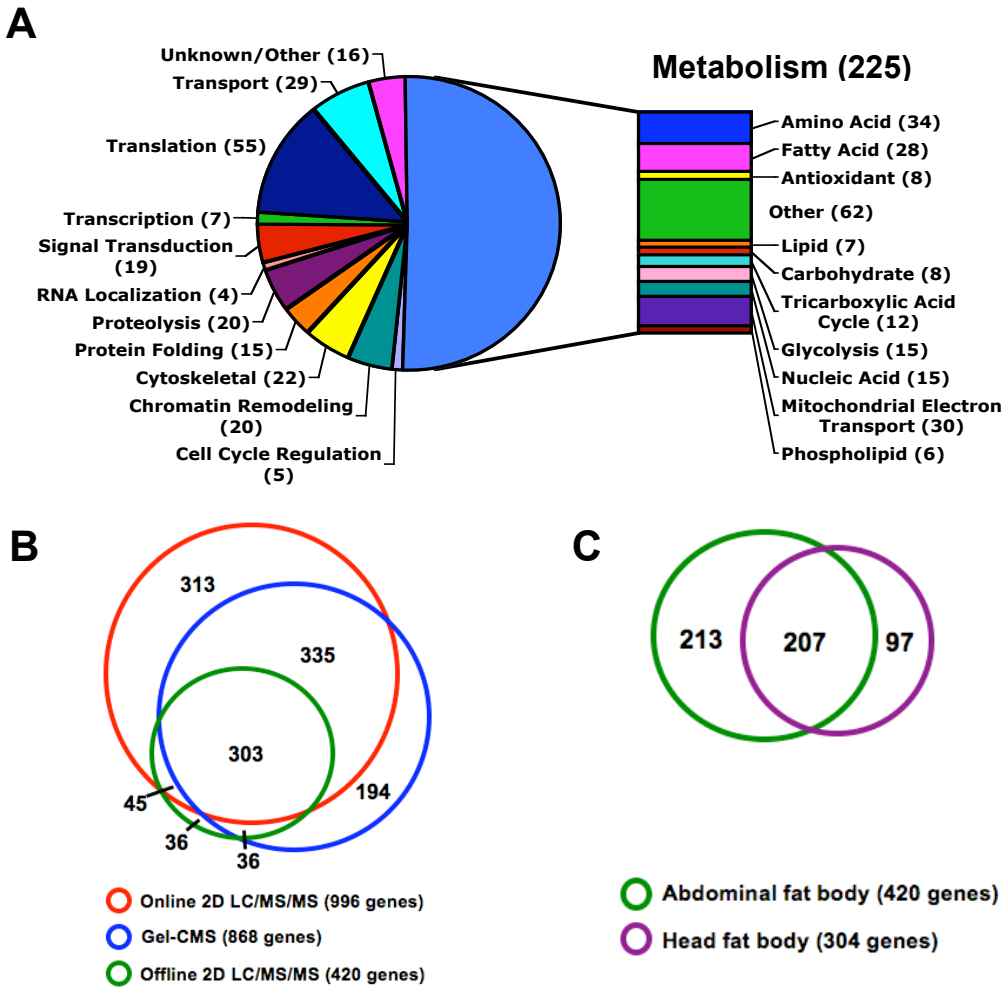

Figure 4.17. Adult female fat body proteome. **(A)** Gene ontology terms for the genes identified in the abdominal fat body using offline 2D LC/MS/MS. **(B)** Overlap of three abdominal fat body datasets using different methods for "shotgun" proteome analysis. **(C)** Overlap of abdominal and head fat body proteomes obtained by offline 2D LC/MS/MS.

There is evidence that the fat body may differ regionally. First, expression of the downstream negative regulator of insulin signaling, *dFOXO*, in the head fat body extends lifespan, while expression in other regions of the fat body does not (Hwangbo et al., 2004). Second, larval serum protein-2 (Lsp-2) is expressed in a gradient in the adult, with the highest levels in the head (80%) and the lowest levels in the abdomen (Benes et al., 1990). I compared the head and abdominal fat body proteomic profiles to test for regional differences in the fat body. Head fat body was manually extracted and analyzed by offline 2D LC-MS/MS and proteins arising from 304 genes were identified. 68% of the head fat body proteome overlapped with that from the abdominal fat body. Many of the non-overlapping proteins appear to be enriched in the nervous system, determined by gene ontology, suggesting contamination from brain and eye tissue (Figure 4.17C). My analysis suggests the head and abdominal fat body do not differ greatly, but a more precise analysis would be necessary to identify true regional differences in the fat body.

To attempt lower fat body tissue proteome complexity, I performed a 1-D separation of proteins by running the fat body sample on a Bis/Tris 10% gel and dividing the lane into eleven regions (see Materials and Methods). Each gel region was in-gel digested and separately loaded onto a column for 2D LC-MS/MS. This method, called Gel-CMS, should increase our identification of low abundance proteins, whose presence may have been previously masked by more abundant and/or larger proteins in a highly complex sample. This approach identified 880 proteins and overlapped with 81% of the proteins identified in the first abdominal fat body trial (Figure 4.17B).

Online 2D LC-MS/MS is reportedly more sensitive than offline 2D LC-MS/MS because samples are run directly from a column to the mass spectrometer instead going

through an additional collection step which can reduce sample volume (Link et al., 1999). This method identified a proteome 15% larger than the Gel-CMS proteome and 137% larger than proteome from our initial offline 2D LC-MS/MS method. 83% of the proteins identified via the offline method were also present in the online method proteomes (Figure 4.17B).

I merged data from all three proteomes, differing only by experimental method of analysis, and performed a bioinformatics analysis using the subcellular localization prediction algorithms pSORT and TargetP (see Material and Methods) to identify predicted extracellular proteins. I removed known extracellular matrix components from the protein list to obtain a final candidate list of 91 proteins, or 81 genes. I selected 35 genes with known mammalian homologs and available RNAi lines to functionally analyze the candidates (Table 4.3). In future studies, RNAi against each candidate gene will be expressed in the adult fat body and those flies will be screened for ovarian phenotypes.

Interestingly, iron-loaded ferritin, a secreted protein present in the candidate list, was recently reported to have a mitogenic role in peripheral cell proliferation during *Drosophila* development (Li, 2010). It is unknown if iron-loaded ferritin has a role in oogenesis, but this result suggests our method can indeed identify secreted proteins that have mitogenic roles in peripheral tissues.

A semi-quantitative proteomics approach to identify dietary-controlled, secreted proteins that regulate oogenesis

I previously hypothesized that when flies are fed a rich diet, the fat body secretes stimulatory factors that regulate oogenesis, and I discussed a proteomics approach aimed at identifying these factors. One weakness of my previous approach is that the fat body

Table 4.3

Potential secreted candidate proteins from proteomics/bioinformatics analysis of the *Drosophila* abdominal fat body

Drosophila gene ID	Mammalian homolog	VDRC RNAi #
CG9429	Calreticulin	51271
CG5474	Signal sequence receptor, beta	12101
CG9022	Oligosaccharyltransferase 48kD subunit	105881
CG2216	Ferritin	102406
CG3373	Adipocyte plasma membrane-associated protein	100286
CG9035	Signal sequence receptor, delta	8759
CG7400	Fatty acid (long chain) transport protein	48719
CG6186	Transferrin 1	106479
CG3359	Transforming growth factor, beta-induced	37888
CG5508[a]	glycerol-3-phosphate acyltransferase	1316
CG6206	Mannosidase	108218
CG32701	Signal sequence receptor, alpha	110344
CG1548	Cathepsin D	109651
CG4666	Mesenchymal stem cell protein DSCD75	109818
CG1837	Thioredoxin domain containing 5	15660
CG1803	regucalcin	105509
CG10992	Cathepsin B	108315
CG7291	Niemann-Pick disease, type C2	106771
CG6453	Protein kinase C substrate 80K-H	37988
CG9342	Microsomal triacylglycerol transfer protein	15775
CG12918	Canopy 2 homolog	38082
CG5532	Transmembrane protein 14C	105693
CG12013	Glutathione peroxidase	100790
CG9953	Serine protease	9024
CG7394	DnaJ (Hsp40) homolog, member 19	101490
CG12582	Mannosidase, beta A	110464
CG11999	Stromal cell-derived factor 2	104384
CG8286	DnaJ (Hsp40) homology, member 3	109649
CG3940	Carbonic anhydrase IV	108233
CG14715	FK506 binding protein 2	12828
CG4572	Carboxypeptidase, vitellogenic-like	101429
CG17271	Neural stem cell-derived neuronal survival protein	103101
CG5112	Fatty acid amide hydrolase	110017
CG18858	Phospholipase A2, group XV	50800
CG31683	Phospholipase A2, group XV	6400

[a] Genes listed in red are uncharacterized, but have predicted mammalian homologs

proteomics data had no information regarding relative protein abundance. In order to identify proteins that are regulated by diet, I and another graduate student, Kate Laws, along with Dr. Robert Cole at the Johns Hopkins School of Medicine Mass Spectrometry Core facility, performed an iTRAQ (isobaric Tags for Relative and Absolute Quantitation) analysis (see Materials and Methods).

We extracted abdominal fat tissue from flies fed either a rich diet or switched to a poor diet for 12 hours—this time point was chosen because it is the earliest time when ovarian proliferation rates are affected by dietary inputs (Drummond-Barbosa and Spradling, 2001). Four replicate samples were prepared for each dietary condition (see Materials and Methods for details). 2,682 total proteins were identified in the final proteome, including many known fat body proteins (such as Imp-L2) not identified in our previous analyses, indicating an increased proteome sensitivity.

I selected proteins from the proteome with significantly altered ratios on a rich compared with a poor diet (outside a 20% confidence interval), then used the aforementioned extracellular prediction programs, pSORT and TargetP, to identify potential secreted proteins. This analysis resulted in a total of 15 proteins upregulated and 12 protein downregulated on a poor diet (Table 4.4). Both Imp-L2, which is known to be more highly expressed on a poor diet, and Yolk Protein 3, which is reduced on a poor diet, were identified using these methods and serve as internal controls validating the analysis. Candidates will be functionally assayed by either mutational analysis or fat body RNAi knockdown as previously described.

Table 4.4

Predicted secreted proteins with altered levels on a rich versus a poor diet

Drosophila gene name	Average ratio[1]
CG11577	1.34
CG11784	1.33
CG14715	1.18
CG2918	1.29
CG6453	1.37
Fkbp13	1.49
microsomal triacylglycerol transfer protein	1.73
Niemann-Pick type C-2g	1.48
Odorant-binding protein 99a	1.47
Retinoid- and fatty acid-binding glycoprotein	1.22
Protein disulfide isomerase	1.33
yolk protein 3[2]	1.44
cathD	.74
CG12163	.71
CG1637	.64
CG17108	.69
CG4115	.78
CG4721	.64
CG5390	.77
CG6206	.70
CG9297	.70
Cystatin-like	.76
Ecdysone-inducible gene L2[3]	.76
ferritin 1 heavy chain homologue	.68
juvenile hormone epoxide hydrolase 2	.80
Larval serum protein 2	.71
thiolester containing protein IV	.69

[1]Ratios in red indicate proteins with reduced levels on a poor diet while those in black indicate proteins with higher levels on a poor diet.

[2]Yolk protein 3 is a known fat body-secreted protein that is downregulated on a poor diet and thus serves as an internal control (Bownes et al., 1988).

[3]Ecdsyone-inducible gene L2 (Imp-L2) is a known fat body-secreted protein that is upregulated on a poor diet and thus serves as an internal control (Honegger et al., 2008).

Discussion

In this chapter I discuss the role of the fat body in the diet-dependent regulation of oogenesis and stem cells. The *Drosophila* fat body, like the adipose tissue of mammals, acts as both a storage and metabolic tissue that modulates whole body homeostasis (Liu et al., 2009). My results indicate that alterations in fat storage levels have a detrimental effect on oogenesis. I also show that nutrient-sensing pathways and potentially adipokine-like signaling may lead to the secretion of factors from the fat body that act on the ovary. I also provide data suggesting *dAdipoR* is required in the ovary for GSC maintenance and proliferation in a diet-dependent manner. My work suggests that further studies in this genetically amenable organism may lead to a better understanding of the highly complex interaction between the adipose tissue signaling and peripheral tissue homeostasis in mammals.

Altered fat storage levels negatively affect reproduction in *Drosophila* and humans

I initially hypothesized that increasing fat body storage levels or insulin signaling in *Drosophila* might increase fertility by producing more proteins and other factors necessary for egg development. Instead, I found that mutants in genes such as *bmm* and *adp*, which have increased fat storage levels, produce fewer eggs than wild-type controls. I also demonstrated that egg production can temporarily elevated by overexpressing *dilp2*, but ultimately long-term egg production decreases. I conclude from these results that alterations in fat storage levels beyond a normal range have a negative impact on oogenesis in *Drosophila*.

Intriguingly, adult human females with fat storage levels outside of a defined normal range (a body mass index, or BMI, of 19-25) are at increased risk for infertility. There are an overwhelming number of studies on the negative effects of obesity (a BMI over 30) on female fertility. It has been observed that obese females have an earlier age of sexual maturation, difficulty conceiving, increased miscarriage, increased pre-term labor, and increased baby birth weight (Lee and Koren, 2010; Rachon and Teede, 2010).

Under nutrition or malnutrition also negatively impact fertility, affecting processes from ovulation to reduced infant birth weight (Muthayya, 2009). Perhaps most disturbingly, there is growing evidence suggesting that a mother's nutrient/metabolic status affects embryonic cellular epigenetic programming *in utero*, potentially increasing a child's risk of developing diseases later in life such as heart disease, type II diabetes, stroke, and hypertension (Barker, 2004). Together these observations suggest that the effects of diet on reproduction via adipose tissue are perhaps greater than imagined. Poor nutrition and metabolic defects, such as altered insulin signaling and adipokine levels during pregnancy, can affect not just the mother, but her offspring and potentially future generations as well via epigenetic imprinting of environmental nutritional conditions received during development (Barker, 2004; Lee and Koren, 2010).

dAdipoR **may sensitize ovarian GSCs and their progeny to insulin**

Adipokine-like signaling serves as a way to communicate dietary status between the fat body and ovarian stem cells. In mammalian muscle, adipocyte-secreted adiponectin is thought to sensitize tissues to insulin by binding its receptors in peripheral tissues and alleviating inhibition of the insulin signaling pathway by S6K (Wang et al., 2007). S6K, a

downstream target of TOR kinase activity, is proposed to be part of a negative feedback loop that keeps TOR activity tightly controlled by suppressing the activity of one of its inputs, the insulin signaling pathway (Kockel et al., 2010). The *Drosophila* ovary is directly regulated by insulin signaling (LaFever and Drummond-Barbosa, 2005) so modulation of insulin signaling activity could be one way the fat body might communicate with ovarian stem cells to modulate their activity in response to diet.

My preliminary data may support the model that adiponectin signaling regulates insulin sensitivity in the *Drosophila* ovary. Based on the proposed mammalian model, on a rich diet, loss of *dAdipoR* in the ovary should lead to increased TOR signaling levels due to loss of upstream TOR repressor activity (Wang et al., 2007). On a poor diet, however, available amino-acids and sugars would be reduced so TOR activity would also be suppressed. I have previously published that increased cell-autonomous TOR activity in the GSCs leads to their loss from the niche. Interestingly, my data suggests that *dAdipoR* mutant GSCs on a rich diet are indeed lost from their niche at a higher frequency than wild-type, but they are not lost at a higher rates on a poor diet, warranting further investigation as to whether or not TOR and insulin signaling activity are altered in these mutant GSCs.

Based on primary sequence analysis, there are no apparent adipokine homologs in insects. It stands to reason that the adiponectin receptor, which is conserved even in yeast, may play a slightly different role in insects than in mammals. Yeast, which have no insulin signaling pathway, have an adiponectin receptor homolog, *PHO36*, that regulates lipid and phosphate metabolism (Narasimhan et al., 2005). Knockdown of *dAdipoR* in the adult fat

body phenocopies knockdown of the TAG lipases, *bmm* and *CG8552*, suggesting the adiponectin receptor may regulate lipid metabolism in the *Drosophila* fat body as well.

The regulation of peripheral tissue homeostasis downstream of adipose tissue nutrient-sensing pathways is conserved

Knockdown of various nutrient-sensing pathway components in the adult female fat body, including *dAdipoR* and *Tor*, results in oogenesis defects, such as altered germline cyst cell number and increased levels of cell death. These results suggest that the fat body communicates with peripheral tissues via secreted factors, one example being the insulin growth factor binding protein homolog, Imp-L2 (Honegger et al., 2008). Other factors are also likely to be required and we currently combining proteomics analysis with functional assays as one method to identify additional fat body secreted factors.

In adult mammals, the adipose tissue secretes a large number of signaling factors such as adipokines, free fatty acids, phospholipids, hormones, and regulatory binding proteins (Alvarez-Llamas et al., 2007), which act on multiple tissues to regulate appetite, tissue growth and homeostasis, fertility, and more (Marshall, 2006). While no known adipokine homologs exist in *Drosophila* based on primary sequence analysis, it is possible that they share homology at the tertiary level and remain to be identified.

CHAPTER V

DISCUSSION AND FUTURE DIRECTIONS

Stem cell activity must be tightly regulated for dying cells to be replenished and injured tissue repaired without leading to tissue overgrowth or cancer. Dietary factors are extremely important for this process as cells need an external source of nutrients for growth, proliferation, and survival. Multiple tissues and signals function in concert to provide a stem cell with information regarding the dietary status of the organism. This dietary information is sensed and received by sophisticated mechanisms that provide a stem cell with the ability to meet the demands of its tissue. In this final chapter I provide further discussion on particular points of interest, discuss the potential impact of my work, and provide suggestions aimed at furthering studies described in earlier chapters.

Before the completion of this body of work, it was known that stem cells and their progeny respond to dietary factors via the insulin signaling pathway, but the mechanisms were unclear. It was also known that many types of cancers have mutations in nutrient-sensing pathways, making studies aimed at understanding how different cell types respond to diet of great importance for the development of future therapies. I used the well-defined *Drosophila* ovarian stem cell model system to examine the role of nutrient-sensing pathways on two stem cell populations and their progeny. This model, with the availability of genetic tools and well-defined cell biology allows a level of experimental control unparalleled in other stem cell model systems. In particular, genetic ovarian mosaic analysis permits mutational analysis of specific cells within a tissue, allowing one to pin-

point where a particular gene function is required. Also, by directly comparing mutant and wild-type cells within the same tissue, mosaic analysis permits quantitation of phenotypes by comparing mutant and wild-type cells within the same tissue so even relatively small differences in cellular proliferation, survival, and growth rates can be monitored *in vivo*.

My studies identified the InR/PI3K branch of the insulin signaling pathway and the TOR nutrient-sensing pathway as having specific roles in GSC regulation in response to diet. Since both of these pathways are highly conserved throughout metazoa, these findings suggest nutrient-sensing mechanisms in mammalian stem cells may also be conserved. I also provide evidence that ovarian cells require signals from other tissues, perhaps from the fat body cells, to regulate their activity. These studies provides a basic mechanistic understanding of how diet regulates ovarian stem cell populations and their progeny and lays groundwork for future studies on the role of diet on stem cell populations.

Germline stem cells respond to diet via insulin signaling, TOR kinase signaling and additional, unknown factors

In the first two chapters, I describe the roles for insulin signaling in the ovarian response to diet. My results demonstrate that insulin signaling via the PI3K branch of the pathway is directly required for GSCs to upregulate proliferation rates in response to diet, but sole activation of insulin signaling is insufficient to bypass the need for nutrients. I take a candidate approach in Chapter III and show that TOR signaling is also required for GSC proliferation, but is regulating proliferation by a different mechanism than insulin signaling. A poor diet, however, slows the cell cycle at both G1 and G2 (Hsu, 2008) (Figure 5.1), suggesting additional factors are involved.

Our laboratory is actively seeking out other players in the ovarian response to diet and DILPs by using candidate approaches and unbiased screening. First, it is possible that a hormonal signal, in addition to the peptide hormone insulin, may regulate GSCs in response to diet. Hormones have clear roles in mammalian stem cell regulation: Follicle-stimulating hormone regulates mammalian testis GSCs, growth hormone stimulates NSCs and mammary stem cells, and estrogen induces mammary epithelial stem cell proliferation (Drummond-Barbosa, 2008). The *Drosophila* steroid hormone ecdysone, has previously published roles in cell growth, proliferation, and survival during development (Fallon and Gerenday, 2010; Mirth and Riddiford, 2007; Yin and Thummel, 2005). Synthesis of ecdysone requires a cholesterol precursor that can only be obtained from diet, thus making ecdysone signaling diet-dependent (Gilbert, 2004). Studies by Dr. Elizabeth Ables in our laboratory identified the ecdysone signaling pathway as being necessary for GSC maintenance via regulation of chromatin remodeling factors and G2 cell-cycle regulation of proliferation (Ables and Drummond-Barbosa, 2010) (Figure 5.1).

To identify dietary regulated proteins in the fat body, brain, and ovary, we have performed a *Drosophila* GFP-protein trap screen. Each GFP-protein trap fly line contains a gene with GFP inserted in frame so that GFP expression should mirror both the localization and levels of the resulting protein (Buszczak et al., 2007; Kelso et al., 2004; Morin et al., 2001; Quinones-Coello et al., 2007). I and a former Vanderbilt Summer Science Academy student, Emily Cross, performed a small pilot GFP-protein trap screen. We fed flies on a rich diet or switched them to a poor diet for 12 hours, then dissected ovary, brain, and fat body tissues, imaged tissues on a fluorescent microscope, and screened for lines with changes in relative GFP intensity levels or localization between

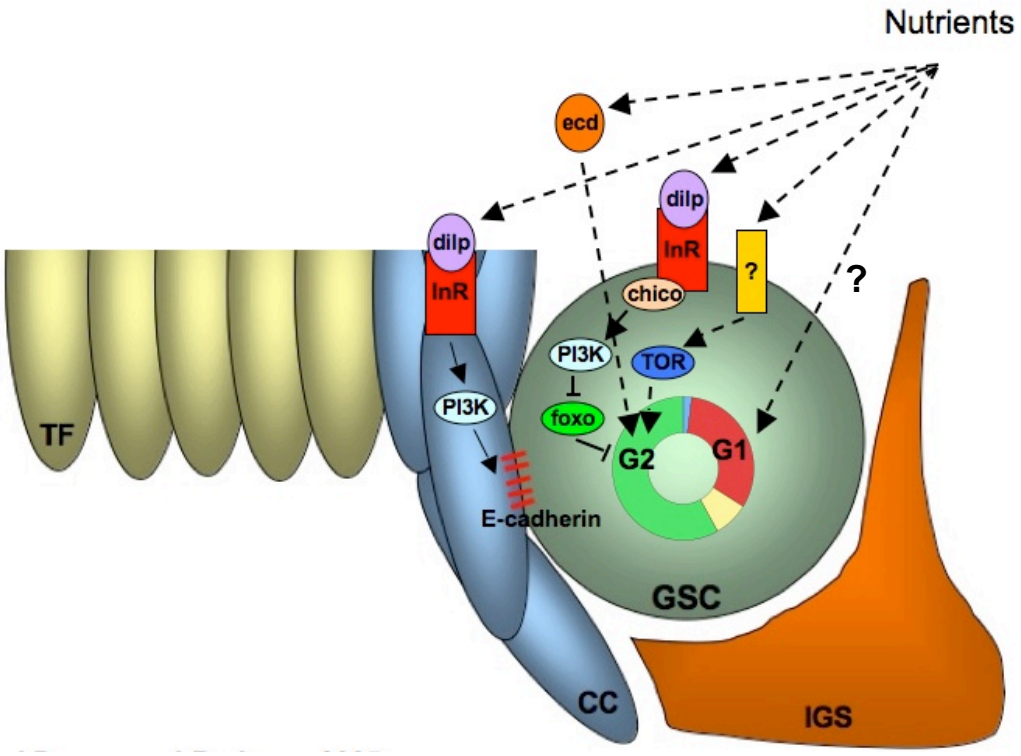

Figure 5.1. Additional unknown factors regulate GSCs in response to diet. A diagram of the GSC and niche cells. GSCs respond to nutrients via insulin, TOR, and ecdysone signaling to regulate the G2 phase of the cell-cycle. Additional unknown factor(s) act at the G1 phase. The upstream activators of TOR signaling in GSCs are also unknown (yellow box with question mark). TF, terminal filament cells (yellow). CC, cap cells (blue). GSC, germline stem cell (green). IGS, inner germarial sheath cell (orange). ecd, ecdysone (orange oval).

dietary conditions. Dr. Hwei-Jan Hsu performed a large-scale screen of the GFP-protein trap lines in the ovary and found several particularly interesting candidates, including Semaphorin-2a (Sema-2a), which has previously published roles in nervous system development. Dr. Hsu found that Sema-2a was expressed at higher levels in GSCs and cystoblasts on a rich diet compared to a poor diet (data not shown). I performed a preliminary ovarian genetic mosaic analysis to examine the role of Sema-2a in the germline. Interestingly, I found that *Sema-2a* mutant GSCs have both a reduced rate of division compared to controls and appear to developmentally arrest or die around a 2-cell germline cyst stage (data not shown). Further studies on the role of Sema-2a in the ovarian response to diet are being completed by Kareshma Mohanty, a Masters of Science student in our laboratory.

Ovarian stem cells and their progeny require factors from multiple organs and tissues to modulate their response to diet.

We hypothesize that the ovary does not receive all nutrient inputs directly, but may sense whole body nutritional status via the brain, the fat body, and other tissues such as the gut and the peripheral nervous system (Figure 5.2). The studies described in Chapter IV focus on the role of the fat body in the ovarian response to diet and DILPs. I have evidence that genetic manipulation of various fat storage, nutrient-sensing, and amino-acid transporter genes in the fat body can affect oogenesis (see Table 4.2 in Chapter IV), but how the ovary senses changes in the fat body is unknown. One possibility is adipokine-like signaling between the fat body cells and the ovary. Future efforts will be made to

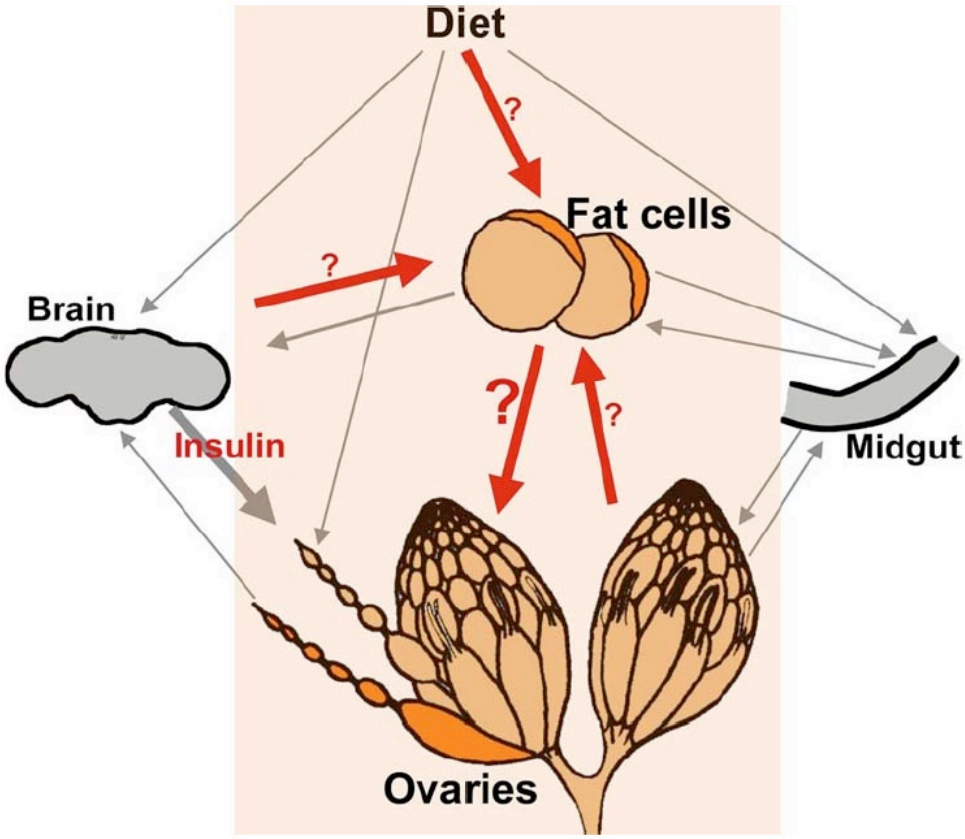

Figure 5.2. The *Drosophila* ovary likely responds to diet via signals from multiple sources. The *Drosophila* ovary responds to diet via insulin signals (DILPs) from the brain. Additional tissues are also likely involved including the fat body. We have evidence that signals from the fat body in response to nutrient-sensing act on the ovary to regulate the ovarian response to diet and DILPs. Figure from Daniela Drummond-Barbosa, unpublished.

identify and understand how factors secreted from the fat body act upon the ovarian stem cells and their progeny.

Future Directions

The studies described in Chapter IV are still incomplete and unpublished. The laboratory will follow up on several aspects of these studies to better characterize the role of the fat body on the ovarian stem cells and their progeny. First, experiments are being designed using lineage tracing to determine how the adult fat body forms, a current black box in the development of *Drosophila melanogaster*. This work should also aid in the development of better tools, such as mosaic analysis, for the study of gene function in the adult fat body. Preliminary data from a new graduate student, Kate Laws, suggests that fat body clones can be induced during the embryonic stage of development. Also, fat body secreted candidates from the four proteomics analyses (offline and online 2D LC-MS/MS, Gel-CMS, and iTRAQ) will be compiled and top genes of interest will be screened for effects on the ovary via the fat body by RNAi knockdown and/or mutational analysis. The largest amount of effort on my part, however, will be focused on better understanding the cell-autonomous and non-cell autonomous effects of *dAdipoR* loss of function on ovarian stem cells and their progeny. For example, I will further test the model that dAdipoR regulates insulin sensitivity by performing a genetic interaction assay between the TOR and insulin signaling pathways and dAdipoR. Since Dr. Hsu previous demonstrated a role for insulin signaling in the GSC niche cap cells, I will also examine the role of *dAdipoR* in those cells by RNAi knockdown. I will also continue to test *dAdipoR* rescue constructs, and perhaps generate new constructs such as dAdipoR isoform B, to try to obtain adult

dAdipoR mutant females for ovarian analysis. Another important experiment to test of dAdipoR acts in a similar manner to mAdipoR is to try to rescue *dAdipoR* mutant phenotypes by transgenic expression of mammalian *AdipoR*. Finally, I will continue to investigate mechanism leading to a 32-cell ovarian cyst phenotype in fat body specific *dAdipoR* knockdown females.

Adult fat body lineage tracing and the development of tools for mutational analysis

To determine when the adult fat body is mitotically active, I attempted to induce clones the LacZ knock-in system (see Figure 4.10) throughout the 3rd larval instar and early adult stages, but failed to identify a developmental time point that allowed positive marking of a significant number of fat body cells. This result suggests the adult fat body is proliferative at an earlier developmental stage. It is important to understand how the adult fat body develops in order to develop tools for mutational analysis and experiments are in progress to systematically test distinct time points using the LacZ knock-in system to identify the adult fat body progenitor population. Several hypotheses can be formed regarding the development of the adult fat body tissue. Current literature favors a model in which the larval fat body breaks down during pupation and the adult fat body forms, likely from cells embedded within the larval body wall or from adepithelial cells associated with imaginal discs, to replace larval fat by 3-4 days post eclosion (Aguila et al., 2007; Miller et al., 2002). It could be imagined, however, that the adult fat body arises from a multinucleated mass formed during embryogenesis that later breaks down to form adult fat body cells at a particular stage of development. A low level of mitotic activity may occur during later stages of development to refine final fat body cell numbers. This second

hypothesis is supported by the fact that I was unable to label more than one or two fat cells during 3rd larval instar stages and the fact that a large percentage of adult fat body cells are multinucleated (Whitten, 1963).

Once it is determined when the adult fat body is mitotically active or if the progenitor population can be identified, tools such as mosaic analysis or the Flp-out technique can be modified to generate mosaic fat tissue for mutational analysis. Both of these techniques (described in earlier sections) can be modified to induce flipase-mediated recombination by *UAS*- or *hsp70-flipase* induction by either a cell-specific Gal4 driver or by heat-shock, respectively. In order to identify genes expressed in the adult fat body progenitor population, a screen of Flybase available Gal4 drivers could be performed. Also, a screen of available enhancer trap lines may also prove useful to identify fat body cell-specific expression patterns.

Adipokinetic regulation of stem cell-based tissues may be conserved in *Drosophila*

Based on the presence of a conserved adiponectin receptor, I hypothesized that adipokinetic signaling may sensitize peripheral tissues, such as the ovary, to insulin in *Drosophila*. My preliminary mutational analyses indicate that the adiponectin receptor appears to have both cell-autonomous and non-cell autonomous roles via the fat body cells on the ovarian stem cell lineages. A detailed mosaic analysis characterization of the role of dAdipoR in the ovary will be performed, much like the study performed in Chapter III on the role of TOR kinase in the ovarian stem cells and their progeny. Additional experiments aimed at testing whether or not TOR activity and insulin signaling sensitivity are affected in the dAdipoR mutant ovarian cells will be tested by genetic interaction experiments and

by direct analysis in the ovary of markers such as p4E-BP staining for TOR activity and p-Akt, FOXO tGPH reporter localization for insulin signaling activity.

The adiponectin receptors belong to a family of receptor proteins called PAQR for the founding members, progesterone and adiponectin (also known as AdipoQ) receptors. Receptors in this family have at least seven transmembrane domains and three conserved motifs—all of which are present in *dAdipoR* (Tang et al., 2005). Conservation at the primary sequence level suggests that *dAdipoR* is an adiponectin receptor homolog, but no functional assay has been performed to demonstrate it functions as a mammalian adiponectin receptor.

It is interesting that loss of *dAdipoR* is lethal in *Drosophila*, but not in other organisms, such as in yeast or mice. Yeast AdipoR, or PHO36, is one of four paralogous steroid receptors that are transcriptionally regulated by both zinc and exogenous fatty acids (Lyons et al., 2004). PHO36 (or IZH2) was identified as the mAdipoR homolog by virtue of its specific sensitivity to osmotin, which also stimulates mAdipoR activity (Narasimhan et al., 2005). Deletion of all four *IZH* genes does not appear to affect yeast cell viability (Lyons et al., 2004) and a mouse double knockout of *mAdipoR1/2* is also viable (Yamauchi et al., 2007). However, some tissues reportedly still expressed *mAdipoR1* at about 50% of wild-type levels, so it is unclear whether complete loss of mAdipoR function might actually cause lethality (Yamauchi et al., 2007). I cannot rule out that dAdipoR may play additional, essential systemic roles in *Drosophila*, especially compared to yeast; but the difference between the mammalian and *Drosophila* mutational analysis is likely due to both redundancy of adiponectin receptors in the mammalian system (AdipoR1, AdipoR2, PAQR3, and T-cadherin all bind adiponectin) and incomplete

knockdown in the mouse mAdipoR1/2 mutant. Both the yeast and mammalian AdipoRs activate the same downstream pathways: AMPK in myocytes (Narasimhan et al., 2005) and suppression of an iron uptake gene, *FET3*, when grown in iron-deficient medium in yeast (Garitaonandia et al., 2009). As such, it would be of interest to test whether dAdipoR stimulates those same pathways in yeast or myocytes, which would suggest functional conservation. We will also obtain human AdipoR1 and AdipoR2 cDNA to examine if replacement of *dAdipoR* with either human receptor can rescue the observed ovarian defects, suggesting a high level of functional conservation.

dAdipoR^{27} developmental lethality rescue

In order to identify adult-specific roles for *dAdipoR* in the ovary and other tissues, I generated transgenic rescue constructs of isoform A/C *dAdipoR*, but transgenic expression of *dAdipoR* during development failed to rescue lethality. Complementation testing indicates lethality is due to loss of *dAdipoR*, so the reason lack of rescue is not likely due to a background mutation. Other possibilities may explain the lack of rescue. First, the *dAdipoR* expression constructs may not be functional, a possibility that can be tested by RT-PCR. Second, *dAdipoR* expression may have isoform-specific requirements during development. In the adult *dAdipoR* isoform B, for instance, appears not to be expressed in the adult ovary, and isoform-specific expression patterns were not tested during the larval stages of development. Thus, it is possible *dAdipoR* isoform A/C alone is insufficient for development. *dAdipoR* isoform B cDNA is now available from the BDGP (Berkeley Drosophila Genome Project) iPCR collection. The iPCR collection contains cDNA clones generated using a screening method called SLIP (Self-Ligation of Inverse

PCR Products); a technique used to recover full-length cDNAs for relatively rare and alternatively spliced transcripts. Therefore, it is possible that transgenic expression of all three *dAdipoR* isoforms may rescue the developmental lethality associated with null alleles of *dAdipoR*. Finally, expression of some genes, *Tor* for instance, must be maintained within "normal" expression levels as either higher or lower expression levels can equally result in larval lethality (Hennig and Neufeld, 2002). It is possible that the expression of *dAdipoR* may also be tightly regulated. Using *dAdipoR* genomic rescue constructs under the control of their own endogenous promoters would be one way to maintain relatively normal levels of expression throughout development.

A role for *dAdipoR* in oogenesis via the fat body

Fat body *dAdipoR* knockdown by RNAi results in 15-20% of germline cysts having 32-cell cysts instead of the normal 16-cell cyst number due to an additional mitotic cell division. Cyclin E levels and expression patterns are altered in about 13% of germaria from $FB>dAdipoR^{RNAi}$ ovaries, which may suggest that, as in other mutants such as *encore* that also exhibit a 32-cell cyst phenotype, rates of proteolysis may be affected. Additional experiments must be performed to confirm this possibility.

I attempted to identify dAdipoR signaling pathway components by screening fat body gene knockdown ovaries for a similar phenotype to *dAdipoR* fat body knockdown. I screened a pool of candidate genes involved in nutrient-sensing and/or fat storage, since mAdipoR has been implicated in regulating both insulin sensitivity via AMPK and TOR kinase and lipid metabolism. I reasoned that if fat body knockdown of a particular gene also results in a 32-cell cyst phenotype it may function within the same pathway as

dAdipoR. I found that fat body knockdown of several genes involved in nutrient-sensing and lipid metabolism led to a 32-cell cyst phenotype, suggesting that, as in mammals, the adiponectin receptor, TOR kinase, insulin signaling, and fat storage pathways are likely interconnected. One hypothesis is that systemic factor(s) are secreted downstream of fat body nutrient-sensing pathways that act upon the ovary to regulate timely mitotic exit in germline cysts. One way to test this hypothesis is to perform an iTRAQ analysis comparing fat body proteomes between wild-type and *FB>dAdipoR*^{RNAi} females to identify differentially expressed fat body secreted proteins. The signal downstream of adiponectin receptor signaling in the fat body, however, may not be a secreted protein, but could be a lipid molecule or a steroid hormone. Differentially expressed enzymes within lipid biogenesis or hormone synthesis pathways present in the iTRAQ data set may provide insights into alternative possibilities regarding signaling downstream of fat body adiponectin receptor signaling.

The fat body produces factors that regulate the ovarian response to diet and DILPs

Production of fat body secreted factors, such as Imp-L2, modulates the ovarian response to diet and DILPs. Neither *Imp-L2* knockdown nor *dilp2* overexpression can bypass the need for dietary nutrients, but both allow for increased egg production on a rich diet, indicating that DILP levels are a limiting factor for oogenesis. Our laboratory has demonstrated that additional, unidentified diet-dependent factor(s) act at the G1/S GSC transition (Hsu et al., 2008). To identify these factors, I performed a fat body proteomics analysis combined with bioinformatics analysis of subcellular localization. 35 candidates with both a mammalian homolog and an available RNAi line were selected for a

secondary functional screen. In addition, our iTRAQ proteomics analysis resulted in 27 proteins that were both predicted to be secreted and exhibit diet-dependent modification of expression levels. Seven proteins overlap between the two datasets, resulting in a total of 55 genes to further screen for a role in the ovary via the fat body. Analysis of differentially expressed enzymes with roles in lipid metabolism or hormone synthesis will address the possibility that non-protein molecules may also be secreted downstream of dietary-regulated pathways in the fat body. These studies will be performed by Kate Laws, a graduate student in our laboratory.

Concluding Statements

My studies suggest the ovarian response to diet is highly complex and requires signals in addition to insulin, that may arise from the fat body. This is also true in mammals, as nutrient sensing entails a network of signals arising from adipose tissue, the brain, pituitary gland and other organs to maintain whole body metabolic homeostasis. Understanding how stem cell activity and maintenance are regulated within tissues would provide much needed insight for the development of better stem cell-based regenerative or cancer therapies. These studies also further our understanding of how stem cells and their progeny sense and respond to dietary signals by providing a detailed description of the roles of insulin and TOR signaling in stem cell maintenance and proliferation and the growth, proliferation, and survival of their differentiated progeny. I also examine potential roles for the fat body in regulating oogenesis via secreted factors and, by proteomics analysis of the adult female fat body, obtained a list of predicted secreted candidate genes that will be functionally screened in the near future. Finally, these studies uncover

parallels between nutrient-sensing in stem cell regulation in insects and mammals, suggesting key regulatory mechanisms may be conserved and further underlining the importance of pursuing studies in *Drosophila* as an important model for mammalian stem cell biology.

REFERENCES

Ables, E. and Drummond-Barbosa, D. (2010). The steroid hormone ecdysone functions with intrinsic chromatin remodeling factors to control female germline stem cells in Drosophila. *Cell Stem Cell* **in press**.

Adhikari, D., Flohr, G., Gorre, N., Shen, Y., Yang, H., Lundin, E., Lan, Z. and Liu, K. (2009). Disruption of Tsc2 in oocytes leads to overactivation of the entire pool of primordial follicles. *Mol Hum Reprod*.

Aguila, J. R., Suszko, J., Gibbs, A. G. and Hoshizaki, D. K. (2007). The role of larval fat cells in adult Drosophila melanogaster. *J Exp Biol* **210**, 956-63.

Alexander, L. S., Mahajan, A., Odle, J., Flann, K. L., Rhoads, R. P. and Stahl, C. H. (2010). Dietary phosphate restriction decreases stem cell proliferation and subsequent growth potential in neonatal pigs. *J Nutr* **140**, 477-82.

Alvarez-Llamas, G., Szalowska, E., de Vries, M. P., Weening, D., Landman, K., Hoek, A., Wolffenbuttel, B. H., Roelofsen, H. and Vonk, R. J. (2007). Characterization of the human visceral adipose tissue secretome. *Mol Cell Proteomics* **6**, 589-600.

Amcheslavsky, A., Jiang, J. and Ip, Y. T. (2009). Tissue damage-induced intestinal stem cell division in Drosophila. *Cell Stem Cell* **4**, 49-61.

Arquier, N., Geminard, C., Bourouis, M., Jarretou, G., Honegger, B., Paix, A. and Leopold, P. (2008). Drosophila ALS regulates growth and metabolism through functional interaction with insulin-like peptides. *Cell Metab* **7**, 333-8.

Arrese, E. L. and Soulages, J. L. (2010). Insect fat body: energy, metabolism, and regulation. *Annu Rev Entomol* **55**, 207-25.

Arsham, A. M. and Neufeld, T. P. (2006). Thinking globally and acting locally with TOR. *Curr Opin Cell Biol* **18**, 589-97.

Arvisais, E. W., Romanelli, A., Hou, X. and Davis, J. S. (2006). AKT-independent phosphorylation of TSC2 and activation of mTOR and ribosomal protein S6 kinase signaling by prostaglandin F2alpha. *J Biol Chem* **281**, 26904-13.

Ashburner, M. and Drysdale, R. (1994). FlyBase--the Drosophila genetic database. *Development* **120**, 2077-9.

Avram, A. S., Avram, M. M. and James, W. D. (2005). Subcutaneous fat in normal and diseased states: 2. Anatomy and physiology of white and brown adipose tissue. *J Am Acad Dermatol* **53**, 671-83.

Avruch, J., Long, X., Ortiz-Vega, S., Rapley, J., Papageorgiou, A. and Dai, N. (2009). Amino acid regulation of TOR complex 1. *Am J Physiol Endocrinol Metab* **296**, E592-602.

Barber, T. M., McCarthy, M. I., Wass, J. A. and Franks, S. (2006). Obesity and polycystic ovary syndrome. *Clin Endocrinol (Oxf)* **65**, 137-45.

Barker, D. D., Wang, C., Moore, J., Dickinson, L. K. and Lehmann, R. (1992). Pumilio is essential for function but not for distribution of the Drosophila abdominal determinant Nanos. *Genes Dev* **6**, 2312-26.

Barker, D. J. (2004). The developmental origins of adult disease. *J Am Coll Nutr* **23**, 588S-595S.

Barthel, A., Schmoll, D. and Unterman, T. G. (2005). FoxO proteins in insulin action and metabolism. *Trends Endocrinol Metab* **16**, 183-9.

Bauer, J. H., Chang, C., Morris, S. N., Hozier, S., Andersen, S., Waitzman, J. S. and Helfand, S. L. (2007). Expression of dominant-negative Dmp53 in the adult fly brain inhibits insulin signaling. *Proc Natl Acad Sci U S A* **104**, 13355-60.

Beller, M., Riedel, D., Jansch, L., Dieterich, G., Wehland, J., Jackle, H. and Kuhnlein, R. P. (2006). Characterization of the Drosophila lipid droplet subproteome. *Mol Cell Proteomics* **5**, 1082-94.

Benes, H., Edmondson, R. G., Fink, P., Kejzlarova-Lepesant, J., Lepesant, J. A., Miles, J. P. and Spivey, D. W. (1990). Adult expression of the Drosophila Lsp-2 gene. *Dev Biol* **142**, 138-46.

Bernal, A. and Kimbrell, D. A. (2000). Drosophila Thor participates in host immune defense and connects a translational regulator with innate immunity. *Proc Natl Acad Sci U S A* **97**, 6019-24.

Bland, M. L., Lee, R. J., Magallanes, J. M., Foskett, J. K. and Birnbaum, M. J. (2010). AMPK supports growth in Drosophila by regulating muscle activity and nutrient uptake in the gut. *Dev Biol* **344**, 293-303.

Bohni, R., Riesgo-Escovar, J., Oldham, S., Brogiolo, W., Stocker, H., Andruss, B. F., Beckingham, K. and Hafen, E. (1999). Autonomous control of cell and organ size by CHICO, a Drosophila homolog of vertebrate IRS1-4. *Cell* **97**, 865-75.

Boyer, D., Quintanilla, R. and Lee-Fruman, K. K. (2008). Regulation of catalytic activity of S6 kinase 2 during cell cycle. *Mol Cell Biochem* **307**, 59-64.

Britton, J. S. and Edgar, B. A. (1998). Environmental control of the cell cycle in Drosophila: nutrition activates mitotic and endoreplicative cells by distinct mechanisms. *Development* **125**, 2149-58.

Britton, J. S., Lockwood, W. K., Li, L., Cohen, S. M. and Edgar, B. A. (2002). Drosophila's insulin/PI3-kinase pathway coordinates cellular metabolism with nutritional conditions. *Dev Cell* **2**, 239-49.

Brogiolo, W., Stocker, H., Ikeya, T., Rintelen, F., Fernandez, R. and Hafen, E. (2001). An evolutionarily conserved function of the Drosophila insulin receptor and insulin-like peptides in growth control. *Curr Biol* **11**, 213-21.

Budak, E., Fernandez Sanchez, M., Bellver, J., Cervero, A., Simon, C. and Pellicer, A. (2006). Interactions of the hormones leptin, ghrelin, adiponectin, resistin, and PYY3-36 with the reproductive system. *Fertil Steril* **85**, 1563-81.

Burgering, B. M. and Kops, G. J. (2002). Cell cycle and death control: long live Forkheads. *Trends Biochem Sci* **27**, 352-60.

Buszczak, M., Paterno, S., Lighthouse, D., Bachman, J., Planck, J., Owen, S., Skora, A. D., Nystul, T. G., Ohlstein, B., Allen, A. et al. (2007). The carnegie protein trap library: a versatile tool for Drosophila developmental studies. *Genetics* **175**, 1505-31.

Cancello, R., Tounian, A., Poitou, C. and Clement, K. (2004). Adiposity signals, genetic and body weight regulation in humans. *Diabetes Metab* **30**, 215-27.

Canto, C. and Auwerx, J. (2010). AMP-activated protein kinase and its downstream transcriptional pathways. *Cell Mol Life Sci*.

Castilho, R. M., Squarize, C. H., Chodosh, L. A., Williams, B. O. and Gutkind, J. S. (2009). mTOR mediates Wnt-induced epidermal stem cell exhaustion and aging. *Cell Stem Cell* **5**, 279-89.

Catania, C., Binder, E. and Cota, D. (2010). mTORC1 signaling in energy balance and metabolic disease. *Int J Obes (Lond)*.

Catania, M. G., Mischel, P. S. and Vinters, H. V. (2001). Hamartin and tuberin interaction with the G2/M cyclin-dependent kinase CDK1 and its regulatory cyclins A and B. *J Neuropathol Exp Neurol* **60**, 711-23.

Chan, S. (2004). Targeting the mammalian target of rapamycin (mTOR): a new approach to treating cancer. *Br J Cancer* **91**, 1420-4.

Chang, Y. Y., Juhasz, G., Goraksha-Hicks, P., Arsham, A. M., Mallin, D. R., Muller, L. K. and Neufeld, T. P. (2009). Nutrient-dependent regulation of autophagy through the target of rapamycin pathway. *Biochem Soc Trans* **37**, 232-6.

Cherbas, L., Hu, X., Zhimulev, I., Belyaeva, E. and Cherbas, P. (2003). EcR isoforms in Drosophila: testing tissue-specific requirements by targeted blockade and rescue. *Development* **130**, 271-84.

Chiarugi, P. and Fiaschi, T. (2010). Adiponectin in health and diseases: from metabolic syndrome to tissue regeneration. *Expert Opin Ther Targets* **14**, 193-206.

Colombani, J., Raisin, S., Pantalacci, S., Radimerski, T., Montagne, J. and Leopold, P. (2003). A nutrient sensor mechanism controls Drosophila growth. *Cell* **114**, 739-49.

Combs, T. P., Pajvani, U. B., Berg, A. H., Lin, Y., Jelicks, L. A., Laplante, M., Nawrocki, A. R., Rajala, M. W., Parlow, A. F., Cheeseboro, L. et al. (2004). A transgenic mouse with a deletion in the collagenous domain of adiponectin displays elevated circulating adiponectin and improved insulin sensitivity. *Endocrinology* **145**, 367-83.

Conlon, I. and Raff, M. (1999). Size control in animal development. *Cell* **96**, 235-44.

Cox, D. N., Chao, A., Baker, J., Chang, L., Qiao, D. and Lin, H. (1998). A novel class of evolutionarily conserved genes defined by piwi are essential for stem cell self-renewal. *Genes Dev* **12**, 3715-27.

de Cuevas, M., Lee, J. K. and Spradling, A. C. (1996). alpha-spectrin is required for germline cell division and differentiation in the Drosophila ovary. *Development* **122**, 3959-68.

de Cuevas, M. and Spradling, A. C. (1998). Morphogenesis of the Drosophila fusome and its implications for oocyte specification. *Development* **125**, 2781-9.

Dean RLLMC, J. V. (1985). in Comprehensive Insect Physiology, Biochemistry and Pharmacology. 155-210.

Delort, L., Kwiatkowski, F., Chalabi, N., Satih, S., Bignon, Y. J. and Bernard-Gallon, D. J. (2009). Central adiposity as a major risk factor of ovarian cancer. *Anticancer Res* **29**, 5229-34.

Deng, W. M., Althauser, C. and Ruohola-Baker, H. (2001). Notch-Delta signaling induces a transition from mitotic cell cycle to endocycle in Drosophila follicle cells. *Development* **128**, 4737-46.

DiAngelo, J. R. and Birnbaum, M. J. (2009). Regulation of fat cell mass by insulin in Drosophila melanogaster. *Mol Cell Biol* **29**, 6341-52.

Diaz-Troya, S., Perez-Perez, M. E., Florencio, F. J. and Crespo, J. L. (2008). The role of TOR in autophagy regulation from yeast to plants and mammals. *Autophagy* **4**, 851-65.

Dietzl, G., Chen, D., Schnorrer, F., Su, K. C., Barinova, Y., Fellner, M., Gasser, B., Kinsey, K., Oppel, S., Scheiblauer, S. et al. (2007). A genome-wide transgenic RNAi library for conditional gene inactivation in Drosophila. *Nature* **448**, 151-6.

DiMascio, L., Voermans, C., Uqoezwa, M., Duncan, A., Lu, D., Wu, J., Sankar, U. and Reya, T. (2007). Identification of adiponectin as a novel hemopoietic stem cell growth factor. *J Immunol* **178**, 3511-20.

Dong, J. and Pan, D. (2004). Tsc2 is not a critical target of Akt during normal Drosophila development. *Genes Dev* **18**, 2479-84.

Dowling, R. J., Topisirovic, I., Alain, T., Bidinosti, M., Fonseca, B. D., Petroulakis, E., Wang, X., Larsson, O., Selvaraj, A., Liu, Y. et al. (2010). mTORC1-mediated cell proliferation, but not cell growth, controlled by the 4E-BPs. *Science* **328**, 1172-6.

Drummond-Barbosa, D. (2005). Regulation of stem cell populations. *In: Meyers, R.A. (Ed.). Encyclopedia of Molecular Cell Biology and Molecular Medicine* **12**, 67-98.

Drummond-Barbosa, D. (2008). Stem cells, their niches and the systemic environment: an aging network. *Genetics* **180**, 1787-97.

Drummond-Barbosa, D. and Spradling, A. C. (2001). Stem cells and their progeny respond to nutritional changes during Drosophila oogenesis. *Dev Biol* **231**, 265-78.

Duffy, J. B. (2002). GAL4 system in Drosophila: a fly geneticist's Swiss army knife. *Genesis* **34**, 1-15.

Duvnjak, L. and Duvnjak, M. (2009). The metabolic syndrome - an ongoing story. *J Physiol Pharmacol* **60 Suppl 7**, 19-24.

Ekholm, S. V., Zickert, P., Reed, S. I. and Zetterberg, A. (2001). Accumulation of cyclin E is not a prerequisite for passage through the restriction point. *Mol Cell Biol* **21**, 3256-65.

El-Hefnawy, T., Ioffe, S. and Dym, M. (2000). Expression of the leptin receptor during germ cell development in the mouse testis. *Endocrinology* **141**, 2624-30.

Fallon, A. M. and Gerenday, A. (2010). Ecdysone and the cell cycle: investigations in a mosquito cell line. *J Insect Physiol* **56**, 1396-401.

Fan, H. Y., Liu, Z., Cahill, N. and Richards, J. S. (2008). Targeted disruption of Pten in ovarian granulosa cells enhances ovulation and extends the life span of luteal cells. *Mol Endocrinol* **22**, 2128-40.

Fingar, D. C., Salama, S., Tsou, C., Harlow, E. and Blenis, J. (2002). Mammalian cell size is controlled by mTOR and its downstream targets S6K1 and 4EBP1/eIF4E. *Genes Dev* **16**, 1472-87.

Fischer, J. A., Giniger, E., Maniatis, T. and Ptashne, M. (1988). GAL4 activates transcription in Drosophila. *Nature* **332**, 853-6.

Fluckiger, A. C., Marcy, G., Marchand, M., Negre, D., Cosset, F. L., Mitalipov, S., Wolf, D., Savatier, P. and Dehay, C. (2006). Cell cycle features of primate embryonic stem cells. *Stem Cells* **24**, 547-56.

Fu, Y., Luo, N., Klein, R. L. and Garvey, W. T. (2005). Adiponectin promotes adipocyte differentiation, insulin sensitivity, and lipid accumulation. *J Lipid Res* **46**, 1369-79.

Fuller, M. T. and Spradling, A. C. (2007). Male and female Drosophila germline stem cells: two versions of immortality. *Science* **316**, 402-4.

Gan, B., Sahin, E., Jiang, S., Sanchez-Aguilera, A., Scott, K. L., Chin, L., Williams, D. A., Kwiatkowski, D. J. and DePinho, R. A. (2008). mTORC1-dependent and -independent regulation of stem cell renewal, differentiation, and mobilization. *Proc Natl Acad Sci U S A* **105**, 19384-9.

Gao, X., Zhang, Y., Arrazola, P., Hino, O., Kobayashi, T., Yeung, R. S., Ru, B. and Pan, D. (2002). Tsc tumour suppressor proteins antagonize amino-acid-TOR signalling. *Nat Cell Biol* **4**, 699-704.

Garitaonandia, I., Smith, J. L., Kupchak, B. R. and Lyons, T. J. (2009). Adiponectin identified as an agonist for PAQR3/RKTG using a yeast-based assay system. *J Recept Signal Transduct Res* **29**, 67-73.

Geminard, C., Rulifson, E. J. and Leopold, P. (2009). Remote control of insulin secretion by fat cells in Drosophila. *Cell Metab* **10**, 199-207.

Gems, D., Sutton, A. J., Sundermeyer, M. L., Albert, P. S., King, K. V., Edgley, M. L., Larsen, P. L. and Riddle, D. L. (1998). Two pleiotropic classes of daf-2 mutation affect larval arrest, adult behavior, reproduction and longevity in Caenorhabditis elegans. *Genetics* **150**, 129-55.

Gibson, M. C. and Perrimon, N. (2005). Extrusion and death of DPP/BMP-compromised epithelial cells in the developing Drosophila wing. *Science* **307**, 1785-9.

Gilbert, L. I. (2004). Halloween genes encode P450 enzymes that mediate steroid hormone biosynthesis in Drosophila melanogaster. *Mol Cell Endocrinol* **215**, 1-10.

Goberdhan, D. C. and Wilson, C. (2003). The functions of insulin signaling: size isn't everything, even in Drosophila. *Differentiation* **71**, 375-97.

Grandison, R. C., Piper, M. D. and Partridge, L. (2009). Amino-acid imbalance explains extension of lifespan by dietary restriction in Drosophila. *Nature* **462**, 1061-4.

Grewal, S. S. (2009). Insulin/TOR signaling in growth and homeostasis: a view from the fly world. *Int J Biochem Cell Biol* **41**, 1006-10.

Grewal, S. S. and Saucedo, L. J. (2004). Chewing the fat; regulating autophagy in Drosophila. *Dev Cell* **7**, 148-50.

Gronke, S., Beller, M., Fellert, S., Ramakrishnan, H., Jackle, H. and Kuhnlein, R. P. (2003). Control of fat storage by a Drosophila PAT domain protein. *Curr Biol* **13**, 603-6.

Gronke, S., Clarke, D. F., Broughton, S., Andrews, T. D. and Partridge, L. (2010). Molecular evolution and functional characterization of Drosophila insulin-like peptides. *PLoS Genet* **6**, e1000857.

Gronke, S., Mildner, A., Fellert, S., Tennagels, N., Petry, S., Muller, G., Jackle, H. and Kuhnlein, R. P. (2005). Brummer lipase is an evolutionary conserved fat storage regulator in Drosophila. *Cell Metab* **1**, 323-30.

Gulati, P., Gaspers, L. D., Dann, S. G., Joaquin, M., Nobukuni, T., Natt, F., Kozma, S. C., Thomas, A. P. and Thomas, G. (2008). Amino acids activate mTOR complex 1 via Ca2+/CaM signaling to hVps34. *Cell Metab* **7**, 456-65.

Gupta, S. and Rosenberg, M. E. (2008). Do stem cells exist in the adult kidney? *Am J Nephrol* **28**, 607-13.

Gutierrez, E., Wiggins, D., Fielding, B. and Gould, A. P. (2007). Specialized hepatocyte-like cells regulate Drosophila lipid metabolism. *Nature* **445**, 275-80.

Gwinn, D. M., Shackelford, D. B., Egan, D. F., Mihaylova, M. M., Mery, A., Vasquez, D. S., Turk, B. E. and Shaw, R. J. (2008). AMPK phosphorylation of raptor mediates a metabolic checkpoint. *Mol Cell* **30**, 214-26.

Hader, T., Muller, S., Aguilera, M., Eulenberg, K. G., Steuernagel, A., Ciossek, T., Kuhnlein, R. P., Lemaire, L., Fritsch, R., Dohrmann, C. et al. (2003). Control of triglyceride storage by a WD40/TPR-domain protein. *EMBO Rep* **4**, 511-6.

Hafen, E. (2004). Cancer, type 2 diabetes, and ageing: news from flies and worms. *Swiss Med Wkly* **134**, 711-9.

Hansen, I. A., Attardo, G. M., Park, J. H., Peng, Q. and Raikhel, A. S. (2004). Target of rapamycin-mediated amino acid signaling in mosquito anautogeny. *Proc Natl Acad Sci U S A* **101**, 10626-31.

Hansen, I. A., Attardo, G. M., Roy, S. G. and Raikhel, A. S. (2005). Target of rapamycin-dependent activation of S6 kinase is a central step in the transduction of nutritional signals during egg development in a mosquito. *J Biol Chem* **280**, 20565-72.

Hardie, D. G. (2004). The AMP-activated protein kinase pathway--new players upstream and downstream. *J Cell Sci* **117**, 5479-87.

Hatfield, S. D., Shcherbata, H. R., Fischer, K. A., Nakahara, K., Carthew, R. W. and Ruohola-Baker, H. (2005). Stem cell division is regulated by the microRNA pathway. *Nature* **435**, 974-8.

Hay, N. and Sonenberg, N. (2004). Upstream and downstream of mTOR. *Genes Dev* **18**, 1926-45.

He, S., Nakada, D. and Morrison, S. J. (2009). Mechanisms of stem cell self-renewal. *Annu Rev Cell Dev Biol* **25**, 377-406.

Heesom, K. J., Gampel, A., Mellor, H. and Denton, R. M. (2001). Cell cycle-dependent phosphorylation of the translational repressor eIF-4E binding protein-1 (4E-BP1). *Curr Biol* **11**, 1374-9.

Hennig, K. M. and Neufeld, T. P. (2002). Inhibition of cellular growth and proliferation by dTOR overexpression in Drosophila. *Genesis* **34**, 107-10.

Hietakangas, V. and Cohen, S. M. (2009). Regulation of tissue growth through nutrient sensing. *Annu Rev Genet* **43**, 389-410.

Hinge, A., Bajaj, M., Limaye, L., Surolia, A. and Kale, V. P. (2009). Oral administration of insulin receptor-interacting lectins leads to an enhancement in the hematopoietic stem and progenitor cell pool of mice. *Stem Cells Dev*.

Honegger, B., Galic, M., Kohler, K., Wittwer, F., Brogiolo, W., Hafen, E. and Stocker, H. (2008). Imp-L2, a putative homolog of vertebrate IGF-binding protein 7, counteracts insulin signaling in Drosophila and is essential for starvation resistance. *J Biol* **7**, 10.

Hsu, H. J. and Drummond-Barbosa, D. (2009). Insulin levels control female germline stem cell maintenance via the niche in Drosophila. *Proc Natl Acad Sci U S A* **106**, 1117-21.

Hsu, H. J., LaFever, L. and Drummond-Barbosa, D. (2008). Diet controls normal and tumorous germline stem cells via insulin-dependent and -independent mechanisms in Drosophila. *Dev Biol* **313**, 700-12.

Hwangbo, D. S., Gershman, B., Tu, M. P., Palmer, M. and Tatar, M. (2004). Drosophila dFOXO controls lifespan and regulates insulin signalling in brain and fat body. *Nature* **429**, 562-6.

Ikeya, T., Galic, M., Belawat, P., Nairz, K. and Hafen, E. (2002). Nutrient-dependent expression of insulin-like peptides from neuroendocrine cells in the CNS contributes to growth regulation in Drosophila. *Curr Biol* **12**, 1293-300.

Inoki, K., Ouyang, H., Li, Y. and Guan, K. L. (2005). Signaling by target of rapamycin proteins in cell growth control. *Microbiol Mol Biol Rev* **69**, 79-100.

Inoki, K., Zhu, T. and Guan, K. L. (2003). TSC2 mediates cellular energy response to control cell growth and survival. *Cell* **115**, 577-90.

Ito, N. and Rubin, G. M. (1999). gigas, a Drosophila homolog of tuberous sclerosis gene product-2, regulates the cell cycle. *Cell* **96**, 529-39.

Jensen, M. and De Meyts, P. (2009). Molecular mechanisms of differential intracellular signaling from the insulin receptor. *Vitam Horm* **80**, 51-75.

Johnston, L. A. (2009). Competitive interactions between cells: death, growth, and geography. *Science* **324**, 1679-82.

Juhasz, G., Erdi, B., Sass, M. and Neufeld, T. P. (2007). Atg7-dependent autophagy promotes neuronal health, stress tolerance, and longevity but is dispensable for metamorphosis in Drosophila. *Genes Dev* **21**, 3061-6.

Juhasz, G., Hill, J. H., Yan, Y., Sass, M., Baehrecke, E. H., Backer, J. M. and Neufeld, T. P. (2008). The class III PI(3)K Vps34 promotes autophagy and endocytosis but not TOR signaling in Drosophila. *J Cell Biol* **181**, 655-66.

Juhasz, G. and Neufeld, T. P. (2008). Drosophila Atg7: required for stress resistance, longevity and neuronal homeostasis, but not for metamorphosis. *Autophagy* **4**, 357-8.

Junger, M. A., Rintelen, F., Stocker, H., Wasserman, J. D., Vegh, M., Radimerski, T., Greenberg, M. E. and Hafen, E. (2003). The Drosophila forkhead transcription factor FOXO mediates the reduction in cell number associated with reduced insulin signaling. *J Biol* **2**, 20.

Kadowaki, T., Yamauchi, T., Kubota, N., Hara, K. and Ueki, K. (2007). Adiponectin and adiponectin receptors in obesity-linked insulin resistance. *Novartis Found Symp* **286**, 164-76; discussion 176-82, 200-3.

Kadowaki, T., Yamauchi, T., Kubota, N., Hara, K., Ueki, K. and Tobe, K. (2006). Adiponectin and adiponectin receptors in insulin resistance, diabetes, and the metabolic syndrome. *J Clin Invest* **116**, 1784-92.

Kao, G. D., McKenna, W. G. and Yen, T. J. (2001). Detection of repair activity during the DNA damage-induced G2 delay in human cancer cells. *Oncogene* **20**, 3486-96.

Kayampilly, P. P. and Menon, K. M. (2007). Follicle-stimulating hormone increases tuberin phosphorylation and mammalian target of rapamycin signaling through an extracellular signal-regulated kinase-dependent pathway in rat granulosa cells. *Endocrinology* **148**, 3950-7.

Kelso, R. J., Buszczak, M., Quinones, A. T., Castiblanco, C., Mazzalupo, S. and Cooley, L. (2004). Flytrap, a database documenting a GFP protein-trap insertion screen in Drosophila melanogaster. *Nucleic Acids Res* **32**, D418-20.

Kim, M. H., Kim, M. O., Kim, Y. H., Kim, J. S. and Han, H. J. (2009). Linoleic acid induces mouse embryonic stem cell proliferation via Ca2+/PKC, PI3K/Akt, and MAPKs. *Cell Physiol Biochem* **23**, 53-64.

Kimble, J. and Crittenden, S. L. (2007). Controls of germline stem cells, entry into meiosis, and the sperm/oocyte decision in Caenorhabditis elegans. *Annu Rev Cell Dev Biol* **23**, 405-33.

Kirilly, D. and Xie, T. (2007). The Drosophila ovary: an active stem cell community. *Cell Res* **17**, 15-25.

Klein, J., Perwitz, N., Kraus, D. and Fasshauer, M. (2006). Adipose tissue as source and target for novel therapies. *Trends Endocrinol Metab* **17**, 26-32.

Kockel, L., Kerr, K. S., Melnick, M., Bruckner, K., Hebrok, M. and Perrimon, N. (2010). Dynamic switch of negative feedback regulation in Drosophila Akt-TOR signaling. *PLoS Genet* **6**, e1000990.

Kos, K., Wong, S. P., Huda, M. S., Cakir, M., Jernas, M., Carlsson, L., Kerrigan, D., Wilding, J. P. and Pinkney, J. H. (2010). In humans the adiponectin receptor R2 is expressed predominantly in adipose tissue and linked to the adipose tissue expression of MMIF-1. *Diabetes Obes Metab* **12**, 360-3.

Kramer, J. M., Davidge, J. T., Lockyer, J. M. and Staveley, B. E. (2003). Expression of Drosophila FOXO regulates growth and can phenocopy starvation. *BMC Dev Biol* **3**, 5.

Kuckelkorn, U., Knuehl, C., Boes-Fabian, B., Drung, I. and Kloetzel, P. M. (2000). The effect of heat shock on 20S/26S proteasomes. *Biol Chem* **381**, 1017-23.

Lachance, P. E., Miron, M., Raught, B., Sonenberg, N. and Lasko, P. (2002). Phosphorylation of eukaryotic translation initiation factor 4E is critical for growth. *Mol Cell Biol* **22**, 1656-63.

LaFever, L. and Drummond-Barbosa, D. (2005). Direct control of germline stem cell division and cyst growth by neural insulin in Drosophila. *Science* **309**, 1071-3.

LaFever, L., Feoktistov, A., Hsu, H. J. and Drummond-Barbosa, D. (2010). Specific roles of Target of rapamycin in the control of stem cells and their progeny in the Drosophila ovary. *Development* **137**, 2117-26.

LaMarca, H. L. and Rosen, J. M. (2008). Minireview: hormones and mammary cell fate--what will I become when I grow up? *Endocrinology* **149**, 4317-21.

Lantz, V., Ambrosio, L. and Schedl, P. (1992). The Drosophila orb gene is predicted to encode sex-specific germline RNA-binding proteins and has localized transcripts in ovaries and early embryos. *Development* **115**, 75-88.

Lavranos, T. C., Mathis, J. M., Latham, S. E., Kalionis, B., Shay, J. W. and Rodgers, R. J. (1999). Evidence for ovarian granulosa stem cells: telomerase activity and localization of the telomerase ribonucleic acid component in bovine ovarian follicles. *Biol Reprod* **61**, 358-66.

Lazaris-Karatzas, A., Montine, K. S. and Sonenberg, N. (1990). Malignant transformation by a eukaryotic initiation factor subunit that binds to mRNA 5' cap. *Nature* **345**, 544-7.

Lee, C. Y. and Koren, G. (2010). Maternal obesity: effects on pregnancy and the role of pre-conception counselling. *J Obstet Gynaecol* **30**, 101-6.

Lee, J. H., Koh, H., Kim, M., Kim, Y., Lee, S. Y., Karess, R. E., Lee, S. H., Shong, M., Kim, J. M., Kim, J. et al. (2007). Energy-dependent regulation of cell structure by AMP-activated protein kinase. *Nature* **447**, 1017-20.

Lee, L. A. and Orr-Weaver, T. L. (2003). Regulation of cell cycles in Drosophila development: intrinsic and extrinsic cues. *Annu Rev Genet* **37**, 545-78.

Li, L. and Clevers, H. (2010). Coexistence of quiescent and active adult stem cells in mammals. *Science* **327**, 542-5.

Li, L., Edgar, B. A. and Grewal, S. S. (2010). Nutritional control of gene expression in Drosophila larvae via TOR, Myc and a novel cis-regulatory element. *BMC Cell Biol* **11**, 7.

Li, L. and Xie, T. (2005). Stem cell niche: structure and function. *Annu Rev Cell Dev Biol* **21**, 605-31.

Li, S. (2010). Identification of iron-loaded ferritin as an essential mitogen for cell proliferation and postembryonic development in Drosophila. *Cell Res*.

Liao, X. H., Majithia, A., Huang, X. and Kimmel, A. R. (2008). Growth control via TOR kinase signaling, an intracellular sensor of amino acid and energy availability, with crosstalk potential to proline metabolism. *Amino Acids* **35**, 761-70.

Lilly, M. A., de Cuevas, M. and Spradling, A. C. (2000). Cyclin A associates with the fusome during germline cyst formation in the Drosophila ovary. *Dev Biol* **218**, 53-63.

Lilly, M. A. and Spradling, A. C. (1996). The Drosophila endocycle is controlled by Cyclin E and lacks a checkpoint ensuring S-phase completion. *Genes Dev* **10**, 2514-26.

Link, A. J., Eng, J., Schieltz, D. M., Carmack, E., Mize, G. J., Morris, D. R., Garvik, B. M. and Yates, J. R., 3rd. (1999). Direct analysis of protein complexes using mass spectrometry. *Nat Biotechnol* **17**, 676-82.

Lippai, M., Csikos, G., Maroy, P., Lukacsovich, T., Juhasz, G. and Sass, M. (2008). SNF4Agamma, the Drosophila AMPK gamma subunit is required for regulation of developmental and stress-induced autophagy. *Autophagy* **4**, 476-86.

Liu, Y., Liu, H., Liu, S., Wang, S., Jiang, R. J. and Li, S. (2009). Hormonal and nutritional regulation of insect fat body development and function. *Arch Insect Biochem Physiol* **71**, 16-30.

Lu, K. and Campisi, J. (1992). Ras proteins are essential and selective for the action of insulin-like growth factor 1 late in the G1 phase of the cell cycle in BALB/c murine fibroblasts. *Proc Natl Acad Sci U S A* **89**, 3889-93.

Lukaszewicz, A. I., McMillan, M. K. and Kahn, M. (2010). Small molecules and stem cells. Potency and lineage commitment: the new quest for the fountain of youth. *J Med Chem* **53**, 3439-53.

Lyons, T. J., Villa, N. Y., Regalla, L. M., Kupchak, B. R., Vagstad, A. and Eide, D. J. (2004). Metalloregulation of yeast membrane steroid receptor homologs. *Proc Natl Acad Sci U S A* **101**, 5506-11.

Maines, J. Z., Stevens, L. M., Tong, X. and Stein, D. (2004). Drosophila dMyc is required for ovary cell growth and endoreplication. *Development* **131**, 775-86.

Margolis, J. and Spradling, A. (1995). Identification and behavior of epithelial stem cells in the Drosophila ovary. *Development* **121**, 3797-807.

Marini, A., Matmati, N. and Morpurgo, G. (1999). Starvation in yeast increases non-adaptive mutation. *Curr Genet* **35**, 77-81.

Marshall, S. (2006). Role of insulin, adipocyte hormones, and nutrient-sensing pathways in regulating fuel metabolism and energy homeostasis: a nutritional perspective of diabetes, obesity, and cancer. *Sci STKE* **2006**, re7.

May, R., Sureban, S. M., Lightfoot, S. A., Hoskins, A. B., Brackett, D. J., Postier, R. G., Ramanujam, R., Rao, C. V., Wyche, J. H., Anant, S. et al. (2010). Identification of a novel putative pancreatic stem/progenitor cell marker DCAMKL-1 in normal mouse pancreas. *Am J Physiol Gastrointest Liver Physiol* **299**, G303-10.

McGuire, S. E., Le, P. T., Osborn, A. J., Matsumoto, K. and Davis, R. L. (2003). Spatiotemporal rescue of memory dysfunction in Drosophila. *Science* **302**, 1765-8.

Michaelson, D., Korta, D. Z., Capua, Y. and Hubbard, E. J. (2010). Insulin signaling promotes germline proliferation in C. elegans. *Development* **137**, 671-80.

Miller, J. M., Oligino, T., Pazdera, M., Lopez, A. J. and Hoshizaki, D. K. (2002). Identification of fat-cell enhancer regions in Drosophila melanogaster. *Insect Mol Biol* **11**, 67-77.

Miron, M., Lasko, P. and Sonenberg, N. (2003). Signaling from Akt to FRAP/TOR targets both 4E-BP and S6K in Drosophila melanogaster. *Mol Cell Biol* **23**, 9117-26.

Miron, M. and Sonenberg, N. (2001). Regulation of translation via TOR signaling: insights from Drosophila melanogaster. *J Nutr* **131**, 2988S-93S.

Mirouse, V., Swick, L. L., Kazgan, N., St Johnston, D. and Brenman, J. E. (2007). LKB1 and AMPK maintain epithelial cell polarity under energetic stress. *J Cell Biol* **177**, 387-92.

Mirth, C. K. and Riddiford, L. M. (2007). Size assessment and growth control: how adult size is determined in insects. *Bioessays* **29**, 344-55.

Mitchell, M., Armstrong, D. T., Robker, R. L. and Norman, R. J. (2005). Adipokines: implications for female fertility and obesity. *Reproduction* **130**, 583-97.

Mitsiadis, T. A., Barrandon, O., Rochat, A., Barrandon, Y. and De Bari, C. (2007). Stem cell niches in mammals. *Exp Cell Res* **313**, 3377-85.

Mohr, S. E. and Boswell, R. E. (2002). Genetic analysis of Drosophila melanogaster polytene chromosome region 44D-45F: loci required for viability and fertility. *Genetics* **160**, 1503-10.

Morin, X., Daneman, R., Zavortink, M. and Chia, W. (2001). A protein trap strategy to detect GFP-tagged proteins expressed from their endogenous loci in Drosophila. *Proc Natl Acad Sci U S A* **98**, 15050-5.

Morrison, S. J., Shah, N. M. and Anderson, D. J. (1997). Regulatory mechanisms in stem cell biology. *Cell* **88**, 287-98.

Morrison, S. J. and Spradling, A. C. (2008). Stem cells and niches: mechanisms that promote stem cell maintenance throughout life. *Cell* **132**, 598-611.

Moumen, A., Patane, S., Porras, A., Dono, R. and Maina, F. (2007). Met acts on Mdm2 via mTOR to signal cell survival during development. *Development* **134**, 1443-51.

Muthayya, S. (2009). Maternal nutrition & low birth weight - what is really important? *Indian J Med Res* **130**, 600-8.

Nakashima, A., Maruki, Y., Imamura, Y., Kondo, C., Kawamata, T., Kawanishi, I., Takata, H., Matsuura, A., Lee, K. S., Kikkawa, U. et al. (2008). The yeast Tor signaling pathway is involved in G2/M transition via polo-kinase. *PLoS One* **3**, e2223.

Narasimhan, M. L., Coca, M. A., Jin, J., Yamauchi, T., Ito, Y., Kadowaki, T., Kim, K. K., Pardo, J. M., Damsz, B., Hasegawa, P. M. et al. (2005). Osmotin is a homolog of mammalian adiponectin and controls apoptosis in yeast through a homolog of mammalian adiponectin receptor. *Mol Cell* **17**, 171-80.

Narbonne, P. and Roy, R. (2006). Regulation of germline stem cell proliferation downstream of nutrient sensing. *Cell Div* **1**, 29.

Narbonne-Reveau, K., Besse, F., Lamour-Isnard, C., Busson, D. and Pret, A. M. (2006). fused regulates germline cyst mitosis and differentiation during Drosophila oogenesis. *Mech Dev* **123**, 197-209.

Niki, Y. (2009). Culturing ovarian somatic and germline stem cells of Drosophila. *Curr Protoc Stem Cell Biol* **Chapter 2**, Unit 2E 1.

Nystul, T. and Spradling, A. (2010). Regulation of epithelial stem cell replacement and follicle formation in the Drosophila ovary. *Genetics* **184**, 503-15.

Nystul, T. G. and Spradling, A. C. (2009). Regulation of Epithelial Stem Cell Replacement and Follicle Formation in the Drosophila Ovary. *Genetics*.

Oh, D. K., Ciaraldi, T. and Henry, R. R. (2007). Adiponectin in health and disease. *Diabetes Obes Metab* **9**, 282-9.

Ohlmeyer, J. T. and Schupbach, T. (2003). Encore facilitates SCF-Ubiquitin-proteasome-dependent proteolysis during Drosophila oogenesis. *Development* **130**, 6339-49.

Oldham, S. and Hafen, E. (2003). Insulin/IGF and target of rapamycin signaling: a TOR de force in growth control. *Trends Cell Biol* **13**, 79-85.

Oldham, S., Stocker, H., Laffargue, M., Wittwer, F., Wymann, M. and Hafen, E. (2002). The Drosophila insulin/IGF receptor controls growth and size by modulating PtdInsP(3) levels. *Development* **129**, 4103-9.

Orme, M. H., Alrubaie, S., Bradley, G. L., Walker, C. D. and Leevers, S. J. (2006). Input from Ras is required for maximal PI(3)K signalling in Drosophila. *Nat Cell Biol* **8**, 1298-302.

Pan, D., Dong, J., Zhang, Y. and Gao, X. (2004). Tuberous sclerosis complex: from Drosophila to human disease. *Trends Cell Biol* **14**, 78-85.

Pasquali, R. (2006). Obesity, fat distribution and infertility. *Maturitas* **54**, 363-71.

Percik, R. and Stumvoll, M. (2009). Obesity and cancer. *Exp Clin Endocrinol Diabetes* **117**, 563-6.

Phillips, S. A. and Kung, J. T. (2010). Mechanisms of adiponectin regulation and use as a pharmacological target. *Curr Opin Pharmacol*.

Piper, M. D., Selman, C., McElwee, J. J. and Partridge, L. (2008). Separating cause from effect: how does insulin/IGF signalling control lifespan in worms, flies and mice? *J Intern Med* **263**, 179-91.

Potten, C. S. and Loeffler, M. (1990). Stem cells: attributes, cycles, spirals, pitfalls and uncertainties. Lessons for and from the crypt. *Development* **110**, 1001-20.

Pritchett, T. L., Tanner, E. A. and McCall, K. (2009). Cracking open cell death in the Drosophila ovary. *Apoptosis* **14**, 969-79.

Prober, D. A. and Edgar, B. A. (2002). Interactions between Ras1, dMyc, and dPI3K signaling in the developing Drosophila wing. *Genes Dev* **16**, 2286-99.

Puig, O., Marr, M. T., Ruhf, M. L. and Tjian, R. (2003). Control of cell number by Drosophila FOXO: downstream and feedback regulation of the insulin receptor pathway. *Genes Dev* **17**, 2006-20.

Puig, O. and Tjian, R. (2006). Nutrient availability and growth: regulation of insulin signaling by dFOXO/FOXO1. *Cell Cycle* **5**, 503-5.

Qatanani, M. and Lazar, M. A. (2007). Mechanisms of obesity-associated insulin resistance: many choices on the menu. *Genes Dev* **21**, 1443-55.

Quinones-Coello, A. T., Petrella, L. N., Ayers, K., Melillo, A., Mazzalupo, S., Hudson, A. M., Wang, S., Castiblanco, C., Buszczak, M., Hoskins, R. A. et al. (2007). Exploring strategies for protein trapping in Drosophila. *Genetics* **175**, 1089-104.

Rachon, D. and Teede, H. (2010). Ovarian function and obesity--interrelationship, impact on women's reproductive lifespan and treatment options. *Mol Cell Endocrinol* **316**, 172-9.

Reddy, P., Liu, L., Adhikari, D., Jagarlamudi, K., Rajareddy, S., Shen, Y., Du, C., Tang, W., Hamalainen, T., Peng, S. L. et al. (2008). Oocyte-specific deletion of Pten causes premature activation of the primordial follicle pool. *Science* **319**, 611-3.

Rodriguez-Viciana, P., Marte, B. M., Warne, P. H. and Downward, J. (1996). Phosphatidylinositol 3' kinase: one of the effectors of Ras. *Philos Trans R Soc Lond B Biol Sci* **351**, 225-31; discussion 231-2.

Royzman, I. and Orr-Weaver, T. L. (1998). S phase and differential DNA replication during Drosophila oogenesis. *Genes Cells* **3**, 767-76.

Rubin, G. M. and Spradling, A. C. (1983). Vectors for P element-mediated gene transfer in Drosophila. *Nucleic Acids Res* **11**, 6341-51.

Sancak, Y., Bar-Peled, L., Zoncu, R., Markhard, A. L., Nada, S. and Sabatini, D. M. (2010). Ragulator-Rag complex targets mTORC1 to the lysosomal surface and is necessary for its activation by amino acids. *Cell* **141**, 290-303.

Schalm, S. S. and Blenis, J. (2002). Identification of a conserved motif required for mTOR signaling. *Curr Biol* **12**, 632-9.

Scherer, P. E. (2006). Adipose tissue: from lipid storage compartment to endocrine organ. *Diabetes* **55**, 1537-45.

Schleich, S. and Teleman, A. A. (2009). Akt phosphorylates both Tsc1 and Tsc2 in Drosophila, but neither phosphorylation is required for normal animal growth. *PLoS One* **4**, e6305.

Serfontein, J., Nisbet, R. E., Howe, C. J. and de Vries, P. J. (2010). Evolution of the TSC1/TSC2-TOR signaling pathway. *Sci Signal* **3**, ra49.

Shen, J. and Dahmann, C. (2005). Extrusion of cells with inappropriate Dpp signaling from Drosophila wing disc epithelia. *Science* **307**, 1789-90.

Shiozaki, K. (2009). Nutrition-minded cell cycle. *Sci Signal* **2**, pe74.

Slaidina, M., Delanoue, R., Gronke, S., Partridge, L. and Leopold, P. (2009). A Drosophila insulin-like peptide promotes growth during nonfeeding states. *Dev Cell* **17**, 874-84.

Smith, E. M. and Proud, C. G. (2008). cdc2-cyclin B regulates eEF2 kinase activity in a cell cycle- and amino acid-dependent manner. *Embo J* **27**, 1005-16.

Song, X. and Xie, T. (2003). Wingless signaling regulates the maintenance of ovarian somatic stem cells in Drosophila. *Development* **130**, 3259-68.

Spradling, A., Drummond-Barbosa, D. and Kai, T. (2001). Stem cells find their niche. *Nature* **414**, 98-104.

Spradling, A. C. (1993). Developmental genetics of oogenesis. **In: Bate, M., Arias, A.M. (Eds), The Development of Drosophila melanogaster, vol. 1. Cold Spring Harbor Laboratory Press, Plainview, NY,**, pp 1-70.

Spritzer, M. D. and Galea, L. A. (2007). Testosterone and dihydrotestosterone, but not estradiol, enhance survival of new hippocampal neurons in adult male rats. *Dev Neurobiol* **67**, 1321-33.

Staiger, H. and Haring, H. U. (2005). Adipocytokines: fat-derived humoral mediators of metabolic homeostasis. *Exp Clin Endocrinol Diabetes* **113**, 67-79.

Stangl, D. and Thuret, S. (2009). Impact of diet on adult hippocampal neurogenesis. *Genes Nutr* **4**, 271-82.

Steller, H. (2008). Regulation of apoptosis in Drosophila. *Cell Death Differ* **15**, 1132-8.

Suh, J. M., Zeve, D., McKay, R., Seo, J., Salo, Z., Li, R., Wang, M. and Graff, J. M. (2007). Adipose is a conserved dosage-sensitive antiobesity gene. *Cell Metab* **6**, 195-207.

Sun, J. and Tower, J. (1999). FLP recombinase-mediated induction of Cu/Zn-superoxide dismutase transgene expression can extend the life span of adult Drosophila melanogaster flies. *Mol Cell Biol* **19**, 216-28.

Tadokoro, Y., Ema, H., Okano, M., Li, E. and Nakauchi, H. (2007). De novo DNA methyltransferase is essential for self-renewal, but not for differentiation, in hematopoietic stem cells. *J Exp Med* **204**, 715-22.

Tanaka, S., Ito, T. and Wands, J. R. (1996). Neoplastic transformation induced by insulin receptor substrate-1 overexpression requires an interaction with both Grb2 and Syp signaling molecules. *J Biol Chem* **271**, 14610-6.

Tanaka, Y., Yujiri, T., Tanaka, M., Mitani, N., Tanimura, A. and Tanizawa, Y. (2009). Alteration of adipokines during peripheral blood stem cell mobilization induced by granulocyte colony-stimulating factor. *J Clin Apher* **24**, 205-8.

Tanapat, P., Hastings, N. B., Reeves, A. J. and Gould, E. (1999). Estrogen stimulates a transient increase in the number of new neurons in the dentate gyrus of the adult female rat. *J Neurosci* **19**, 5792-801.

Tang, Y. T., Hu, T., Arterburn, M., Boyle, B., Bright, J. M., Emtage, P. C. and Funk, W. D. (2005). PAQR proteins: a novel membrane receptor family defined by an ancient 7-transmembrane pass motif. *J Mol Evol* **61**, 372-80.

Tapon, N., Ito, N., Dickson, B. J., Treisman, J. E. and Hariharan, I. K. (2001). The Drosophila tuberous sclerosis complex gene homologs restrict cell growth and cell proliferation. *Cell* **105**, 345-55.

Tastan, O. Y., Maines, J. Z., Li, Y., McKearin, D. M. and Buszczak, M. (2010). Drosophila Ataxin 2-binding protein 1 marks an intermediate step in the molecular differentiation of female germline cysts. *Development*.

Teleman, A. A., Chen, Y. W. and Cohen, S. M. (2005a). 4E-BP functions as a metabolic brake used under stress conditions but not during normal growth. *Genes Dev* **19**, 1844-8.

Teleman, A. A., Chen, Y. W. and Cohen, S. M. (2005b). Drosophila Melted modulates FOXO and TOR activity. *Dev Cell* **9**, 271-81.

Teleman, A. A., Hietakangas, V., Sayadian, A. C. and Cohen, S. M. (2008). Nutritional control of protein biosynthetic capacity by insulin via Myc in Drosophila. *Cell Metab* **7**, 21-32.

Terskikh, A. V., Bryant, P. J. and Schwartz, P. H. (2006). Mammalian stem cells. *Pediatr Res* **59**, 13R-20R.

Thibault, S. T., Singer, M. A., Miyazaki, W. Y., Milash, B., Dompe, N. A., Singh, C. M., Buchholz, R., Demsky, M., Fawcett, R., Francis-Lang, H. L. et al. (2004). A complementary transposon tool kit for Drosophila melanogaster using P and piggyBac. *Nat Genet* **36**, 283-7.

Thomer, M., May, N. R., Aggarwal, B. D., Kwok, G. and Calvi, B. R. (2004). Drosophila double-parked is sufficient to induce re-replication during development and is regulated by cyclin E/CDK2. *Development* **131**, 4807-18.

Trotman, L. C. and Pandolfi, P. P. (2003). PTEN and p53: who will get the upper hand? *Cancer Cell* **3**, 97-9.

Tsuchida, A., Yamauchi, T., Ito, Y., Hada, Y., Maki, T., Takekawa, S., Kamon, J., Kobayashi, M., Suzuki, R., Hara, K. et al. (2004). Insulin/Foxo1 pathway regulates

expression levels of adiponectin receptors and adiponectin sensitivity. *J Biol Chem* **279**, 30817-22.

Ueishi, S., Shimizu, H. and Y, H. I. (2009). Male germline stem cell division and spermatocyte growth require insulin signaling in Drosophila. *Cell Struct Funct* **34**, 61-9.

Van Buskirk, C., Hawkins, N. C. and Schupbach, T. (2000). Encore is a member of a novel family of proteins and affects multiple processes in Drosophila oogenesis. *Development* **127**, 4753-62.

Van Der Heide, L. P., Hoekman, M. F. and Smidt, M. P. (2004). The ins and outs of FoxO shuttling: mechanisms of FoxO translocation and transcriptional regulation. *Biochem J* **380**, 297-309.

Vereshchagina, N. and Wilson, C. (2006). Cytoplasmic activated protein kinase Akt regulates lipid-droplet accumulation in Drosophila nurse cells. *Development* **133**, 4731-5.

Viollet, B., Horman, S., Leclerc, J., Lantier, L., Foretz, M., Billaud, M., Giri, S. and Andreelli, F. (2010). AMPK inhibition in health and disease. *Crit Rev Biochem Mol Biol* **45**, 276-95.

Wang, C., Mao, X., Wang, L., Liu, M., Wetzel, M. D., Guan, K. L., Dong, L. Q. and Liu, F. (2007). Adiponectin sensitizes insulin signaling by reducing p70 S6 kinase-mediated serine phosphorylation of IRS-1. *J Biol Chem* **282**, 7991-6.

Wang, X. and Proud, C. G. (2009). Nutrient control of TORC1, a cell-cycle regulator. *Trends Cell Biol* **19**, 260-7.

Wang, Y. and Riechmann, V. (2007). The role of the actomyosin cytoskeleton in coordination of tissue growth during Drosophila oogenesis. *Curr Biol* **17**, 1349-55.

Wang, Z. and Lin, H. (2005). The division of Drosophila germline stem cells and their precursors requires a specific cyclin. *Curr Biol* **15**, 328-33.

Weissman, I. L. (2000). Stem cells: units of development, units of regeneration, and units in evolution. *Cell* **100**, 157-68.

Whitehead, J. P., Richards, A. A., Hickman, I. J., Macdonald, G. A. and Prins, J. B. (2006). Adiponectin--a key adipokine in the metabolic syndrome. *Diabetes Obes Metab* **8**, 264-80.

Whittaker, A. J., Royzman, I. and Orr-Weaver, T. L. (2000). Drosophila double parked: a conserved, essential replication protein that colocalizes with the origin recognition complex and links DNA replication with mitosis and the down-regulation of S phase transcripts. *Genes Dev* **14**, 1765-76.

Whitten, J. (1963). Haemocytes and the metamorphosing tissues in Sarcophaga bullata, Drosophila melanogaster and other cyclorrhaphous Diptera. *J Insect Physiol* **10**, 447-450.

Wiese, S., Reidegeld, K. A., Meyer, H. E. and Warscheid, B. (2007). Protein labeling by iTRAQ: a new tool for quantitative mass spectrometry in proteome research. *Proteomics* **7**, 340-50.

Williams, T. and Brenman, J. E. (2008). LKB1 and AMPK in cell polarity and division. *Trends Cell Biol* **18**, 193-8.

Wong, G. W., Wang, J., Hug, C., Tsao, T. S. and Lodish, H. F. (2004). A family of Acrp30/adiponectin structural and functional paralogs. *Proc Natl Acad Sci U S A* **101**, 10302-7.

Wong, M. D., Jin, Z. and Xie, T. (2005). Molecular mechanisms of germline stem cell regulation. *Annu Rev Genet* **39**, 173-95.

Wu, M. Y., Cully, M., Andersen, D. and Leevers, S. J. (2007). Insulin delays the progression of Drosophila cells through G2/M by activating the dTOR/dRaptor complex. *Embo J* **26**, 371-9.

Wu, X., Tanwar, P. S. and Raftery, L. A. (2008). Drosophila follicle cells: morphogenesis in an eggshell. *Semin Cell Dev Biol* **19**, 271-82.

Xi, R. and Xie, T. (2005). Stem cell self-renewal controlled by chromatin remodeling factors. *Science* **310**, 1487-9.

Xie, T., Song, X., Jin, Z., Pan, L., Weng, C., Chen, S. and Zhang, N. (2008). Interactions between stem cells and their niche in the Drosophila ovary. *Cold Spring Harb Symp Quant Biol* **73**, 39-47.

Xie, T. and Spradling, A. C. (1998). decapentaplegic is essential for the maintenance and division of germline stem cells in the Drosophila ovary. *Cell* **94**, 251-60.

Yaba, A., Bianchi, V., Borini, A. and Johnson, J. (2008). A putative mitotic checkpoint dependent on mTOR function controls cell proliferation and survival in ovarian granulosa cells. *Reprod Sci* **15**, 128-38.

Yamauchi, T., Kamon, J., Ito, Y., Tsuchida, A., Yokomizo, T., Kita, S., Sugiyama, T., Miyagishi, M., Hara, K., Tsunoda, M. et al. (2003). Cloning of adiponectin receptors that mediate antidiabetic metabolic effects. *Nature* **423**, 762-9.

Yamauchi, T., Nio, Y., Maki, T., Kobayashi, M., Takazawa, T., Iwabu, M., Okada-Iwabu, M., Kawamoto, S., Kubota, N., Kubota, T. et al. (2007). Targeted disruption of AdipoR1 and AdipoR2 causes abrogation of adiponectin binding and metabolic actions. *Nat Med* **13**, 332-9.

Yan, Y. P., Sailor, K. A., Vemuganti, R. and Dempsey, R. J. (2006). Insulin-like growth factor-1 is an endogenous mediator of focal ischemia-induced neural progenitor proliferation. *Eur J Neurosci* **24**, 45-54.

Yates, J. R., 3rd, Eng, J. K., McCormack, A. L. and Schieltz, D. (1995). Method to correlate tandem mass spectra of modified peptides to amino acid sequences in the protein database. *Anal Chem* **67**, 1426-36.

Yenush, L., Fernandez, R., Myers, M. G., Jr., Grammer, T. C., Sun, X. J., Blenis, J., Pierce, J. H., Schlessinger, J. and White, M. F. (1996). The Drosophila insulin receptor activates multiple signaling pathways but requires insulin receptor substrate proteins for DNA synthesis. *Mol Cell Biol* **16**, 2509-17.

Yilmaz, O. H., Valdez, R., Theisen, B. K., Guo, W., Ferguson, D. O., Wu, H. and Morrison, S. J. (2006). Pten dependence distinguishes haematopoietic stem cells from leukaemia-initiating cells. *Nature* **441**, 475-82.

Yin, V. P. and Thummel, C. S. (2005). Mechanisms of steroid-triggered programmed cell death in Drosophila. *Semin Cell Dev Biol* **16**, 237-43.

Yue, L. and Spradling, A. C. (1992). hu-li tai shao, a gene required for ring canal formation during Drosophila oogenesis, encodes a homolog of adducin. *Genes Dev* **6**, 2443-54.

Zagon, I. S., Klocek, M. S., Sassani, J. W. and McLaughlin, P. J. (2007). Use of topical insulin to normalize corneal epithelial healing in diabetes mellitus. *Arch Ophthalmol* **125**, 1082-8.

Zahn, J., Doormann, P., Dorn, A. and Dorn, D. C. (2007). Apoptosis of male germ-line stem cells after laser ablation of their niche. *Stem Cell Res* **1**, 75-85.

Zhang, C. C. and Lodish, H. F. (2004). Insulin-like growth factor 2 expressed in a novel fetal liver cell population is a growth factor for hematopoietic stem cells. *Blood* **103**, 2513-21.

Zhang, H., Stallock, J. P., Ng, J. C., Reinhard, C. and Neufeld, T. P. (2000). Regulation of cellular growth by the Drosophila target of rapamycin dTOR. *Genes Dev* **14**, 2712-24.

Zhang, N., Xie, T. (2009). Extrinsic and Intrinsic Control of Germline Stem Cell Regulation in the Drosophila ovary. *Regulatory Networks in Stem Cells* **Stem Cell Biology and Regenerative Medicine**, 155-163.

Zhang, R. L., Zhang, Z. G., Zhang, L. and Chopp, M. (2001). Proliferation and differentiation of progenitor cells in the cortex and the subventricular zone in the adult rat after focal cerebral ischemia. *Neuroscience* **105**, 33-41.

Zhang, Y., Billington, C. J., Jr., Pan, D. and Neufeld, T. P. (2006). Drosophila target of rapamycin kinase functions as a multimer. *Genetics* **172**, 355-62.

Zhang, Y., Proenca, R., Maffei, M., Barone, M., Leopold, L. and Friedman, J. M. (1994). Positional cloning of the mouse obese gene and its human homologue. *Nature* **372**, 425-32.

Zid, B. M., Rogers, A. N., Katewa, S. D., Vargas, M. A., Kolipinski, M. C., Lu, T. A., Benzer, S. and Kapahi, P. (2009). 4E-BP extends lifespan upon dietary restriction by enhancing mitochondrial activity in Drosophila. *Cell* **139**, 149-60.